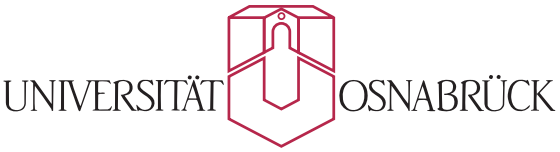

Electrophysiological Signatures of Active Vision

Dissertation
zur Erlangung des Grades
"Doktor der Naturwissenschaften"
im Fachbereich Humanwissenschaften
der Universität Osnabrück

vorgelegt von Christine Carl

Hamburg, 2013

Abstract

Active movements are a key feature of human behavior. Even when we do not move our limbs we almost never stop guiding our eyes. As a minimal but omnipresent form of behavior, fast eye movements, called saccades, sample the visual world and determine to a large extent what we perceive. Despite being an integral part of visual perception, prevalent research practice treats the human subject as a passive observer who fixates a spot on the screen and is not allowed to move. Yet, learning sensorimotor interactions by active exploration in order to predict future changes and guide actions seems to be a fundamental principle of neural organization. This results in neural patterns of active behavior that can be fundamentally different from the neural processes revealed in movement-restricted laboratory settings questioning the transferability of results from experimental paradigms demanding fixation to real-world free viewing behavior. In this thesis, we aim at studying the neural mechanisms underlying free viewing behavior. In order to assess the fast, flexible and possibly distributed neural dynamics of active vision, we established a procedure for studying eye movements in magnetoencephalography (MEG) and investigated oscillatory signatures associated with sensorimotor processes of eye movements and saccade target selection, two fundamental processes of active vision.

Electroencephalography (EEG) and MEG can non-invasively measure fast neural dynamics and hence seem ideally suited for studying active vision in humans. However, artifacts related to eye movements confound both EEG and MEG signals, and a thorough handling of these artifacts is crucial for investigating neural activities during active movements. Mostly, cleaning of ocular artifacts has been performed for occasional eye movements and blinks in fixation paradigms in EEG. Less is known about the impact of ocular artifacts and especially the saccadic spike on MEG. As a first step to enable active vision studies in MEG, we investigated ocular artifacts and possible ways of their separation from neural signals in MEG. We show that the saccadic spike seriously distorts the spatial and spectral charac-

teristics of the MEG signal (Study 2). We further tested if electrooculogram (EOG) based regression is feasible for corneo-retinal artifact removal (Study 1). Due to an often-raised concern, we addressed if EOG regression eliminates neural activity when applied for MEG. Our results do not indicate such susceptibility and we conclude that EOG regression for removing the corneo-retinal artifact in MEG is suitable. Based on insights from both studies, we established an artifact handling procedure including EOG regression and independent component analysis (ICA) to assess the neural dynamics of active vision.

In Study 3, we investigated spectral signatures of neuronal activity across cortex underlying saccade preparation, execution and re-fixation in a delayed saccade task. During preparation and execution, we found a dichotomic signature of gamma power increases and beta power decreases in widespread cortical areas related to saccadic control, including fronto-parietal structures. Saccade direction specific signatures resided in hemisphere lateralized changes in low gamma and alpha power in posterior parietal cortex during preparation extending to extrastriate areas during re-fixation.

Real-world behavior implies the constant need to flexibly select actions between competing behavioral alternatives depending on both sensory input and internal states. In order to assess internally motivated viewing behavior, we compared neuronal activity of externally cued saccades with saccades to freely chosen, equally valuable targets. We found gamma band specific power increases in fronto-parietal areas that are likely to reflect a fast transient process of action guidance for sensory-guided saccades and a sustained process for internally selecting between competing behavioral alternatives. The sustained signature of internal action selection suggests that a decision between spatially oriented movements is mediated within sensorimotor structures by neural competition between assemblies encoding parallel evolving movement plans. Since our observations support the assumption that a decision emerges through the distributed consensus of neural activities within effector specific areas rather than in a distinct decision module, they argue for the importance of studying mental processes within their ecologically valid and active context.

This thesis shows the feasibility of studying neural mechanisms of active vision in MEG and provides important steps for studying neurophysiological correlates of free viewing in the future. The observed spectrally specific, distributed signatures highlight the importance of assessing fast oscillatory dynamics across the cortex for understanding neural mechanisms mediating real-world active behavior.

Acknowledgements

Great thanks go to Prof. Andreas Engel for supervising and supporting me as a PhD student in his institute through these years. With his liberal attitude he gave a lot of freedom for the own scientific work. Particular thanks also go to Prof. Peter König, who supervised my thesis and gave great scientific advice.

I specially thank Joerg Hipp with whom I worked on all my PhD projects. He gave me excellent support and advice throughout my PhD time and taught me a lot, especially about neuroscientific data analysis. For helpful discussions and advice I would also like to thank Alper Açık. Prof. Thomas Gruber kindly agreed to be the third referee for my thesis, many thanks for this.

I would further like to thank Christiane Reißmann and Gerhard Steinmetz for their help during the measurements and recruitment of participants. I was very happy about the nice company and fruitful discussions with my colleagues in Hamburg as well as in Osnabrück. Especially my office mates, that made me laugh at least once a day, have to be mentioned here. Particular thanks go to Hanna, Inga, David, Immanuel, Florian, Jonas, Till, Gernot, Nora and Frank.

Finally, I would like to thank my family. Sven has given me great motivational support and many helpful comments on the thesis manuscript. He was always there for me and made me feel greatly accepted in every difficult moment. I also have to thank him for all the hours I spent in the institute or was busy, while he was with our daughter Marlene. Being forced to take a break every day in order to spend time with Marlene was the best that could happen to me and helped me not to stress out too much when finishing the thesis. I am also deeply grateful for my parents who always supported me and gave me the opportunity to study what I wanted without any financial worries.

Contents

List of Figures

List of Abbreviations

BOLD blood-oxygen-level dependent

CRP corneo-retinal potential

EEG electroencephalography

EOG electrooculogram

FDR false discovery rate

fMRI functional magnetic resonance imaging

FWHM full width at half maximum

GFP global field power

ICA independent component analysis

iEEG intracranial electroencephalography

IPS intraparietal sulcus

LFP local field potential

LIP lateral intraparietal area

MEG magnetoencephalography

MRI magnetic resonance image

NAI neural activity index

REOG radial electrooculogram

ROI region of interest

SF saccadic spike field

SP saccadic spike potential

SRP saccade related potential

TMS transcranial magnetic stimulation

Abbreviations for ROIs:

aIPS anterior intraparietal sulcus

dLPFC dorsolateral prefrontal cortex

FEF frontal eye fields

mIPS medial intraparietal sulcus

pIPS posterior intraparietal sulcus

SEF supplementary eye fields

V1 primary visual cortex

Seeing is a way of acting.
O'Regan and Noë (2001)

1

General Introduction

Understanding the mechanisms of human real-world behavior is one of the central interests in the field of cognitive science. The interaction with a complex world produces constant demands for actions and makes active movements of the limbs and eyes an essential part of behavior. Especially the eyes never stay still for a prolonged period of time; instead, humans continuously sample the visual scene by making fast eye movements denoted as saccades.

Eye movements are not only an omnipresent feature of everyday behavior but also fulfill fundamental roles for perception and goal-orientedness. Since humans have evolved with eyes that allow precise and colorful vision only at their foveal centers, much of the visual input that is processed by the brain requires individuals to actively direct their senses through movements (Schroeder et al., 2010). In addition, where and when individuals look is both task and context dependent (for reviews see Hayhoe and Rothkopf, 2011, Schütz et al., 2011, Tatler et al., 2011) so that grasping a jar of jam and putting on its lid dependably results in distinct eye positions (Hayhoe et al., 2003). Consequently, perception does not only guide human actions, but these actions also determine what we perceive. By emphasizing different aspects of the world through directing gaze, we construct a unique visual experience.

Notably, the conviction that vision is a process involving both movement and sensation was already stated over a hundred years ago:

> *We find that we begin not with a sensory stimulus, but with a sensori-motor coördination* [sic]*, the optical-ocular, and that in a certain sense*

> *it is the movement which is primary, and the sensation which is secondary.... In other words, the real beginning is with the act of seeing; it is looking, and not a sensation of light. The sensory quale gives the value of the act, just as the movement furnishes its mechanism and control, but both sensation and movement lie inside, not outside the act.* – Dewey (1896, pp.358f.)

Despite these early attempts towards an active account of vision, neuroscientific practice of the past century has mostly tackled mental processes from the perspective of a passive observer. Consequently, determining which physical properties of a stimulus cause changes in neuronal activity has long been the primary focus in the neurosciences of vision. These studies have relied on the assumption that the mechanisms of vision (and, correspondingly, any other mental processes) can be assessed analytically, by investigating neural responses to simplified visual stimulation in isolation. Experiments were and still are often conducted in artificial settings with movement-restricted subjects that fixate spots on the screen and perform tasks upon visual presentations on a trial-by-trial basis. In these settings, periods with movements indicating task-specific responses are usually discarded from the analysis.

On the upside, these procedures have allowed studying mental processes within the technical and methodological constraints of the time. In particular, since signal distortions of neurophysiological measurements through movements are substantial, excluding movements from the experimental analysis has helped to prevent these kinds of artifacts (cf. Talsma and Woldorff, 2005). Importantly, however, real-world behavior unfolds in a complex and dynamic environment that constantly involves active processes such as eye movements, working memory, information selection mechanisms, decision making, and action control. These processes often work interactively and in parallel and rely on internal and spontaneous action selection mechanisms (Cisek and Kalaska, 2010). Therefore, isolating single mental functions through artificial experimental settings will not be sufficient for understanding the full complexity of real-world goal-driven behavior.

Instead, it is our opinion that the neurosciences will have to move from passive and artificial stimulation towards research paradigms that investigate behavior in increasingly natural settings that mirror everyday situations. These settings require that subjects are able to move unrestrictedly and spontaneously. An important first step towards this paradigm is allowing the subjects to move their eyes, when

investigating underlying neural dynamics.

Two key approaches for studying these possibly fast neural dynamics in the human brain are electroencephalography (EEG) and magnetoencephalography (MEG). These techniques allow non-invasive recordings across the whole cortex and with high temporal resolution. However, they are highly susceptible for ocular artifacts arising from eye and eyelid movements that mask underlying neural signals. Consequently, separating cerebral from artifactual sources is a significant challenge impeding neuroscientific investigation of real-world human behavior.

The primary goal of this thesis is to study the electrophysiological signatures of active human vision. To this end we first address methodological problems related to eye movement artifacts in EEG and MEG. Subsequently, we investigate oscillatory cortical control mechanisms that are associated with the planning and execution of saccades, as well as subsequent re-fixation. Finally, we proceed towards the investigation of spectral signatures associated with intentional action selection of saccade targets, a key process in real-world goal-oriented behavior.

In detail, this thesis is organized as follows: Within the introductory chapter, we demonstrate the importance of evolving current movement-restricted paradigms towards action-oriented paradigms: First, we report on illustrative neuroscientific evidence suggesting that visual sensation and action are causally linked and that visual perception is a constructive process based on actions (Section 1.1). Second, we incorporate this idea in the larger context of action-oriented accounts on mental processes that argue for holistic investigations of any cognitive phenomena by taking their embodied nature and action-dependence into account (Section 1.2). Sections 1.1 and 1.2 are not a pre-requisite in order to understand the thesis but provide a general subsumption into the field of cognitive science and neuroscience. Subsequently in Section 1.3, we introduce the specific scientific background of the experimental work in this thesis and refer to the contributions that this thesis provides to the field.

Following the general introduction we present the experimental work itself. Section 2 describes a procedure for investigating saccade related potentials (SRPs) during active vision. The presented project includes an MEG experiment for applied ocular artifact cleaning, which has been the author's (Christine Carl) contribution and which is therefore focussed on when discussing this project in the thesis. In Section 3, we provide a characterization of the saccadic spike artifact in MEG, an ocular artifact that has previously been investigated extensively in EEG only. In Section

4, we present work that investigates the spectral signatures of saccade control and target selection. The concluding general discussion in Section 5 holds a summary of the results and offers an outlook on future directions of the field of active vision.

1.1 Active Vision

In this section, we would like to motivate that eye movements are not only an omnipresent and essential aspect of human real-world behavior but might also be linked to vision in a more fundamental manner than is immediately apparent. In addition to being a subject of interest in itself, studying the neural correlates of eye movements and saccade selection is therefore relevant for understanding vision and real-world behavior in general.

Due to the anatomical structure of the human body and, in particular, the inhomogeneous sensor distribution in the retina, human vision captures only a fraction of the environment at any given time. In order to alleviate this circumstance and provide increased visual access to the environment, humans employ fast movements of the eye, termed saccades, that drastically change gaze position multiple times per second[1]. Eye movements occur during sleep and with eyes closed. Even while attempting to fixate a target for a prolonged time, small saccades, termed microsaccades, occur every $1-2$ times per second (Martinez-Conde et al., 2013)[2].

This omnipresence of eye movements suggests that they are a substantial component of vision in general. Neurophysiological studies indicate that vision critically depends on temporal modulation for optimal stimulation (Arend, 1973, Ditchburn and Ginsborg, 1952, Kelly, 1981, Yarbus, 1957). Eye movements are one source of this temporal change. Some researchers have suggested that saccades and microsaccades in particular counteract a fading of vision resulting from prolonged fixation due to adaptation mechanisms of sensory neurons (Martinez-Conde et al., 2006, McCamy et al., 2012, for a review see also Martinez-Conde et al., 2013).

Apart from their fundamental role in visual perception, eye movements subserve behavior by selecting and emphasizing information out of the vast amount of possi-

[1] In this thesis, we focus on saccadic eye movements, although other types of eye movements exist such as smooth pursuit, tremor, and drift.

[2] Recent evidence suggests that fixational vision and saccades form a continuum and should not be seen as two opposing states (Otero-Millan et al., 2013). This is supported by evidence suggesting a common generator for micro- and regular saccades (cf. Martinez-Conde et al., 2013, for a review).

ble visual input from the world. By initiating systematic patterns of eye and head movements, humans actively sample the visual scene (Schumann et al., 2008), a process that we here refer to as active sensing (modality indifferent) or more specifically active vision (Maldonado et al., 2009, Schroeder et al., 2010)[3]. The temporally discrete sampling of saccadic vision in particular seems to be an optimal strategy for acquiring information. This assumption is supported by anecdotal evidence from a patient suffering from extraocular muscular fibrosis: Unable to move the eyes, the patient showed head movements with spatio-temporal dynamics strikingly similar to those of saccades from healthy controls. These head movements seemed to ensure surprisingly normal perception (Gilchrist et al., 1997, 1998).

This active sensing seems to select information for guiding future actions. It is long known that the spatial and temporal distribution of eye movements and fixations correlate with attentional attribution and other cognitive aspects in favor of achieving specific goals (Buswell, 1935, Kowler, 1990, Yarbus, 1967/1965). This becomes evident, for example, by the fact that selected fixation positions usually fall on task relevant objects (Hayhoe et al., 2003, Land et al., 1999) or anticipate relevant locations for actions (Land, 2006, Pelz and Canosa, 2001). Also, attentional processes that enhance input relevant for behavioral goals at the expense of other distractions usually go together with overt active sensing in real-world behavior (Schroeder et al., 2010). Both processes are mediated partly by the same networks (Corbetta et al., 1998, Kustov and Robinson, 1996) and many studies report evidence that suggests attentional allocation as a planned but not executed movement (Craighero et al., 2001, Moore and Armstrong, 2003, Moore and Fallah, 2001), thereby arguing in favor of the premotor theory of attention (Rizzolatti et al., 1987). Even microsaccades during fixations are modulated in occurrence, amplitude and direction by visual stimulation or cognitive and attentional factors (Engbert and Kliegl, 2003, Hafed and Clark, 2002, Valsecchi and Turatto, 2008, Yuval-Greenberg et al., 2008). Because of these tight correlations to cognitive functions, eye movements have been considered as a window of the mind (e.g., van Gompel et al., 2007) and viewing behavior has served as a surrogate for revealing underlying cognitive processes.

Additionally, behavioral studies in humans have shown evidence for the causal effect of eye movements on visual experience (e.g., Hafed and Krauzlis, 2006). Study-

[3]This term is mainly used in the field of robotics, but we think it is appropriate here in order to emphasize the role of motor sampling routines for vision.

ing ambiguous line drawings, Kietzmann et al. (2011) could demonstrate that eye movements prior to conscious precept of an object causally influence what humans perceive. Furthermore, later fixation positions were chosen in favor of this initial percept. In these studies, action precedes perception – an observation that is at odds with the majority of neuroscientific studies in which the experimental paradigm already imposes a fixed sequence of sensation, cognition and subsequent motor response.

From these observations, we can conclude two practical implications for neuroscientific research in general. First, the omnipresence of eye movements and their systematical modulation in combination with other mental processes make eye movements a concern in any investigation about the human brain even if one is not interested in eye movements themselves. More specifically, even if subjects are instructed to fixate, small fixational eye movements occur and may covary with experimental manipulations, thus, inevitably confounding measurements. For electrophysiological recordings, this impact is especially detrimental because of artifactual signal distortions produced by eye movements (see Section 1.3.1). Second, these observations show that active vision is a critical part of real-world goal-oriented behavior. This is not reflected in most current scientific paradigms in which subjects are passively stimulated and are allowed motor responses only at the end of a trial according to task instructions. Real-world behavior will probably only be understood in its entirety if we move away from these restricted paradigms towards settings that allow for active vision. Critically, assessing the neural correlates of such active processes requires the characterization of cortical mechanisms associated with eye movements.

In the following, we go a step further and argue that vision and related mental processes are inherently active and might be inseparable from action. There exists a large body of neuroscientific evidence supporting the hypothesis that perception is grounded in action (cf. Engel et al., 2013, for a review on action-oriented paradigms), meaning that perception arises from learning the laws of sensorimotor interactions and dependencies in order to predict future movement related changes and guide behavior. Consequently, studying vision and its neural correlates without considering motor components poses the danger of disregarding the fundamental nature of visual perception. In the following, we report illustrative examples from the neuroscientific literature that suggest such tight and possibly inseparable linkage between action and perception.

If perception results from learning sensorimotor contingencies, the development

of perceptual capacities should strongly depend on the ability to move. Indeed, many neuroscientific studies have shown that the development of perceptual skills, sensorimotor adaptations, and neuroplasticity critically depends on active exploration in order to learn sensorimotor interactions for action guidance. An influential study by Held and Hein (1963) proved that kittens showed defective development in visually guided behavior if they were deprived of self-produced movements but otherwise received the same visual input as an actively moving control group. Another example comes from studies in non-human primates investigating changes in receptive fields based on active tool use. Visual receptive fields in intraparietal visuo-tactile neurons of these primates usually covering the hand or the arm were shown to enlarge in order to include the tool or the newly accessible space resulting from its use. Critically, this modification only took place if the monkeys were allowed to intentionally use the tool for food retrieval. Passive holding of the tool did not produce any adaptation (Iriki et al., 1996). In humans, experiments of sensory substitution have investigated perceptual learning by translating visual input from a camera to tactile or auditory stimulation (Amedi et al., 2007, Bach-y Rita et al., 1969, 2003). After active exploration with the translating device subjects reported having visual-like experiences. Again, learning to predict the dependencies between active manipulation of the camera and resulting changes in the sensory input were necessary for developing this experience (Bach-y Rita, 1972, 1984).

The above-mentioned examples demonstrate that abilities for active modification of sensory input and learning the laws of sensorimotor interactions are critical for sensorimotor adaptation and perceptual development. This interdependence of sensation and action in learning results in neuronal activity patterns that often change drastically with behavioral context. In particular, neuronal responses to identical visual stimulation are often different in moving compared to passively stimulated animals. For example, responses of motion-processing interneurons in the visual cortex of Drosophila melanogaster double as soon as the animal flies in comparison to responses during rest (Maimon et al., 2010). In monkeys, rhythmic theta band activity in the hippocampus, a cerebral structure that is crucial for memory consolidation, is modulated by saccadic exploration through phase resetting (Jutras et al., 2013). This modulation might contribute to optimal conditions for stimulus encoding. A drop in performance in an object discrimination and recognition task when preventing eye movements during learning supports this assumption in humans (Nazir and O'Regan, 1990).

Eye movements, in particular, influence visual processing throughout the cortex. In order to differentiate self-movement related changes from sensory changes induced by the environment, corollary discharges from movement related regions initiate predictive and modulatory processes in sensory areas (for a review see Crapse and Sommer, 2008). Consistently, pre- and perisaccadic suppressions of visual responses (e.g., Sylvester et al., 2005, Watson and Krekelberg, 2009, Wurtz, 2008)[4] as well as predictive remapping[5] and postsaccadic enhancements of visual responses (e.g., Dorr and Bex, 2013, Duhamel et al., 1992, Ibbotson et al., 2008, Ito et al., 2011, Merriam et al., 2003, Nakamura and Colby, 2002, Rajkai et al., 2008) have been observed throughout the visual pathway in brains of humans and other primates (for a review see Ibbotson and Krekelberg, 2011, Martinez-Conde et al., 2013).

We conclude from this evidence that changes in neural activity due to movements are not restricted to areas that are primarily involved in motor control. Rather, action related activity modulates almost all stages of visual processing in the brain (cf. Engel et al., 2013, Hafed and Krauzlis, 2006).

On the single neuron level, sensory and motor processes are so closely intertwined in some parietal and premotor areas of the monkey brain that these neurons' activities are hard to attribute exclusively to motor or perceptual functions. For example, in anti-saccade tasks, where a saccade is performed in the opposite direction to an appearing visual stimulus, single neurons in lateral intraparietal area (LIP) seem to switch between sensory and motor related functions (Zhang and Barash, 2000). The group of Rizolatti and colleagues reported that mirror cells in premotor cortex, a region previously assumed to be purely motor related, did not only fire when an action is executed but also when it is visually observed in another individual (di Pellegrino et al., 1992, for a review see Casile, 2013). As reviewed in Lebedev and Wise (2002), on the neural population level, most higher brain areas of primates cannot be functionally specified to solely visuomotor or perceptual functions, but participate in both, arguing against a functionally modularized brain structure in space.

To summarize, the presented evidence shows widespread and multi-level action-modulation and action-dependence of perceptual activity, suggesting that vision is

[4]Some studies have questioned an extra-retinal movement induced suppression of visual activity during the saccade (e.g., Dorr and Bex, 2013).

[5]Predictive remapping refers to the phenomenon that some cells in retinotopically organized brain areas increase activity in anticipation of a saccade that will bring stimuli in their receptive fields.

fundamentally grounded in action. Furthermore, evidence suggests that processes are inherently distributed and cannot easily be separated in solely sensory, cognitive or motor related modules. All these phenomena imply that studying vision without allowing eye movements will result in studying a perceptual system that is different from the one that occurs under real-world behavior. As O'Regan and Noë (2001, p.947) stated: "Seeing involves testing the changes that occur through eye, body, and attention movements. Seeing without such movements is ... a subspecies of seeing: an exception." Therefore, it is questionable how many of the experimental results from movement-restricted paradigms can be readily transferred to settings involving real-world active behavior. Conclusively, we have to begin studying the neurophysiological correlates of eye movements and associated processes that occur under active vision.

1.2 Embodied Accounts of Cognition and Perception

In this section, we would like to embed the active and ecological view on vision presented in Section 1.1 in the context of cognitive science. Embodied or action-oriented accounts of cognition[6] are increasingly gaining support in the cognitive science community. It is our belief that active vision is an important component and starting point of this new research agenda, which motivates a brief outline of these embodied views here[7].

Before the rise of action-oriented views on cognition, cognitive science was founded on a computational metaphor (Fodor, 1981, 2000, Marr, 1982, Newell and Simon, 1963/1961, Newell and Simon, 1972) where cognition is seen as abstract, rule-based computation on symbolic mental representations within the brain. According to this view, cognition can be fully understood by focusing on the organism's internal mental processes. Sensations and motor control are considered to be merely peripheral inputs and outputs of the system and are thus separated from cognition. Departing from this classical representationalist view, assumptions of a modular brain with separate perceptual, cognitive, and motor units that operate in a serial manner have been inherent to many studies in the field of neurosciences (cf. Cisek and Kalaska, 2010, for a comprehensive description of the impact of the representationalist view on the scientific practice in psychology and neuroscience).

In the context of visual neuroscience, this has led to research paradigms that treat subjects as passive observers merely retrieving and representing information

[6]Depending of the specific conceptions, various terms have been employed to describe these paradigms besides *embodied* cognition (e.g., Clark, 1999, Shapiro, 2011, Varela et al., 1993), among them *enactive* (Varela et al., 1993) and *grounded* (Barsalou, 2008) cognition. Others have emphasized the *distributed* (Barrett, 2011) or situated (Clancey, 1997) nature of cognition. Engel et al. (2013) has employed the term action-oriented views on cognitive science to subsume different embodied accounts on cognition. While terms are not consistently used throughout the literature and *action-oriented* accounts on cognition are diverse, most conceptions assume embodiment as a necessary part of cognition. Therefore, we use the term *embodied cognition* in the following in order to refer to all approaches that base cognition within the context of an active organism's sensorimotor capacities and the resulting unique interactions within its specific environment.

[7]For the sake of brevity, this chapter does not aim at an extensive description of the different and often divergent and still developing theories within the field of embodied cognition or their philosophical implications (see e.g., Engel, 2010, Shapiro, 2011, Wilson, 2002, for reviews on different concepts). While the experimental work that we present later on contributes to realizing action-based paradigms in the future, it is not primarily designed to argue in favor of a particular embodied approach.

about pre-given features in the world as presented to their sensors. Inherent in the classical representationalist account on perception is the assumption that perception is flawed, in the sense that sensors only capture a fraction of the reality of the outside world. The brain – seen as the only problem-solving device available to cognitive agents – has to solve tasks and produce intelligent behavior solely based on this incomplete sensor information. According to the representationalist view this is achieved by internal cognitive representations stored in the neural structures that reconstruct the real world in a mirror-like version (cf. Marr, 1982). The experience of seeing then directly arises from the activation of these internal representations.

The classical representationalist view has led to several important insights regarding neural mechanisms of the brain. These insights primarily resulted from analytical decomposition of complex real-world and interactive behavior into small controllable units that could be separated from presumed confounding factors and thus investigated for their neural correlates. However, even without relating to the various critical arguments coming from embodied accounts on cognition[8], is should be evident that these restrictive paradigms are very far from ecologically relevant goal-oriented behavior. For example, until today, neurophysiological recordings in humans usually require the subject to refrain from eye movements and blinks during visual stimulation. Given the prominence of eye movements in real-world behavior and the close relation of eye movement to other mental functions (see Section 1.1), it is especially undesirable that even such minimal way of active behavior is prevented.

In contrast to this prevalent research practice of the past century, arguments for an active and constructive account on perception, in particular on vision, have been raised for a long time and started long before the recent rise of embodied approaches to cognition (e.g., Dewey, 1896, Gibson, 1966, 1979, Merleau-Ponty, 1963/1942, von Helmholtz, 1867, pp.442ff.). Gibson (1966, 1979) has claimed that humans have a direct and high quality access to the world by active sensing using the ability to move eyes, head and body. Consequently, he has argued that in order to perceive and act upon the world humans do not need realistic and complete internal representation of the environment but can obtain information whenever needed by directly probing the world as best and veridical source of knowledge (see also Noë, 2005, O'Regan and Noë, 2001 for a more recent elaboration on active perception)[9]. The evidence of

[8]Among them is, for example, the symbol-grounding problem (Harnad, 1990, Searle, 1980), which, in short, asks how the symbolic representations in the brain acquire meaning.

[9]Indeed, eye movement studies have shown that observers acquire the information they need

a tight coupling between perception and action and the goal-orientedness of active sensing as reviewed in the last section seems to support this assumption from the neuroscientific side.

With this direct and goal-driven perceptual access to the environment via actions, internal knowledge and mirror-like internal representations of the world that are disconnected from sensorimotor processes loose their primary role in cognition and problem solving. Instead, resources distributed over environment, body, and brain may participate in cognition and remove the brain from its island position of being the only and isolated structure able to generate intelligent behavior (Barrett, 2010, 2011).

Within this line of thinking, a shift in paradigm has started in the different cognitive sub-disciplines in the last decades towards more action-oriented accounts on mental processes (e.g., Agre, 1997, Ballard et al., 1997, Cisek and Kalaska, 2010, Clark, 1997, Noë, 2005, Pulvermüller and Fadiga, 2010, Thelen et al., 2001, Varela et al., 1993, see Engel, 2010, for a recent review of this *pragmatic* turn). These accounts describe cognition to result from the real-time goal-directed exploration within the world. It is by actively exercising movements that organisms develop an understanding of the lawful relationship between sensory changes and own actions and learn about their sensorimotor capacities within the bodily and environmental constraints and possibilities. These sensorimotor experiences have been suggested to be a first essential step for developing more complex cognitive capabilities like object categorization (cf. Beauchamp and Martin, 2007, Maye and Engel, 2011). While there exist different theories on action-oriented accounts to cognition, most different conceptions claim that embodiment is a crucial part for developing cognition. An often-cited quote that explains this central claim originates from Esther Thelen:

> *To say that cognition is embodied means that it arises from bodily interactions with the world. From this point of view, cognition depends on the kinds of experiences that come from having a body with particular perceptual and motor capabilities that are inseparably linked and that together form the matrix within which reasoning, memory, emotion, language, and all other aspects of mental life are meshed.*
> –Thelen et al. (2001, p.1)

A well-known example that illustrates the full explanatory power of embodied

just-in-time when the information is required for the behavioral task (Ballard et al., 1995).

accounts on intelligent behavior is the outfielder problem (see Wilson and Golonka, 2013, for a detailed description). How does a baseball outfielder catch a highflying ball? Classical representationalist accounts on this problem suggested that, based on the initially perceived flying parameters of the ball, a simulation about the balls motion is computed in the outfielder's brain in order to predict the ball's landing position (Saxberg, 1987a,b). However, given the initially perceived information of the very distant ball, it was shown that such a prediction is highly error prone and probably not the way, the task is solved (Shaffer and McBeath, 2005). In contrast, the embodied solutions to the problem rely on the kinematics of the ball perceived by the outfielder in constant interaction with his own movements: One solution suggests that the outfielder will align his running path with the ball so that in appears to move with constant velocity (Chapman, 1968, Fink et al., 2009). The second solution assumes that the fielder will move in a way so that the ball appears to fly in a straight line (McBeath et al., 1995). Evidence suggests that both strategies are indeed used in real-time behavior depending on the position of the fielder (Fink et al., 2009, McBeath et al., 1995). Both solutions show that optimizing through action the moment-to-moment relationship between perceptional information of the flying ball and the outfielder can replace an internal complex computation of the ball's flying trajectory within the outfielder's brain[10].

Radical approaches to embodied cognition deny any representation of the outside world in the brain. Instead, these accounts claim that most abstract cognitive concepts like language acquisition or mental calculation arise from the organism's sensorimotor activities and interactions with its environment. Based on this view, a living organism constructs or enacts a world by generating action relevant structures (Varela et al., 1993). Other conceptions of embodied cognition suggest action-oriented (Clark, 1997, 1999) representations that incorporate context sensitive and action-related information. The sensorimotor contingency theory assumes that the knowledge and mastery of the rules of sensory transformation according to motor actions constitutes cognition (O'Regan and Noë, 2001). According to this view, the role of the brain in visual perception is to "enable the knowledge and exercise of sensorimotor contingencies. Seeing ... is constituted by the brain's present attunement to the changes that would occur as a consequence of an action on the part

[10]Barrett (2011) describes in her book other various compelling examples of embodied cognition from the animal kingdom that demonstrate how intelligent behavior can arise based on bodily design and coevolution even under conditions of limited computational capacity of the brain.

of the perceiver" (O'Regan and Noë, 2001, p.968). Despite their variety, all these concepts of embodied cognition call for studying mental processes of an organism in a dynamic and ecologically valid context that takes into account the relationship between body, mind, and environment in real-time goal-oriented behavior[11]. Apart from developing suitable experimental paradigms, action-oriented accounts require rethinking the role of neural activity in generating intelligent behavior. Instead of studying neural activity as implementation of internal representations, neural patterns need to be understood as being primarily determined by their functions to guide action in a situated and behaviorally relevant manner (cf. Engel et al., 2013).

Assuming that cognition is a distributed process emerging from real time interactive behavior probably implies distributed as well as non-linear dynamics on the neural level and questions a classical separation of the brain into functional and often serially operating modules (cf. Cisek and Kalaska, 2010, Engel, 2010, Flusberg et al., 2010, Fox and Friston, 2012, Maldonado, 2007, Rohde, 2010, pp.36f.). In particular, neural activity underlying action guidance is most likely organized in flexible networks of tightly coupled sensorimotor processes interacting with memory processing and intentional states important for action guidance (cf. Engel et al., 2013).

How do these fast changing and distributed neuronal networks arise? More specifically, how are interactions between brain areas established in a flexible and yet highly specific way? Coherent oscillatory activities especially in the gamma range have been suggested to enhance both inter- and intra-areal communication by inducing non-linear increases in input gain in downstream neurons (Salinas and Sejnowski, 2001, Womelsdorf et al., 2007). This makes frequency specific correlated oscillations a key candidate for dynamically setting up distributed networks of neural assemblies with possibly large-scale interaction between areas (Engel et al., 2001, Fries, 2005, see also Fries, 2009, Maldonado, 2007, Siegel et al., 2012). Hence, Engel (2010) suggests that these dynamic oscillatory patterns might, on the neural side, contribute to implementing the procedural knowledge of the lawful interaction in sensorimotor couplings.

Entrainment of sensory oscillatory activity to the rhythmicity of active sampling mechanisms further highlights the importance of oscillatory activity in active exploratory behavior (Schroeder et al., 2010). During active viewing, saccades occur

[11] See Wilson and Golonka (2013) on an elaborate suggestion for a radical turn in experimental paradigms that we clearly not pursuit in this thesis.

with an average frequency of 3 Hz. Corollary discharges that inform sensory areas about each performed eye movement seem to modulate ongoing oscillations in visual areas in human (Ossandón et al., 2010) and non-human primates (Bartlett et al., 2011, Rajkai et al., 2008). This motor related information seems to prepare visual areas for the temporal pattern of visual input by establishing a coupling between sensory and motor rhythms. Even during fixation, microsaccades impose a similar rhythm in visual processing and modulate synchronized gamma band activity (Bosman et al., 2009).

In order to assess such oscillatory neural signatures that are part of human active behavior in real-time, neurophysiological measures are required that can resolve fast and distributed dynamics across the cortex. MEG and EEG provide non-invasive measurements of neural population activity across the whole cortex and allow assessing spectral signatures of fast dynamics. Since both technologies face methodological problems induced by movement artifacts (see Section 1.3.1), studying active movements in general and eye movements in particular is currently rare in scientific practice.

To summarize, the pragmatic turn in cognitive science questions whether we can understand the actual nature of mental processes without studying active real-world behavior in a holistic way by taking into account the dynamic, situated, and embodied nature of cognition. This approach calls for new methods and paradigms in the field of neuroscience that allow unrestrictive dynamic behavior like free viewing. If methodological problems concerning movement artifacts can be overcome, MEG and EEG are optimal measurement methods to investigate these paradigms due to their ability to access the probably distributed and fast dynamics of active behavior.

1.3 Neurophysiological Recordings of Active Vision

As detailed in previous sections, allowing free eye movements as well as studying the underlying neural correlates of these movements is an important aspect of research paradigms that investigate human real-world behavior. A first step into this direction is to investigate the cortical dynamics of saccade control and target selection mechanisms, which underlie each free viewing behavior. This is the aim of the thesis. However, artifacts induced by eye movements still pose serious prob-

lems for investigating the neurophysiological signatures during eye movements in humans. Therefore, the first part of the thesis contributes to a better understanding and handling of these artifacts. Subsequently, we investigate cortical signatures of active vision and target selection during a delayed saccade task. We assess the oscillatory population dynamics of planning and execution of saccades as well as internal mechanisms of target selection across a wide range of frequencies and across the cortex. By investigating saccade related sensorimotor activities in the cortex we provide the foundation for studying real-world free viewing behavior in humans.

In the following sections, we introduce the neuroscientific background and our contributions to the fields of ocular artifacts (Section 1.3.1) and neural signatures of active vision (Section 1.3.2).

1.3.1 Ocular Artifacts

When studying the physiology of free viewing behavior with MEG or EEG, potential or field changes we measure during movements of the eyes do not solely origin from underlying brain activities but also from non-cerebral sources related to the motion itself. These so-called ocular artifacts arise from eye and eyelid movements, as well as from associated muscle activity. The amplitude of the potential or field change of these ocular artifacts can be orders of magnitude higher than the signal of interest, thus yielding small signal-to-noise ratios for investigating underlying neural processes (Fatima et al., 2013, Talsma and Woldorff, 2005). Consequently, ocular artifacts lead to experimental confounds that mask the neural signals that the experiment was originally designed to measure. Separating these artifacts from cerebral sources out of the mixed sensor data is therefore a major challenge for EEG/MEG investigations.

1.3.1.1 Types of ocular artifacts

There are at least three types of ocular artifacts with distinct underlying mechanisms and significant impact on neurophysiological measurements. These are the corneo-retinal artifact, the eyelid artifact, and the saccadic spike artifact (for a comprehensive review on these artifacts see Plöchl et al., 2012). We shortly introduce these artifacts in the following.

The *corneo-retinal* artifact is a prominent offset in potential or field strength of the EEG or MEG, respectively. The artifact is caused by eye movements and

arises from the rotation of the eyeballs. Between cornea and retina resides a potential difference that can be described by an equivalent dipole in the optic axis of the eyeball with a positively charged cornea relative to the retina (Mowrer et al., 1935, cf. also Arden and Constable, 2006, Pasik et al., 1965 on details about the physiological causes of this dipole). Following the direction of gaze, this dipole alters its orientation and hereby produces changes in the electrical potential at the periorbital surface. These changes depend on the amplitude and direction of the eye movement as well as on alterations in light intensity (Malmivuo and Plonsey, 1995, pp.440-442).

The *eyelid* artifact, occurring when the eyelid slides over the eyeballs, is mostly elicited during blinks and in association with upward saccades (Barry and Jones, 1965, Lins et al., 1993a,b, Picton et al., 2000a, Plöchl et al., 2012). Eyelid movements change the geometry of the volume conductor, so that the eyelid acts as a sliding electrode that short circuits the positively charged cornea to the surrounding skin, producing a current upwards to the forehead (Antervo et al., 1985, Barry and Jones, 1965, Lins et al., 1993b, Matsuo et al., 1975).

The *saccadic spike* artifact, a transient deviation in voltage, reflects the cumulative, synchronized activity of recruited motor units of the extraocular muscles when initiating saccades (Boylan and Doig, 1989b, Kovach et al., 2011, Moster and Goldberg, 1990, Riemslag et al., 1988, Thickbroom and Mastaglia, 1985, Yuval-Greenberg et al., 2008). Its appearance changes with direction, and amplitude of the movement (Carl et al., 2012, Keren et al., 2010a, Kovach et al., 2011), or the initial position of the eye (Plöchl et al., 2012). This artifact can have prominent effects on the EEG/MEG signal even during fixations since also microsaccades produce a saccadic spike artifact that induces transient high frequency distortions from roughly 30 to 120 Hz (Jerbi et al., 2009, Yuval-Greenberg et al., 2008).

1.3.1.2 Practical implications for neurophysiological experiments

A diligent handling of the ocular artifacts is important for a number of reasons: The low signal-to-noise ratio of artifact contaminated data goes in hand with usually small effect sizes of the experimental contrasts of interest. Consequently, true effects might be hidden due to the artifact induced high variance of the data. More importantly, systematic changes of artifact occurrence can seriously distort statistical analysis so that signal cancellation hides true experimental effects (Hipp and

Siegel, 2013) or apparently significant effects result from eye movements rather than the experimental contrast of interest (Hillyard and Galambos, 1970, Low et al., 1966, Yuval-Greenberg et al., 2008). Indeed, eye movements and associated artifacts often co-vary with experimental conditions. This is even true for periods where subjects are required to fixate: The rate and metrics of microsaccades, which occur on average $1-2$ times per second during fixations (Martinez-Conde et al., 2013), is modulated by visual and auditory stimulation (Engbert and Kliegl, 2003, Hipp and Siegel, 2013, Rolfs et al., 2008) and other cognitive factors like shifts in spatial attention (Engbert and Kliegl, 2003, Hafed and Clark, 2002, Laubrock et al., 2005) and working memory (Valsecchi et al., 2007). Similarly, the occurrence of blinks is linked to attentional processes and cognitive load (Oh et al., 2012, Siegle et al., 2008, Smilek et al., 2010), or social communication (Nakano and Kitazawa, 2010).

Ocular artifacts may be considered in the analysis by approaches with varying complexity. A basic strategy for dealing with these artifacts consists of simply rejecting all contaminated data periods. When investigating active vision and perisaccadic neuronal signatures, this is infeasible since rejecting data implies loosing the signal of interest. However, because eye movements are present even during fixations and may correlate with experimental factors, selecting and rejecting periods containing artifacts may in any case introduce bias in data selection and thus influence the experimental contrast of interest.

A more advanced method for controlling the effects of ocular artifacts is to closely monitor their occurrence, directions, and amplitudes with the help of an eye tracker or the electrooculogram (EOG) (cf. Keren et al., 2010a). This procedure allows for additional analyses of artifact statistics, which may uncover possible systematic effects of ocular artifacts on the experimental results.

Last, several analysis approaches have been published that aim to reduce the amount of the artifactual signal within the data. These cleaning procedures try to separate the artifact from the cerebral sources. Since the true distribution of artifactual and cerebral sources is generally unknown, an objective evaluation of cleaning methods is difficult. Still, results suggest that, so far, no cleaning procedure is able to perfectly separate cortical from artifactual signals in all situations (Keren et al., 2010a, Nottage, 2010, Shackman et al., 2010). Despite these drawbacks, artifact cleaning is a common and useful analysis procedure for neuroscientific investigations and we present the most applied approaches in the next section.

Finally, we note that appropriate source localization techniques can mitigate

the detrimental impact of eye movements on measurements (Hipp and Siegel, 2013, see also Section 3). However, even analysis in source space does not completely prevent contamination by artifacts especially in frontal and temporal sources (Carl et al., 2012, Fatima et al., 2013). Therefore, source localization techniques may be considered additions rather than alternatives to artifact cleaning.

Irrespective of the specific approach chosen for handling ocular artifacts, spatial, spectral, and temporal characteristics of the ocular artifacts have to be known in order to identify systematic contamination (in case the artifacts have not been removed at all) or possibly remaining contamination (in case artifact cleaning has been used). While details about the characteristics of the presented artifacts are known in EEG, the appearance of the saccadic spike artifact in MEG has not yet been addressed in the literature.

1.3.1.3 Procedures for cleaning the ocular artifact in MEG and EEG

Several different approaches exist for the cleaning of ocular artifacts. Among them are EOG based linear least square regression (Croft and Barry, 2000b, Elbert et al., 1985, Gratton, 1998, Schlögl et al., 2007), blind source separation techniques like independent component analysis (ICA) (Hyvärinen and Oja, 2000, Jung et al., 2000b) or principal component analysis (Ille et al., 2002, Lins et al., 1993b), dipole modeling (Berg and Scherg, 1991, Lins et al., 1993b), as well as methods based on a Bayesian estimation (Fujiwara et al., 2009, Kierkels et al., 2007). We here focus on EOG based linear least square regression and ICA since these approaches are among the most frequently used in the literature and their performance has been extensively evaluated.

Cleaning based of the EOG signals exploits the fact that the EOG depicts potential changes next to the eye and is therefore dominated by changes resuming from eye movements. By volume conduction, these potential changes are propagated across the skull and diminish with increasing distance to the eye. Consequently, eye movement related signals are measured to different degrees by the MEG/EEG electrodes. Given that electromagnetical signal propagation in the head can be considered to be linear and instantaneous (i.e., without a delay between sensors; Nunez and Srinivasan, 2006), ocular artifacts within MEG/EEG signals can be removed by subtracting the properly weighted EOG from the MEG/EEG. This way, any activity in the MEG/EEG that is correlated with the EOG as a measure of the artifact will

be eliminated.

Often bipolar EOG electrodes capturing horizontal and vertical potential differences (measured as difference between supra- and infra-orbital or left and right EOG recordings, respectively) are used as a measure of the corneo-retinal dipole rotations for saccades covering all directions. Regression coefficients are then derived according to the model:

$$EEG(t) = S(t) + \beta_1 vEOG(t) + \beta_2 hEOG(t) \tag{1.1}$$

with $S(t)$ being the potential difference of underlying true cerebral sources at any measured point in time t, EEG being the measured EEG (or MEG) signal, $vEOG$ and $hEOG$ being the vertical and horizontal EOG, respectively, and β_1 and β_2 being the regression coefficients.

EOG regression provides some important benefits. First, the cleaning procedure is both, fast and automatic. Second, the regression coefficients can be derived from a relatively small dataset. Third, the coefficient can be applied to any number of MEG or EEG channels. Hence, small amounts of experimental data or only few measured EEG/MEG channels argue for EOG based regression (cf. Hoffmann and Falkenstein, 2008).

Several variants of this approach exist that employ different electrode montages of the EOG or exploit event related data for estimation of coefficients (see Croft et al., 2005). Dependent on the spatial arrangement and referencing of the EOG, different ocular artifacts may be preferentially depicted by the EOG and can consequently be subtracted from the EEG/MEG signal. Removal of the saccadic spike artifact with an EOG based regression, for instance, requires an axial EOG component with reference to posterior electrodes for optimal results (usually referred to as radial EOG (REOG) component, cf. Plöchl et al., 2012).

Various studies have compared EOG regression to other cleaning methods such as ICA (Hoffmann and Falkenstein, 2008, Plöchl et al., 2012, Wallstrom et al., 2004) or have evaluated the relative performance of different regression approaches (Croft et al., 2005, Pham et al., 2011, Plöchl et al., 2012), yielding somewhat contradictory conclusions. A recent study suggests that using EOG regression is problematic if all ocular artifacts are cleaned simultaneously (Plöchl et al., 2012). It may, however, be feasible for removing only the corneo-retinal or eye lid artifact.

Another common approach for artifact cleaning is ICA. ICA is a data-driven ap-

proach that assumes that the multiple sensor measurements represent mixtures of mutually statistically independent sources. These sources can be of cerebral origin as well as physiological or environmental artifacts. In order to uncover the original sources, ICA aims at finding a (usually linear) transformation of the sensor data that de-mixes the measured signal into estimates of minimally dependent source signals (independent components). In the context of electrophysiological recordings, it is usually further assumed that the measured signals are an instantaneous linear mixture of the electromagnetic activity from the neuronal and artifactual sources, and that the number of sources equals (or is less than) the number of sensors. Additionally, both the source signals and the mixing process are presumably stationary. Notably, for ocular artifacts these assumptions either have been proven to be reasonably satisfied or their violation has been shown to produce only minimally detrimental effects (Debener et al., 2011, James and Hesse, 2004, Vigario and Oja, 2008, Vigario et al., 2000).

The performance of ICA depends on the choice of algorithm, the definition of training dataset, and the selection of independent components that – in case of artifact cleaning – represent the artifact.

Algorithms for ICA can be roughly differentiated into approaches that exploit higher order statistics assuming non-gaussian distributions of sources and second order methods that rely on different spectra of sources (for reviews see: James and Hesse, 2004, Vigario and Oja, 2008). As a consequence of these assumptions, which group of approaches will perform better depends on the characteristics of the data. To date, according to Delorme et al. (2012), the algorithms most commonly applied to EEG data are – from the first group – *FastICA* (Hyvärinen, 1999) and *(extended) Infomax ICA* (Bell and Sejnowski, 1995, Lee et al., 1999) and – from the second group – *Second-Order Blind Identification* (Belouchrani and Cichocki, 2000).

For a good separation of the artifact from cerebral sources, training data used for ICA should contain all cortical signals under investigation. At the same time, the proportion of the artifact that is to be be removed should be maximized in the signal. This might require special preprocessing of the data. In order to remove the saccadic spike artifact, for example, Kovach et al. (2011) improved separation by filtering the data to its characteristic frequency range. Our observations as well as those of others (Hipp and Siegel, 2013) suggest that successfully cleaning each dataset from the saccadic spike artifact may indeed require training data tailored to the specific artifact. This can result in the necessity of repeatedly applying ICA

with differently tailored training data for removing distinct artifacts (cf. Section 4 and 5).

ICA does not provide the researcher with any information about which independent component represents an artifactual source. Often components for ocular artifact rejection are selected by visual inspection based on pre-known qualities of the specific artifact, like topographic distribution, the temporal evolution of single trials or of averaged time courses, or spectral composition (e.g., Fatima et al., 2013, Hipp and Siegel, 2013, Hoffmann and Falkenstein, 2008, Keren et al., 2010a). Automatic procedures for independent component selection have been suggested (Joyce et al., 2004, Kovach et al., 2011, LeVan et al., 2006, Nolan et al., 2010) for ocular artifact cleaning, but usually do not provide a full rejection of all three major types of ocular artifacts. Recently Plöchl et al. (2012) showed that this is feasible in a fully automated way for EEG. This approach exploits additional information about eye movement occurrence using an eye tracker and selects independent components based on the relative variance of component activity during saccades and fixations.

Conclusively, selecting independent components and appropriate training datasets are not trivial, and either require a competent user or additional information. In addition, reliable ICA results are more difficult to achieve for small amounts of data (see Debener et al., 2011). Apart from these limitations, ICA has been shown to perform well as a tool for eliminating corneo-retinal and blink artifacts in EEG (Joyce et al., 2004, Jung et al., 2000b) and MEG (Barbati et al., 2004, Fatima et al., 2013, Vigario et al., 1998) and has been used extensively in practice (Vigario and Oja, 2008). Only recently, it has been shown that ICA is also appropriate for removing the saccadic spike artifact in EEG and intracranial EEG (iEEG) (Hassler et al., 2011, Hipp and Siegel, 2013, Keren et al., 2010a, Kovach et al., 2011). However, removal of this artifact has not yet been systematically investigated for MEG.

Due to the missing ground truth, objective evaluation of cleaning methods can be considered difficult. In general, cleaning procedures can either over- or under-correct the EEG/MEG signal. While under-correction results in residual artifactual signal in the cleaned data, over-correction results in loss of true cerebral sources or the addition of noise to the data. To validate performance, spectral components or event related averages of cleaned and raw data have been visualized for periods with and without eye movements, respectively (Hoffmann and Falkenstein, 2008, Plöchl et al., 2012, Schlögl et al., 2007). Ideally for such a comparison, an eye tracker yields an independent measurement in order to detect the occurrence of

eye movements (cf. Keren et al., 2010a, Kierkels et al., 2007, Plöchl et al., 2012). Alternatively, quantification of cleaning performance is based on simulated data containing artifacts (e.g., Hoffmann and Falkenstein, 2008, Kierkels et al., 2007, Ma et al., 2011).

This thesis provides contributions for better evaluating artifact cleaning and identifying artifact contamination. First, by using source reconstruction, we evaluate the cleaning based separation of artifacts from true cerebral source. Second, we characterize the saccadic spike artifact in MEG in order to allow identification of the artifact when using this technology.

1.3.1.4 Contributions of this thesis

For EOG regression analysis any potential change that is measured at the skull propagates by volume conduction to other regions. Hence, not only do we measure a mixture of cerebral and artifactual sources at the EEG electrodes, but also the EOG might depict to some degree potential changes originating from true cerebral sources (Iacono and Lykken, 1981). Consequently, it has been criticized that EOG based regression might also subtract true cerebral sources from the MEG/EEG signal (Ille et al., 2002). In Section 2 we introduce an approach based on source reconstructions to investigate the amount of loss of cerebral sources by regression analysis and show that the applied EOG based regression is not susceptible to removing true cerebral sources.

In Section 3 we provide a detailed spatial, temporal and spectral characterization of the saccadic spike artifact in MEG. While the characteristics of eyelid and corneo-retinal artifact have been examined extensively, the saccadic spike artifact has only recently recaptured awareness with the advent of frequency specific analyses of neuronal data that are prone to being contaminated by this artifact. A thorough characterization of this artifact for MEG has been missing. It has even often been assumed that MEG is not seriously affected by this kind of artifact. By providing a description of saccadic spike characteristics for MEG in Section 3, we show that this artifact seriously affects the MEG in frontal and temporal electrodes. In addition, we further investigate how adaptive source reconstructions can help to reduce the impact of this artifact.

Finally, in Section 4 we describe a cleaning procedure that combines EOG based regression with ICA for reducing saccade related artifacts in MEG in a conservative

manner. In particular, similar to previous reports on EEG data (Hassler et al., 2011, 2013, Hipp and Siegel, 2013, Keren et al., 2010a, Kovach et al., 2011), we found that ICA successfully separates an independent component representing the saccadic spike artifact also in MEG. By analyzing the cleaned signals in source space we further reduced the risk of residual artifact distortions even after cleaning.

1.3.2 Neural Signatures of Active Vision

As stated in Section 1.2, the assumption of an embodied and action-oriented nature of mental processes implies searching for their neural correlates in a holistic manner that assesses possibly fast changing and distributed dynamics of interdependent processes. Oscillatory mechanisms have been proposed as key candidates for implementing these action-based structures on the neural level, and we assume that these mechanisms likewise play an important role in the neural correlates of active vision.

Functional magnetic resonance imaging (fMRI) studies have revealed relevant cortical structures involved in eye movement control in humans (for reviews see McDowell et al., 2008, Sweeney et al., 2007). However, due to measuring blood-oxygen-level dependent (BOLD) activity, fMRI cannot reveal fast temporal dynamics associated with saccades. While studies on the neural dynamics of saccades and saccade selection mechanisms in monkey (Johnston and Everling, 2008, Kable and Glimcher, 2009) have access to fast neural dynamics, these studies are invasive and therefore not appropriate for studying the human system. In addition, low spatial coverage across the cortex and limitations to measuring single neurons with specific response patterns have prevented many studies from assessing presumably distributed neural population dynamics for active vision. Only recently, neural activities in animals have been recorded at the network level in order to reveal large-scale communication in distributed networks (e.g., Bosman et al., 2012, Rubehn et al., 2009). Consequently, MEG and EEG are to date the methods of choice for measuring the supposed distributed oscillatory population dynamics underlying active vision in humans[12].

After carefully addressing saccade induced artifact problems as outlined in the previous section, we present spectral signatures of saccadic control and saccade selection mechanisms in MEG (see Section 4). Understanding these cortical dynamics

[12]We deliberately did not mention electrocorticography here, since this method is limited to a specific patient group.

provides the foundation for revealing neural mechanisms of active vision in goal-oriented real-world settings on the system level. In the following, we introduce the background on saccadic control and saccade selection in separate subsections.

1.3.2.1 Dynamics of cortical control of saccades

It is widely accepted from monkey neurophysiology, human functional imaging, and lesion studies that cortical areas involved in saccade programming include frontal and supplementary eye fields, the parietal eye fields (known as LIP in monkeys) within the intraparietal sulcus, and dorsolateral prefrontal cortex (for reviews see Johnston and Everling, 2008, McDowell et al., 2008, Munoz and Everling, 2004). Within the cortical oculomotor network, the parietal and frontal eye fields have been attributed to spatial aspects of orienting behavior and sensorimotor transformations from stimulus encoding to motor planning of the saccade (Andersen and Cui, 2009, Medendorp et al., 2011)[13].

These fronto-parietal structures exhibit spectrally specific changes in local population dynamics associated with saccadic control. In monkeys, LIP shows direction-selective increases in rhythmic synchronization in gamma frequency range (25-90 Hz) with increases in local field potential (LFP) power, spiking activity and LFP-spike coherence when planning memory-guided saccades (Pesaran et al., 2002). Analogous observations in frequencies starting from 50 Hz on have been made in posterior parietal cortex when recording the spectral signatures of memory-guided saccades in humans measuring MEG (Buchholz et al., 2011, Medendorp et al., 2007, Van Der Werf et al., 2013, 2008, 2010).

Memory-guided delayed saccade tasks are a common paradigm for studying preparatory activity, since the neural signatures can be investigated in an artificially prolonged period of saccade planning. In these paradigms, because of the memory delay, motor preparation is tightly coupled to attentional processes and memorizing the stimulus location (for a discussion see Andersen and Cui, 2009, Medendorp et al., 2011, Van Der Werf et al., 2009). By dissociating the motor component en-

[13] Animal and fMRI studies have revealed a spatially detailed and distributed organization of the fronto-parietal structures including several distinct topographic maps reflecting spatial orienting, as well as effector-specific encoding patterns reflecting movement preparation (Gallivan et al., 2011, Pertzov et al., 2011, Silver and Kastner, 2009). Since these detailed maps do not mirror the signals that are usually encountered when studying preparatory signals of saccades in MEG or EEG, we do not decribe them in detail. Instead, we focus on evidence on oscillatory signatures of saccade preparation and execution.

coding the upcoming saccade goal during the memory delay from the initial sensory component, it could be shown that sustained local gamma band oscillations in the posterior parietal cortex are a neural correlate of the preparatory set for the upcoming saccade (Van Der Werf et al., 2008, cf. Zhang and Barash, 2000, 2004, for comparable results recording single cell firing rates in monkeys).

Accompanying these direction specific increases in gamma power, prolonged contralateral alpha band suppression was observed in posterior parietal and extrastriate areas around the lateral occipital cortex as a signature of a general regulatory mechanism, allocating resources for processing sensory information (Medendorp et al., 2007, Van Der Werf et al., 2008). Lateralization of alpha band was also shown to follow the fast dynamics of overt attention[14] in non-delayed saccades (Belyusar et al., 2013) in EEG. In addition, ongoing pre-trial phase of alpha oscillations in EEG in frontal and occipital areas predict variability in saccadic control capabilities like reaction time and performance in anti-saccade tasks (Drewes and VanRullen, 2011, Hamm et al., 2010, 2012) and might reflect fluctuations of excitability (Mathewson et al., 2011).

In parietal and occipital areas, beta band power was shown to be also suppressed with a weaker direction specificity during saccade planning and bilateral power reductions after saccade onset (Hinkley et al., 2011, Medendorp et al., 2007). Beta band power was suggested to be essential for linking sensory evidence to motor plans for upcoming movements (Gregoriou et al., 2012, Hinkley et al., 2011, Siegel et al., 2008, 2011).

There is little evidence for a direction specific enhanced gamma band activity in the frontal and supplementary eye fields during saccade preparation in humans (Lachaux et al., 2006) – although expected from their involvement in saccade generation of visually and memory-guided saccades in humans as well as monkeys (Bruce and Goldberg, 1985, Curtis and Connolly, 2008, Curtis and D'Esposito, 2006, Dias and Segraves, 1999, Prime et al., 2010, Schall et al., 2002). Gamma increases have been observed in supplementary eye fields and frontal eye fields during execution (Hinkley et al., 2011, Lachaux et al., 2006), but direction specificity is weak or absent (cf. also Kagan et al., 2010, for an fMRI study). In monkeys, direction specific spike-LFP coherence and LFP power in the beta frequency range within frontal eye

[14]The term overt attention focuses on the act of directing sense organs, e.g. by moving the eyes, towards the attended stimulus and is used in contrast to covert attention, where stimuli are mentally focussed on without movements, e.g. by maintaining eye fixation.

fields was suppressed during saccade planning in memory-guided saccades, while direction selective LFP gamma power was slightly increased in the same area (Gregoriou et al., 2012).

1.3.2.1.1 Contributions of this thesis

To circumvent problems of ocular artifacts during saccade execution, most electrophysiological studies in humans focused on the preparatory phase of saccade generation and stopped analysis before the saccade is actually executed (e.g., Brignani et al., 2010, Buchholz et al., 2011, Cordones et al., 2013, Hamm et al., 2010, 2012, Lee et al., 2011, Medendorp et al., 2007, Moon et al., 2007, Van Der Werf et al., 2008, 2010). Only recently, dynamics during saccades were investigated while carefully controlling for artifacts (e.g., Ossandón et al., 2010, Van Der Werf et al., 2013).

Conclusively, while saccade direction specific modulation in local oscillatory population activity within frontal and parietal structures has been implicated in the process of saccade planning, little is known about the spectral dynamics of the human cortical saccade network involved in eye movement execution. Further studies are needed to reveal the metric specific spectral signatures of the saccade related network during execution while carefully accounting for movement induced artifacts that can distort the oscillatory signatures (see Section 3 for an example of artifact generated changes in spectral power).

In Section 4 we examine saccade metric specific spectral signatures of the network involved in saccade generation, execution, and re-fixation in a delayed saccade task. Because of the high dimensionality of data when studying oscillatory processes across the cortex, the majority of existing studies in the field restrict analysis to sensor space or depict very narrow temporal, spectral, or spatial regions of interest (but see Hinkley et al., 2011). In contrast to this common procedure, we present spectral power changes at source level cortex-wide and across a broad temporal and spectral range. While physiological investigations of oscillatory mechanisms of saccade control in humans focused mostly on the aspect of motor preparation for externally guided saccades, we show saccade specific cortical dynamics not only for visually guided behavior but also for internal selection of saccade goals.

1.3.2.2 Saccadic decisions

So far we have considered guided saccades, where a movement is performed according to fixed instructions. In real-world ongoing behavior, humans seldom have to respond with a predefined action to a sensory cue. Rather, they repeatedly have to choose between several competing behavioral alternatives. Action selection is therefore an integrative part of ecologically relevant behavior, and it most probably involves voluntary and internally motivated processes that are absent in guided actions. Humans constantly decide when and where to look, and these decisions influence to a great extent what is perceived at any moment in time. Consequently, uncovering the neural correlates of saccadic decisions is a crucial step towards real-world action based paradigms in vision.

Behavioral studies have identified various internal and external aspects that influence our decisions where to look such as current behavior goals, saliencies of a visual scene, object identification, indirect values and intrinsic motivations (for reviews see Einhäuser and König, 2010, Hayhoe and Rothkopf, 2011, Schütz et al., 2011). Despite this variety, neural correlates of saccadic decision making have mostly been investigated in non-human primates as a model for value learning and encoding in the field of neuroeconomics (Glimcher, 2003, 2009, 2011, Sugrue et al., 2005). While saccadic decisions in ongoing free viewing behavior rather rely on indirect values (see Schütz et al., 2011, and Section 5), saccadic decisions in these neuroeconomic studies have usually been based on stimuli associated with direct rewards that are experimentally manipulated by the researcher.

Consequently, studies from the field of neuroeconomics have found subjective value related responses in primate ventromedial prefrontal areas and striatum (see Kable and Glimcher, 2009, for a review). Activity specific for action value learning and linking of abstract rewards to actions has been found in anterior cingulate cortex (Hayden and Platt, 2010, cf. also Kennerley et al., 2006, for a non-saccadic decision task). The areas from the valuation circuitry are strongly influenced by midbrain dopaminergic neurons implicated in reinforcement learning (Kable and Glimcher, 2009). Representations of context dependent rules have often been suggested to originate from dorsolateral prefrontal cortex (see Bunge et al., 2005, for a review).

Interestingly, saccade decision related signals are not only restricted to the aforementioned areas but can also be identified in a multitude of distributed regions, namely in sensorimotor structures like the frontal (Coe et al., 2002, Schall and

Hanes, 1998) and parietal eye fields (Dorris and Glimcher, 2004, Platt and Glimcher, 1999, Sugrue et al., 2004, Yang and Shadlen, 2007), and superior colliculus (Basso and Wurtz, 1998)[15], that means regions that have traditionally been implicated in the process of motor control (for a review see Cisek and Kalaska, 2010, Gold and Shadlen, 2007, Kable and Glimcher, 2009). These areas of sensorimotor transformation seem to encode the subject's choice preference (e.g., by encoding *relative* reward values based on the available options) and mediate the choice of a specific action towards a movement command (Glimcher, 2009, Gold and Shadlen, 2007, Kable and Glimcher, 2009, see also de Jong, 2011, Hare et al., 2011, Trommershäuser et al., 2009, for studies focussing on the human system).

Since a multitude of sensorimotor related areas were shown to simultaneously encode parallel evolving competing movement plans and potential targets for saccades and other skeletal movements (Basso and Wurtz, 1998, Cisek and Kalaska, 2005, Cui and Andersen, 2007, Klaes et al., 2011, McPeek et al., 2003, Mysore and Knudsen, 2011, Pastor-Bernier and Cisek, 2011, Pastor-Bernier et al., 2012, Platt and Glimcher, 1999, Powell and Goldberg, 2000, Scherberger and Andersen, 2007, Shadlen and Newsome, 2001), it has been suggested that the decision for a specific motor outcome emerges from the competing distributed activations within these structures (Cisek, 2006, 2007, Cisek and Kalaska, 2010, Shadlen et al., 2008). In support of this assumption, competitive neural activities strongly inhibit each other if they relate to potential movements that are mutually exclusive (e.g., movements in opposite directions), while mutual inhibition for choices of similar actions is weaker and might even allow a mixture of both movements (Pastor-Bernier and Cisek, 2011). Indeed, spatially close target alternatives can lead to movements that are in-between both presented alternatives (Chapman et al., 2010). These observations illustrate how a competition between cell populations that define the physical properties of an action can lead to a decision about the action itself.

The aforementioned observations put to question – at least for decisions leading ultimately to a movement – classic representationist models, which define decision making as an isolated cognitive operation in a sequential and modular process of sensation, decision, and subsequent movement preparation. Rather, these observations argue in favor of an action-based framework of decision making where movement

[15]In this thesis we focus on the structures of the cerebral cortex that we investigated in the MEG analysis, although the superior colliculus plays an important role in saccade selection (e.g., Glimcher, 2009, Mysore and Knudsen, 2011).

preparation and the choice of an action are formed in an integrated and distributed manner to ensure flexible adjustments in interactive real-world behavior (Cisek and Kalaska, 2010). Cisek claims that throughout evolutionary history, the individual was constantly faced with the requirement of adapting quickly to fast changing behavioral context during ongoing behavior. These evolutionary demands favored development of a system that can operate action preparation and selection in parallel so that actions can be flexibly modified on the fly. This system is supposed to work in close interaction with other processes originating for example from frontal regions that might either bias the fronto-parietal competition by providing information about value and behavioral relevance, or mediate more abstract decisions independent of immediate actions (cf. Cisek, 2012). Cisek proposes that from such a parallel architecture, decision emerges as a "consensus distributed among a variety of representations" (Cisek, 2012, p.933), rather than resulting from the activity of a central executive brain structure.

As discussed in Section 1.2, we hypothesize that neural oscillations play an important role in the flexible implementation of such a proposed distributed and interacting network of internal choice. For reaching movements, stronger oscillatory couplings between frontal and parietal areas were indeed attributed to the process of internally selecting between equally valuable reach targets in monkeys (Pesaran et al., 2008). For perceptual decisions, where individuals accumulate sensory evidence over time before making a discriminatory judgment about what they have perceived, investigations in animals and humans have emphasized the importance of oscillatory population activity in sensorimotor areas (Donner et al., 2009, Haegens et al., 2011, Siegel et al., 2011, Wyart et al., 2012, see also Gould et al., 2012).

1.3.2.2.1 Contributions of this thesis

Evidence supporting the presented distributed and integrative view on action selection with sensorimotor areas as key structures primarily originates from animal studies. Some studies in humans have argued so far for response competition between simultaneously activated movements plans, for example for reaching movements in posterior parietal cortex (Coulthard et al., 2008, Oliveira et al., 2010). If human internal choice of saccade target is mediated by parallel evolving movements plans within sensorimotor structures and if oscillatory processes play a key role in guiding this competitive saccadic choice remains unclear.

In case response competition between behavioral alternatives is indeed reflected in enhanced synchronized oscillatory activity within or in between areas, then the choice between many equally valuable saccade targets should maximally drive spectral changes presumably in distributed fronto-parietal networks. Therefore, we investigated the oscillatory mechanisms associated with selecting a saccade target between equally rewarding behavioral alternatives (Section 4). This way action selection was relatively independent from sensory input. Consequently, our investigation emphasized internally motivated or voluntary action selection, which we consider a crucial part of active real-world behavior. This aspect has been rather absent in studies of neuroeconomic and perceptual decisions involving saccades. Also, the role of oscillatory dynamics in human voluntary action selection has not been addressed yet.

Consequently, the experimental work presented in this thesis will add to our understanding of neural and in particular oscillatory mechanisms of voluntary saccade target selection and saccadic control, which are two fundamental processes of real-world free viewing behavior.

2

Towards Active Vision in EEG and MEG (Study 1)

The content of this chapter is based on an internal report, which was originally written in 2009. For the thesis, the author (Christine Carl) has adapted the report to address some recent publications of high relevance. The authors of the report are: Joerg F Hipp[1,2], Alper Açık[3], Christine Carl[2,3], Kai Görgen[3,4], Andreas K Engel[2] & Peter König[3]

[1]Centre for Integrative Neuroscience, University of Tübingen, Germany [2]Department of Neurophysiology and Pathophysiology, University Medical Center Hamburg-Eppendorf, Germany [3]Institute of Cognitive Science, University of Osnabrück, Germany [4]Bernstein Center for Computational Neuroscience, Berlin, Germany

J F Hipp, A Açık and K Görgen designed the research, performed the experimental recordings and data analysis in EEG. C Carl performed the experimental recordings and data analysis in MEG. J F Hipp and A Açık wrote the manuscript part concerning the EEG study and J F Hipp contributed to the manuscript part concerning the MEG study. C Carl wrote the manuscript part concerning the MEG study and contributed to the part concerning the EEG study. A Engel and P König provided general ideas and contributed to the manuscript. The Bachelor thesis of K Görgen was based upon the here presented EEG study (Görgen, 2010).

2.1 Introduction

Every second, humans perform approximately three fast, ballistic eye-movements, called saccades, in order to project different portions of the visual scene onto the fovea where it is processed with maximal acuity. This makes saccadic eye-movements a key feature of our visual system (Sparks, 2002).

EEG and MEG are the means to non-invasively study fast neuronal dynamics in the human brain. However, the electrical properties of the eye cause severe methodological problems when studying natural vision with EEG/MEG. The eye is the source of an electric potential that can be described as a dipole with a positive pole at the cornea and a negative pole at the retina with a potential difference of 0.4 to 1.0 mV (Malmivuo and Plonsey, 1995, pp.440-442). Consequently, an eye movement causes change in electrical potential around the eyes, which is commonly referred to as the corneo-retinal potential (CRP) or corneo-retinal artifact (Lins et al., 1993a, Mowrer et al., 1935). This change can be measured with the EOG but also confounds EEG/MEG signals, that are applied in order to measure neuronal activity fluctuations. Together with the saccadic spike artifact, a transient deflection resulting from the concurrent recruitment of motor units at saccade initiation (Thickbroom and Mastaglia, 1985), the CRP is a major source of EEG/MEG distortion due to eye movements. Consequently, to allow the interpretation of EEG/MEG signals as genuine changes in neural activity, the vast majority of experiments demand steady fixation – a rather unnatural constraint. This discrepancy between experiments and natural vision raises a fundamental question: Do findings from experiments with steady fixation generalize to natural conditions with eye movements?

Some of the existing studies investigating saccade related processes in humans have indicated a close relation between covert attention and gaze shifts (Rizzolatti et al., 1987, Schafer and Moore, 2007, Wauschkuhn et al., 1998). Others have shown saccade induced modulations of visual responses like saccadic suppression and predictive remapping or updating processes that rely on information of self-induced saccadic movements by corollary discharges (Dodge, 1900, Haarmeier et al., 1997, Merriam et al., 2003, Parks and Corballis, 2010, Peterburs et al., 2011, Wurtz, 2008). These findings indicate that eye movements are indeed key for understanding natural vision. In order to address ecological validity concerns of passive stimulation paradigms we have to fortify the research of active vision and the study of neural

processes of saccade performance in EEG/MEG. This requires a thorough handling of the eye movement artifacts.

Until today, many researchers are reluctant to use artifact cleaning procedures in order to study the active performance of eye movements. Researchers interested in saccade related processes often focus on the preparatory phase of saccades and stop analysis before the saccade is executed (e.g., Brignani et al., 2010, 2007, Cordones et al., 2013, Gutteling et al., 2010, Lee et al., 2011, Medendorp et al., 2007). There exist only a few studies that investigate active execution of regular saccades. Some of them try to separate the artifactual from cortical signals by employing artifact cleaning procedures (e.g., Bellebaum and Daum, 2006, Van Der Werf et al., 2013). Others investigate saccade related activity without cleaning for artifacts (e.g., Belyusar et al., 2013, Hinkley et al., 2011, Moon et al., 2007, Peterburs et al., 2011), following the reasoning that e.g. posterior sensors are not affected by the artifacts (Belyusar et al., 2013), or with the underlying assumption that reconstructed cortical sources are artifact-free (cf. Herdman and Ryan, 2007, Hinkley et al., 2011). It was also proposed to subtract different saccade conditions to remove eye movement artifacts (Parks and Corballis, 2010), or average equal amounts of rightward and leftward saccades (Kleiser and Skrandies, 2000, Kurtzberg and Vaughan, 1982). This way, the CRPs of opposing directions cancel out.

Although disentangling motor commands, visual responses, remapping processes, and eye movement artifacts remains a challenge for EEG/MEG research, we think that eye movement artifact cleaning methods are pivotal for active vision studies. Balanced designs as mentioned above can address only those SRP components that are common to saccades into both directions. In contrast, artifact cleaning can help to uncover cerebral lateralized potentials related to saccade direction (cf. Bellebaum and Daum, 2006, Bellebaum et al., 2005, Wauschkuhn et al., 1998). Furthermore, studying neuronal processes underlying natural human vision demands a procedure that allows arbitrary fixation statistics and single trial analysis. This is not possible when relying on balanced designs for artifact reduction. Finally, it was shown that ocular artifacts (i.e., from blinks and eye movements) can contaminate even channels distant from the eyes, such as those above occipital areas (cf. Plöchl et al., 2012), or reconstructed cortical sources (Fatima et al., 2013). Consequently, restriction to distant sensors or an analysis in source space may be not sufficient to prevent artifact contamination. This makes reliable cleaning procedures for ocular artifact reduction extremely relevant.

Since the seventies, there have been attempts to subtract ocular artifacts from the recorded data by employing mathematical models (Quilter et al., 1977, Whitton et al., 1978). Such methods include regression techniques (Croft and Barry, 2000a), making use of the EOG recorded concurrently with EEG, and blind source separation techniques such as ICA (Jung et al., 2000a). Automated and easily employable routines based on linear regression have been shown to return satisfactory results as validated by experts' inspections of the cleaned data (Schlögl et al., 2007). Mostly, these routines have been tested for cleaning the data from ocular artifact contaminations due to small and unintentional eye-movements, rather than for developing paradigms that allow natural unrestricted viewing behavior. More importantly, linear regression methods have repeatedly been accused of removing parts of the cortical potentials of interest together with the CRP (Ille et al., 2002, Jung et al., 2000a,b). Such concerns may be another reason why many researchers refrain from studying active vision and using cleaning procedures to reduce the related artifacts.

The goal of this study is to re-evaluate if regression cleaning is an appropriate tool for studying regular saccades in order to provide a procedure that allows studying active vision in EEG. To do so, we recorded, in separate experiments, EEG and MEG employing an active vision task and applied an EOG regression procedure to subtract eye movement artifacts. Concurrent eye tracking provided accurate information on gaze position and allowed the detection of saccades. As a proof of principle, we aimed at assessing direction specific cortical signatures of saccades that are normally covered by the CRP. We further used source reconstruction of the MEG data to evaluate what parts of the data are subtracted by the EOG regression.

2.2 Materials and Methods

2.2.1 Stimulation and Behavioral Task

For the main EEG experiment subjects performed a continuous guided saccade task. Stimuli were presented on a CRT-monitor that covered horizontally 15° of visual angle (stimuli were presented using Presentation software, Neurobehavioral Systems, San Francisco, CA). A target, either a white Gaussian patch (0.25° full width at half maximum (FWHM), probability 0.8) or a radially contracting grating (probability 0.2, data not analyzed here) was presented at one of 9 possible locations on a gray background screen (see Figure 2.1B; possible locations: 3×3 grid; horizontal/vertical

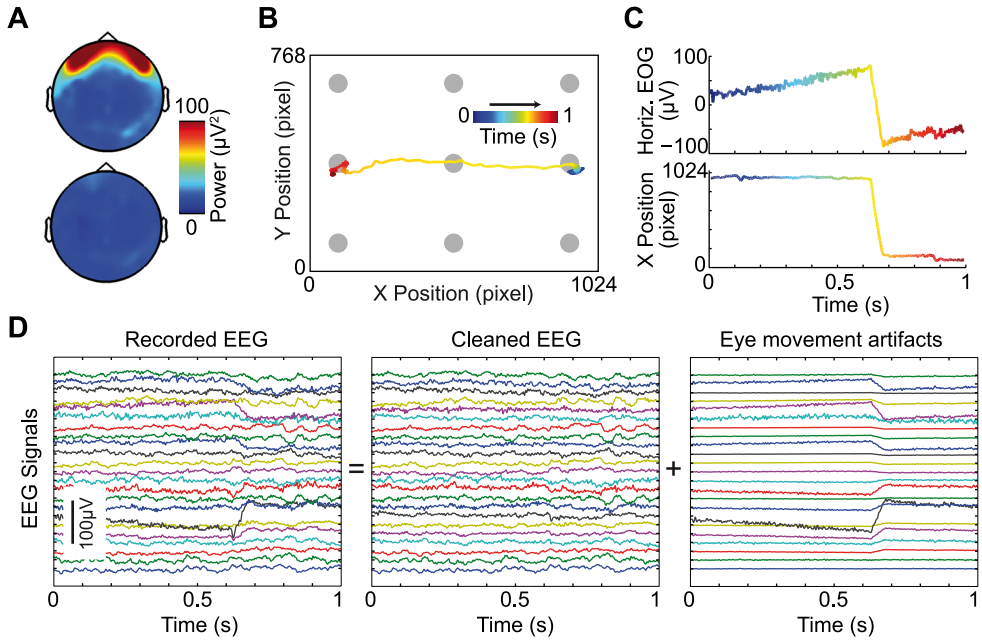

Figure 2.1: Removing eye movement artifacts. A. Grand average broadband power of the EEG in 1 s periods around detected saccades during the 3 min session of voluntary eye movements with (bottom) and without (top) EOG regression cleaning (average over trials, subjects, and time). B. Temporal evolution (color-coded) of gaze position during one representative trial of the continuous guided saccade task. The rectangle represents the stimulation screen and the gray circles indicate all possible target locations. Note that the screen during the experiment only showed one target at a time, with white target on a gray background. In this representative trial, a horizontal saccade from the right to the left target location is executed between 0.6 and 0.7 s. C. Corresponding EOG (top) and horizontal gaze position (bottom). D. Illustration of the EOG regression cleaning. The recorded EEG (left) can be decomposed into a cleaned EEG signal (middle) and corneo-retinal potential (right). Data recorded concurrently to eye position (B, C) and EOG (C).

spacing 6°/5.5° of visual angle respectively). The target remained at a location for $1 - 1.5$ s (flat probability distribution) before it disappeared, just to re-appear at another randomly chosen location. The task was to fixate the target and follow it upon changes in location. This required the subjects to perform saccades with a minimal and maximal distance of 5.5° and 16.3° of visual angle respectively.

An experimental block was organized in 40 sections of 20 s each (∼16 saccades) intermitted by breaks. 9 Subjects performed 1 to 3 blocks with a total of 14 blocks. Each section started with the presentation of a central fixation cross that had to be fixated stably for 1 s before the task began. The fixation cross was used for drift correction of the eye tracker data. Before each experimental block subjects per-

formed 3 min of voluntary eye movements. Subjects were presented a gray screen and were instructed to perform arbitrary, self-paced saccades within the screen borders. The identical protocol with 2×3 min voluntary eye movements was recorded in a separate MEG experiment.

2.2.2 Analysis Software

All data analyses were performed in Matlab (MathWorks, Natick, MA) with custom software and several open source Matlab-toolboxes: Fieldtrip (`http://www.ru.nl/fcdonders/fieldtrip/`), SPM2 (`http://www.fil.ion.ucl.ac.uk/spm/`), FastICA (`http://www.cis.hut.fi/projects/ica/fastica/`), and BioSig (`http://biosig.sourceforge.net/`).

2.2.3 Participants

Nine healthy volunteers participated in the experiment (4 female, mean age 26) and received monetary compensation for their participation. All participants had normal or corrected-to-normal vision (visus > 0.9) and had no history of neurological or psychiatric illness. The study was conducted in accordance with the Declaration of Helsinki, and informed consent was obtained from all participants prior to the recordings.

2.2.4 EEG and Eye Tracker

2.2.4.1 EEG/EOG recording and preprocessing

Subjects were seated in a sound isolated and electrically shielded chamber. Continuous EEG data were collected from 124 scalp sites using active ring electrodes mounted on an elastic cap (Falk Minow Services, Herrsching, Germany). The left mastoid was used as reference. Four additional electrodes were positioned around the eyes to record the EOG. The data were recorded with an analog passband of $0.016-250$ Hz and digitized at a sampling rate of 1000 Hz using BrainAmp amplifiers (BrainProducts, Munich, Germany).

Offline, the EEG and EOG data were band-pass filtered (0.3 Hz high-pass, 150 Hz low-pass, zero phase Butterworth IIR filter, filter order 3). Noisy channels (9 ± 4, mean $\pm$ sd) were interpolated. Data segments with obvious muscle artifacts or

eye blinks were detected manually and excluded from further analysis. The EEG data were re-referenced to average reference. The EOG channels were re-referenced against one of the channels reducing EOG channels to three, positioned above the nasion and below the outer canthi of each eye (cf. Schlögl et al., 2007).

2.2.4.2 Eye tracker recording and preprocessing

Simultaneous to EEG/EOG we recorded the eye position using a high-speed eye tracker system (iView X Hi-Speed 1250, SMI, Berlin, Germany). The system was placed in front of the subject inside the recording chamber. The system monitors the left eye with an infrared camera to detect the pupil center and the corneal reflection of the infrared light source. After calibration (13 points) the system determines the gaze direction from the relative position of pupil and the corneal reflection at a rate of 1250 Hz. The system was placed without a chin-rest and without direct contact to the participant in order to keep the viewing behavior of the subject as unrestrained as possible. To ensure good acuity we calibrated the eye tracker before each experimental block and validated the accuracy frequently.

Offline, the eye tracker signal (x/y gaze position and pupil diameter) was down-sampled from 1250 Hz to the sampling rate of the EEG system (1000 Hz). We excluded all data from the analysis showing one of the following characteristics: (a) blinks (regions in which the pupil-diameter size approached or reached 0) (b) extreme and as such erroneous position values (if the x/y position exceeded ± 3 sd from the median of the all recorded data) (c) regions with instantaneous jumps in the pupil diameter values (caused by errors in the pupil detection). Data were smoothed and differentiated (Savitzky-Golay filter, 1st order, 61 ms, Savitzky and Golay, 1964) to derive the eye-movement speed. We defined all those periods as saccades in which the speed profiles were higher than $25°/s$ for a duration of at least 15 ms. Given the simple, stereotypical saccades demanded by the paradigm and the absence of smooth-pursuit movements, additional threshold parameters, such as acceleration, were not needed. The first time point in the saccadic interval was defined as the saccade onset and the last point as the saccade offset. We then merged all saccades that were closer than 75 ms to a single saccade with the onset of the earlier saccade to avoid miss-categorizing saccadic periods as fixations. All other periods were labeled fixations. On average, 3 out of 16 saccades in each trial were excluded from analysis. Saccades were categorized into rightwards and leftwards

saccades with a tolerance aperture angle of 45°.

2.2.4.3 Eye tracker performance

We used two approaches to quantify the precision of eye tracking. First, before and after each experiment, we validated the calibration of the eye tracking system. For validation subjects had to fixate the same 13 positions as for calibration presented in a random order. During an experimental block the mean validation errors increased from 0.4° and 1.0° before, to 0.6° and 1.2° after the block. Second, for the continuous guided saccade task, we computed the distance to the target location for each fixation. In the ideal case this distance should be zero, assuming that the subjects always perfectly fixate the center of the target stimulus. For 5587 valid fixations detected in the continuous saccade data, we computed the distances to the center of the target location. The mode, median, and the mean of this distance distribution were 0.48°, 0.88° and 1.76°, respectively. In summary, during the whole experiment, the accuracy of the eye-position data provided by the tracker was sufficient to be employed in the active viewing task.

2.2.4.4 Alignment of EEG/EOG and eye tracker signals

To synchronize the EEG/EOG and eye tracker signals, we simultaneously sent triggers to the EEG/EOG and the eye tracker system. However, the EEG/EOG and eye tracker system temporally differed in storing the trigger relative to their recorded signals. To account for the remaining offset we computed the cross-correlation of EOG and eye tracker signals of the 3 min voluntary eye movements for each experimental block. For both signal types (EOG and eye tracker) we extracted the first principal component, rectified and smoothed the signal. Then, we identified the latency of the peak in the cross-correlogram between the signals. This latency corresponds to the difference in trigger alignment and was corrected for in order to achieve optimal alignment of EEG/EOG and eye tracker signals.

2.2.4.5 Cleaning data from artifacts related to the movements of the eye

To clean the EEG/MEG signal from eye movement artifacts we performed a two-step process. First, the corneo-retinal artifacts were removed by linear regression based

on the EOG signals. Second, facial muscle activity was attenuated by removing corresponding independent components of the data.

2.2.4.6 Multiple linear regression

To remove corneo-retinal artifacts we used an EOG based linear regression technique (Croft and Barry, 2000b, Gratton et al., 1983, Quilter et al., 1977, Schlögl et al., 2007). The reasoning is as follows: The EOG signal provides a measure of the CRP. Given that electromagnetical signal propagation in the head can be considered instantaneous (i.e., without a delay between sensors; Nunez and Srinivasan, 2006) and linear (assuming the relation between sensor and source locations are fixed), one can remove the corneo-retinal artifacts by subtracting the properly weighted EOG from the EEG/MEG.

Before the main experiment we recorded 3 min of voluntary eye movements on a gray screen. These signals were cleaned and preprocessed and then served to compute the linear relation between the EOG sensors (in EEG: 3 EOG electrodes that were referenced against a fourth electrode under the right eye, in MEG: 7 EOG electrodes referenced against an electrode at the nose and reduced to 3 dimensions using principal component analysis) and each EEG/MEG channel (Schlögl et al., 2007). EEG/MEG data were then cleaned by subtracting the weighted EOG signal.

2.2.4.7 Removing independent components

Eye movements come along with changes in facial muscle activity. To account for these artifacts, we computed an independent component analysis using the FastICA algorithm (`http://www.cis.hut.fi/projects/ica/fastica/`, Hyvärinen, 1999) and removed artifactual components (22 ± 10 of 124 components per subject, mean $\pm$ sd). The selection of artifact components was based on visual inspection of their topography and power spectrum. Note that we used ICA to remove facial muscle activity only, and neither corneo-retinal artifacts nor the spike potential as proposed by others (Barbati et al., 2004, Ille et al., 2002, Joyce et al., 2004, Keren et al., 2010a).

2.2.4.8 Data analysis

We used global field power (GFP) as an unbiased measure that quantifies the temporal evolution of event related potentials on the scalp (Lehmann and Skrandies,

1980). In detail, GFP is defined as:

$$GFP(t) = \sqrt{\frac{1}{N}\sum_{s=1}^{N} SRP(t)_s{}^2} \tag{2.1}$$

where s is an index for the EEG/MEG sensors, N denotes the number of EEG sensors ($N = 124$), t is the time point, and SRP is the saccade related potential. Since we re-referenced the EEG signal to average reference, the GFP summarizes the potential differences across all channels and provides a global and unbiased index of changes in the scalp potential. We computed a GFP for every subject and averaged across subjects.

For calculating the difference of the SRP between leftwards and rightwards saccades, we matched the number of rightwards and leftwards saccades, as well as their amplitudes. To test for statistically significant increases in GFP for right versus left saccades, we used a random permutation test (Nichols and Holmes, 2002). We derived a null-hypothesis distribution by $10,000$ times randomly permuting saccade labels *right* and *left* and computing the corresponding GFP. By computing in each iteration the GFP of a random permutation in each subject and averaging over subjects we derived a fixed effects statistics. Then we derived a p-value for each time point as the fraction of random samples that was larger than the true GFP.

2.2.5 MEG

We performed an additional MEG experiment to investigate the source locations of the portions of the MEG signal that had been subtracted by the EOG regression[1]. To do so, we evaluated regression cleaning on both datasets of 3 min length. Each dataset had been cleaned before employing the regression coefficients computed with the other dataset, respectively.

2.2.5.1 Participants

Fifteen healthy volunteers participated in the experiment (7 female, mean age 25.7$\pm$ 3.3) and received monetary compensation for their participation. All participants had normal or corrected-to-normal vision (visus > 0.9) and had no history of neurological or psychiatric illness. The study was conducted in accordance with the

[1]The data analyzed here have also been used in Study 3.

Declaration of Helsinki and informed consent was obtained from all participants prior to the recordings.

2.2.5.2 MEG/EOG recording and preprocessing

We recorded MEG continuously with a 275-channel whole-head system (CTF275, VSM MedTech) in a magnetically shielded room. Seven electrodes referenced to the nose tip were positioned around the eyes to record the EOG. Impedances were kept below 10 kΩ. MEG and EOG data were sampled with 1200 Hz (MEG: 300 Hz low-pass filter, EOG $0.16 - 300$ Hz band-pass filter). Offline, we removed line-noise with notch-filters (at 50, 100, 150 Hz), band-pass filtered the data ($1 - 170$ Hz) and down-sampled to 400 Hz. Data periods contaminated by eye blinks, muscle artifacts, and signal jumps were rejected offline using semi-automated procedures.

2.2.5.3 Saccade detection and alignment

In order to access the effect of the EOG regression cleaning on broadband power in sensor space, we identified MEG trials aligned to a saccade out of the continuous MEG recordings during free viewing. Therefore, we identified windows of 1 s length within which the horizontal or vertical EOG changed by more than 72 μV. We realigned data to the time of maximal saccade velocity measured as the largest signal change in the EOG within such windows. Saccade trials extended ± 0.5 s around this time point. Note that an alignment to the exact onset of the saccade was not crucial since we were only interested in the mean broadband power over time and trials.

2.2.5.4 Source reconstruction

We used adaptive linear spatial filtering (beamforming; Van Veen et al., 1997) with coherent source suppression (Dalal et al., 2006) to localize the sources of the artifactual signal components removed by linear regression. Coherent source suppression accounted for the highly synchronized electrical activity of the two eyes. In short, for each source location, a linear filter was computed that passes activity from that location with unit gain and blocks activity from the opposite hemisphere's eyeball location, while maximally suppressing activity from other sources. Forward models were computed using individual single-shell volume conductor models based on the individual T1-weighted structural magnetic resonance image (MRI) and the

measured head positions (Nolte, 2003). Whole-head source reconstructions were performed on a regular 3D grid of 1 cm resolution. The grid incorporated source locations within and around the eyeballs.

For each subject we localized mean broadband source power of signals with and without the linear regression cleaning procedure. Since linear regression always reduces signal power (even if there is no relation between EOG and EEG/MEG) the cleaned source power is negatively biased. To overcome this problem we replaced the *no cleaning* condition by regression cleaning with a miss-aligned EOG signal (EOG and MEG signals were randomly taken from different times). This procedure was repeated 100 times and averaged to get a robust source estimate for the *no cleaning* condition with the same negative bias as the *cleaning* condition. For each subject we then computed the relative change of *no cleaning* and *cleaning*, isolating the fraction of source power that was subtracted by linear regression at each source location. These values were linearly aligned to a template brain (Montreal Neurological Institute; using SPM2). We then computed the average of these values over subjects. For illustration purposes values were interpolated to 1 mm resolution and overlaid on the structural MRI of the template brain.

2.3 Results

Eye movements cause changes in electrical potential, confounding the EEG signal that we use to measure fluctuations of the brain's neuronal activity. This effect is illustrated in Figure 2.1A (top) where we show the topography of the broadband EEG power while subjects performed saccades. The topography is dominated by massive broadband signal power at frontal sensors reflecting eye movement artifacts. A part of these artifacts can be removed by subtracting the linearly weighted EOG. To illustrate how eye movement artifacts and cerebral sources add to the EEG signal, we show a one second period within which a subject performed a guided saccade. The time course of the eye position recorded with an eye tracker (see Figure 2.1B and 2.1C, bottom) revealed that the subject first fixated on the right and then, starting at 0.65 s, performed a saccade of approximately 12° visual angle to the left. The change in electrical potential caused by the eye movement (CRP) was measured with the EOG (Figure 2.1C, top). Crucially, this change in potential was also reflected in and even dominated the raw EEG signal (Figure 2.1D, left), which

is supposed to provide a measure of changes in neuronal activity. Using multiple linear regression with EOG sensors (see Section 2.2.4.6) we decomposed the raw EEG signal (Figure 2.1D, left) into a cleaned EEG signal (Figure 2.1D, center) and corneo-retinal artifacts (Figure 2.1D, right). Subsequently, we used ICA to remove facial muscle activity that comes along with eye movements. The effect of this cleaning procedure is reflected in the dramatic change of EEG signal power around the eyes (Figure 2.1A, bottom, in comparison to Figure 2.1A, top). Thus, the cleaning procedure removes a substantial part of artifactual signal and clears the way to analyze smaller neuronal signals.

2.3.1 SRPs

In order to demonstrate the feasibility of the EOG regression cleaning procedure, we recorded EEG, EOG, and eye position simultaneously while subjects performed an active vision task. Subjects followed a visual object with their eyes that changed its position once every 1.25 s with a jitter of 0.25 s (9 possible positions, Figure 2.1B). Using the eye position signal derived with the eye tracker, we detected saccade onsets and aligned the signals to these events (Figure 2.2). The changes in eye position and EOG magnitude relative to a pre-saccadic baseline (-300 to -200 ms) revealed the time course of the average saccade across directions (average of the absolute value). The average saccade duration was approximately 60 ms. To quantify the temporal evolution of the SRP measured with EEG, we computed the GFP for all saccades to the right (Figure 2.2B, top) with (black line) and without (gray shading) EOG regression cleaning. The cleaning of eye movement artifacts had a dramatic effect. The GFP of the raw, non-cleaned signal increased to more than 9 μV after saccade onset. In contrast, GFP of the cleaned EEG did not exceed 4 μV and revealed a rich temporal structure: First, the GFP monotonically increased from approximately 100 ms prior to the saccade to saccade onset and was characterized by a peak at parietal sensors (Figure 2.2C, first row). Second, shortly before the saccade onset a sharp spike with frontally negative and posteriorly positive topography occurred (Figure 2.2C, second row). Third, during saccade execution the scalp potential increased at occipito-parietal sensors (Figure 2.2C, third row). Fourth, a prolonged change at occipito-parietal sensors followed the saccade offset (Figure 2.2C, fourth row). Importantly, these potentials after saccade onset were buried in ocular artifacts if no EOG regression was applied (compare Figure 2.2C and D). The result for saccades

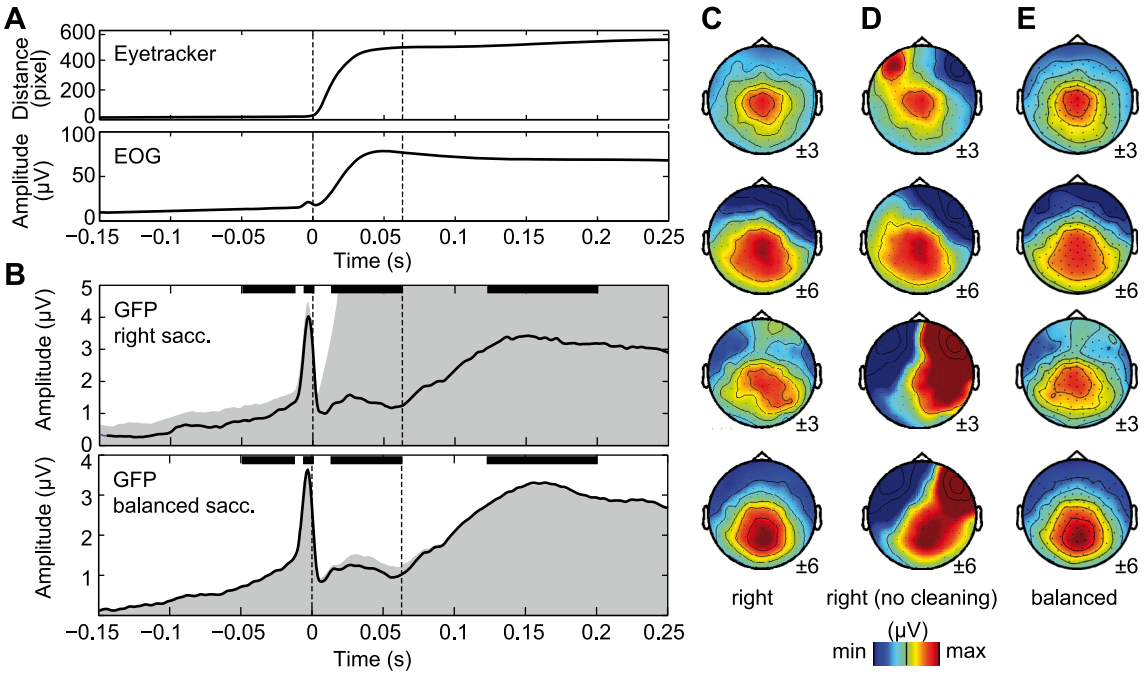

Figure 2.2: Saccade related potentials. All signals are aligned to saccade onset (first dashed line at time $t = 0$ ms, second dashed line denotes the average saccade offset at $t = 60$ ms). A. Top: Change in gaze position relative to baseline (−300 to −200 ms). Bottom: Change in EOG magnitude relative to baseline. B. Top: GFP for saccades to the right with (black line) and without EOG regression cleaning (gray shading; reaches > 9 μV around saccade offset). Bottom: GFP for leftwards and rightwards saccades (balanced) with (black line) and without (gray shading) EOG regression cleaning. Black bars indicate the intervals of the topographies in panels C–E. C. Topographies of SRPs for saccades to the right with EOG regression cleaning. First row: antecedent potential (−50 to −10 ms). Second row: saccadic spike potential (−8 to 0 ms). Third row: during saccade execution (10 to 60 ms). Forth row: lambda response (120 to 200 ms). D. Topographies of SRPs for saccades to the right without cleaning (raw signal). E. Topographies of SRPs for balanced horizontal saccades without cleaning.

to the left were mirror symmetric but otherwise identical. This demonstrated that EOG regression allows cleaning of eye movement artifacts and uncovers neuronal signals associated with active viewing behavior that remains hidden otherwise.

For experimental designs with balanced saccade statistics, where for each saccade a corresponding saccade in the opposite direction with identical amplitude is performed, the corneo-retinal artifacts may cancel out in the SRP. We tested this by computing the SRP of matched leftwards and rightwards saccades (Figure 2.2B, bottom, Figure 2.2E). In this case, the GFP of the cleaned (black line) and raw (gray shading) signals were highly similar.

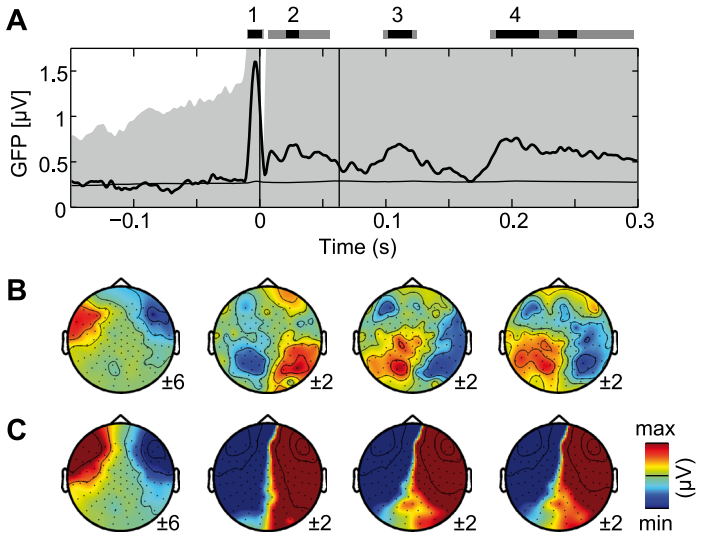

Figure 2.3: Direction specific saccade related potentials. A. GFP for difference of saccades to the left from saccades to the right (saccade onset at time = 0) with (black line) and without (gray shading; reaches > 11 μV around saccade offset) EOG regression cleaning. The bars above the plot indicate statistically significance GFP (gray: $p < 0.05$; black: $p < 0.01$). B. Topographies of SRPs difference of the cleaned signal at four different latencies as indicated by numbers in A. First: saccadic spike potential (-8 to 0 ms). Second: during saccade execution (10 to 60 ms). Third and forth: difference topographies after saccade execution (100 to 120 ms; 190 to 220 ms, respectively). C. Same as in B but without regression cleaning.

Next, we investigated direction specific effects of the SRP by computing the difference of saccades to the left from saccades to the right of the cleaned EEG signal (Figure 2.3, black line, here the difference of the SRP entered the GFP computation). The analysis of the GFP revealed a distinct temporal structure in the direction specific signal (Figure 2.3A): We found a lateralized spike potential with a frontal topography starting approximately 8 ms before saccade onset ($p < 0.01$, random permutation test; the corresponding topography is shown in Figure 2.3B, first column). During saccade execution ($\sim 0 - 60$ ms) we found a lateralized occipito-parietal potential ($p < 0.05$, random permutation test; topography in Figure 2.3B, second column). The potential was positive on the ipsilateral side. After saccade execution a potential with similar topography but opposite polarity reappeared twice ($100 - 120$ ms; $190 - 220$ ms; $p < 0.01$, random permutation test; topographies in Figure 2.3B, third and fourth column). These findings critically depended on cleaning the EEG signal. The difference SRP derived from the raw signal (Figure 2.3A, gray shading; Figure 2.3C) was entirely dominated by eye movement artifacts.

2.3.2 Does the EOG Regression Accidentally Remove Brain Signal?

Since the EOG might not only measure the CRP but also pick up some cerebral activity, subtracting a linearly weighted EOG from the EEG might substantially alter the measured neuronal activity. To address this issue, we performed an MEG experiment. We analyzed signals from 15 subjects that performed 3 minutes of voluntary eye movements each. After preprocessing we applied the linear EOG regression to clean the MEG data. Figure 2.4A shows sensor topographies of the grand average broadband signal power before (top) and after EOG regression cleaning (bottom). The cleaning procedure removed a large part of the signal power at lateral frontal sensors. Next, we localized the subtracted signal using source reconstruction based on adaptive linear spatial filtering (see Section 2.2.5.4; Figure 2.4C). This revealed bilateral sources within the eyeballs. Source power smoothly decayed from the maxima reflecting the limited spatial resolution of MEG source analysis. Importantly, no cortical sources of the subtracted signal were revealed.

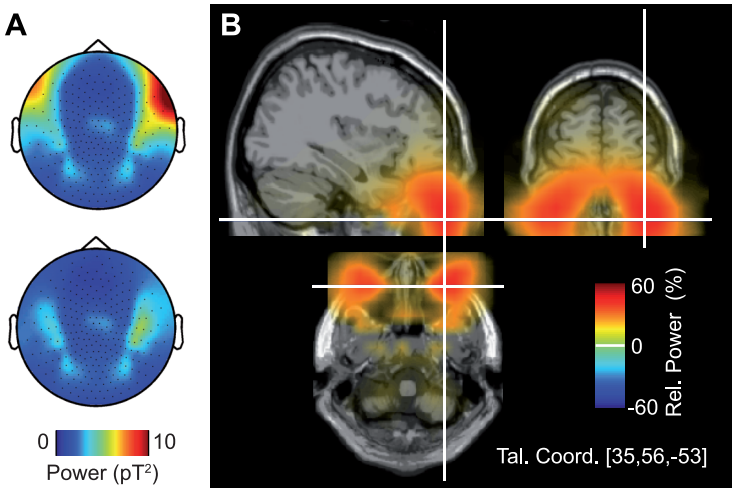

Figure 2.4: Source localization of removed corneo-retinal artifacts. A. Broadband power at MEG sensors of the raw signal (top, with eye movement artifacts) and after EOG regression cleaning (bottom). MEG analog to Figure 2.1A. B. Fraction of source power removed by the EOG regression cleaning procedure (Tal. Coord.: Talairach coordinate).

2.4 Discussion

Studying neuronal processes underlying natural human vision in EEG/MEG requires good procedures for artifact reduction and concurrent information about gaze position. Here, we demonstrate a procedure that allows studying cortical signatures of active vision by simultaneously recording EEG/MEG, EOG, and eye position.

Eye tracker and EOG signals have different properties that complement each other. The eye tracker provides accurate information about absolute gaze position and eye movement dynamics, but, given its complicated nonlinear relation to the corneo-retinal artifacts, it is not well suitable for EEG/MEG artifact cleaning. In contrast, the EOG signal allows for efficient artifact cleaning using regression based methods, but, because of drifts in electrical potential, necessary filtering, and the high noise level of the ongoing signal, it is less appropriate to detect saccades and to determine the absolute gaze position.

We employed this setup in an active vision task and analyzed saccade related signal properties. The source analysis based on MRI guided MEG demonstrated that the removed signal originated exclusively from around the eyeballs. Besides well-known SRPs, our analysis revealed saccade related components, which are ipsilateral to horizontal saccade direction during the execution of the saccade and contralateral after the saccade offset. Below we discuss the significance of the findings in regard to artifact cleaning methods and SRPs.

2.4.1 EOG Regression Procedures

To date EOG regression is mainly used: (1) to increase the number of valid trials by removing ocular artifacts due to accidental eye blinks and eye movements (e.g., Pieszek et al., 2013), (2) to allow single trial analysis of brain signals e.g. for brain computer interface applications (e.g., Spüler et al., 2012), (3) to allow studies with subjects that cannot or will not cooperate in avoiding eye movements, such as children and certain groups of patients (e.g., Meier et al., 1998). Just a few studies (e.g., Bellebaum and Daum, 2006, Wauschkuhn et al., 1998) used regression based approaches in order to study saccade related signals.

Here, we used EOG regression cleaning to study active vision, where eye movements are not an unavoidable evil but are a crucial part of the object of investigation. A major challenge with any artifact cleaning procedure is to validate the success in removing ocular artifacts and to demonstrate that no true cerebral sources were removed.

Due to the lack of ground truth control data, a standard procedure is to validate the success of artifact cleaning by a subjective evaluation of the cleaned signals by experts (Joyce et al., 2004, Schlögl et al., 2007, Verleger et al., 1982). Similarly, we affirmed that corrected signals look reasonable, both on the single trial as well as

in the event related average. In particular, we inspected saccade direction specific potentials that are time-locked to saccade onset. This way, remains of the artifact should be apparent, since they would systematically add up and show the artifact specific topography of the CRP.

The EOG regression cleaning seems to reasonably reduce the CRP. After cleaning, we did not find the lateralized topography specific for this artifact. Moreover, we were able to reveal peri- and post-saccadic event related potentials that would otherwise have been buried by the corneo-retinal artifact (see Section 2.3.1).

A recent study by Plöchl et al. (2012) that compared two EOG regression based approaches with ICA seems to be at odds with our results. The authors investigated if EOG regression can clean the CRP, the saccade spike artifact, and blinks at the same time. When employing an arrangement of EOGs that was roughly comparable to our setting, they found an under-correction of the CRP and an over-correction of blinks. This seems to contradict our findings. However, in contrast to Plöchl et al. (2012), we eliminated blink artifacts before the removal of the CRP by EOG regression. Concurrent removal of blinks and CRP might lead to suboptimal correction coefficients because they propagate differently onto the scalp (Croft et al., 2005, Gratton et al., 1983, Picton et al., 2000b). We conclude that regression might provide best results if applied only for reducing the corneo-retinal artifact.

In contrast to the successful reduction of the corneo-retinal artifact, another prominent eye movement artifact remained almost unaffected in the data: Shortly before saccade onset the cleaned data reveal a sharp peak with a fronto-parietal gradient. This potential is known from the literature as the saccadic spike potential, which originates from ocular muscle activity (Becker et al., 1972, Keren et al., 2010a, Yuval-Greenberg et al., 2008). Since it can seriously affect signal measurements especially in high frequency bands (Yuval-Greenberg et al., 2008), it has to be carefully controlled for. For its removal independent component analysis was shown to yield satisfactory results (Hassler et al., 2011, Keren et al., 2010a, Kovach et al., 2011).

We conclude that EOG regression is able to reduce the CRP and can uncover SRPs of probably cerebral origin. For reducing the saccadic spike artifact, however, the regression at least with the current EOG arrangement is not suitable. An REOG component where the signals of a posterior electrode is subtracted from frontal EOG would help to emphasize the saccadic spike artifact in the EOG signal (Carl et al., 2012) and thus support its removal by EOG regression. However, we do not

recommend using such an REOG for regression due to risk in signal loss of true cerebral activity (see below in the same section).

The second concern is the accidental removal of meaningful brain activity. Because volume conduction results in portions of the EEG/MEG signal appearing in the EOG channels, a regression might eliminate true neural activity. It could also artificially introduce neural activity in other EEG/MEG channels. This problem is ignored in most studies employing regression based methods while it is used as counter argument in studies promoting alternative methods (Ille et al., 2002, Jung et al., 2000a,b, Plöchl et al., 2012). In practice, unintentional removal of cerebral sources can occur to all artifact cleaning methods because one can assume that no analysis approach is able to find a complete perfect separation in all situations (Keren et al., 2010a, Nottage, 2010, Shackman et al., 2010). Since experimental evidence for a particular susceptibility of EOG regression to removing cerebral sources is rare (Berg and Scherg, 1994, Croft and Barry, 2002), we directly addressed this problem by localizing the sources of the removed signal in an additional MEG experiment. This source analysis shows that the subtracted signal originated specifically from the eyeballs. Since relative power changes are limited to this area, this source reconstruction suggests that no cortical signal was accidentally removed or added. Consequently, at least for MEG analysis, our results contradict the often-raised critics and suggest that EOG regression can reliably reduce corneo-retinal artifacts without eliminating true neural sources.

Please note that this conclusion solely holds for an EOG regression based on the current EOG electrode setting. Studies using an REOG component where the signal of a posterior electrode is subtracted from frontal EOG have claimed a distortion of cerebral sources by EOG regression (cf. Berg and Scherg, 1994, Croft and Barry, 2002, Plöchl et al., 2012). This probably results from a massive introduction of correlated neural activity by the posterior electrode into the EOG measurements.

To summarize, while regression might be problematic for reducing all ocular artifacts at the same time, our results provide new evidence that supports the validity of EOG regression procedures for removing the corneo-retinal artifact from EEG/MEG.

2.4.2 SRPs

Our results reveal three SRPs that are well-known from the literature (for a review see Jagla et al., 2007). The *antecedent potential* starting approximately $100 - 150$ ms before the saccade onset is considered to be a correlate of saccade preparation. The component monotonically increases up to saccade onset and is characterized by a parietal topography (Csibra et al., 1997, Kurtzberg and Vaughan, 1982). Since it appears before saccade execution the CRP does not substantially affect its appearance. The *saccadic spike artifact* follows at saccade onset. Usually characterized by a biphasic peak, its monophasic appearance in our data suggests that saccade onset might not be precisely aligned but jittered by a few milliseconds (cf. Keren et al., 2010a). The largest component of the SRP is the occipito-parietal, positive *lambda response*, which was reported to peak between $100 - 200$ ms after saccade onset. The lambda response is thought to reflect the processing of the visual input at the new location of fixation (Jagla et al., 2007, Kazai and Yagi, 2003, Thickbroom et al., 1991). In short, our analysis reproduced the known potentials related to saccade planning, ocular muscle contraction and post-saccadic visual processing.

2.4.3 Lateralized SRPs during Saccade Execution

After CRP removal, our analysis of direction specific signatures of horizontal saccades revealed lateralized parietal potentials. In particular, during the time of saccade execution, the SRP was larger at ipsilateral than at contralateral occipito-parietal sensors. This time span is critical for trans-saccadic perception (Melcher and Colby, 2008): Although humans perform approximately 3 saccades a second causing major changes of the retinal image, we perceive the visual input as smooth and predictable. Corollary discharge signals, which convey a copy of the motor command signal to visual processing regions, are thought to be one mechanism that allows the visual system to compensate for the self-generated movement induced changes in visual input (Sommer and Wurtz, 2008). The lateralized component we find during saccade execution might be related to processes of sensory prediction due to corollary discharges. We elaborate on this in the following.

Lateralized responses of sensorimotor regions like the parietal eye fields are known to be preferentially contralateral to both, the stimulus and the direction of the upcoming saccadic movement (Everling et al., 1998, Kagan et al., 2010, Silver

and Kastner, 2009, Van Der Werf et al., 2008, Van Pelt et al., 2010). During saccade execution, we found an occipito-parietal increase in amplitude of the SRP, that was lateralized to the ipsilateral side of saccade direction. This might be surprising at first sight, given the contralateral preference during saccade preparation.

One obvious candidate for this lateralized potential would be residual activity from the CRP. This seems unlikely, given its topographic distribution and the fact that the polarity of the lateralization switches 100 ms after saccade onset. Such a polarity switch is not easily explainable by potential residuals of the CRP, which would presumably be unchanged 100 ms after the saccade onset (cf. the raw signal in Figure 2.3C, third column). Also, such topography is unlikely to result from the saccadic spike potential, which shows a very different topographic distribution in the *right-left* contrast (cf. first column of Figure 2.3B and 2.3C).

Ipsilateral signals related to saccades have been observed in so-called remapping paradigms in human electrophysiological and fMRI studies (Bellebaum and Daum, 2006, Merriam et al., 2003, Parks and Corballis, 2010). In these paradigms a large saccade between two horizontally placed fixation targets shifts the cortical representation of a peripheral stimulus in between them from one hemisphere to the other. Hence, the future post-saccadic location of the stimulus representation is ipsilateral to the saccade direction. Interestingly, neural activities for this future visual stimulation have been observed already before and during the saccade. And neural activities can encode the remapped visual stimulus after the saccade in conditions where the visual stimulus has already disappeared by then (cf. Duhamel et al., 1992, for a study in monkeys showing both phenomena). Remapping has been interpreted as a predictive activity of future sensory events based on incoming information about the saccade.

Our experimental paradigm was not designed to show such remapping processes. In contrast to the mentioned studies, we find an ipsilateral bias during the execution of saccades to fixation targets in *absence* of additional visual stimuli. Therefore, we can only hypothesize that a remapping might have occurred. For example the illuminated screen in contrast to the darkened room might have been remapped when a saccade was required from one border of the screen to the other. In many other ways, our paradigm is not comparable to the existing electrophysiological studies on remapping. For example, both, Parks and Corballis (2010) and Bellebaum and Daum (2006) compared the remapping condition to a control condition where a saccade was performed without a visual stimulus presentation. Therefore, it is too

hypothetical to compare our results in detail to these existing findings. During eye movements in the dark ipsilateral increases in occipital channels shortly after saccade onset ($\sim 72 - 92$ ms afterwards) were also found by Skrandies and Laschke (1997) and related to inputs from corollary discharges. However, they did not report any ocular artifact correction procedure, which could possibly have distorted results. We conclude that further studies are needed to confirm that the observed ipsilateral potentials during execution are indeed related to updating processes based on corollary discharges. Most importantly, we consider the appearance of such a lateralized potential during the saccade execution, where artifact contamination is maximal, as a proof of principle for the success of the EOG regression cleaning.

2.5 Conclusion

We demonstrated that the analysis of potentials appearing during gaze shifts is possible after the removal of the corneo-retinal artifact with EOG regression. As a first step towards active vision paradigms, we have characterized the electrophysiological correlates of visually guided saccades and revealed saccade direction specific mechanisms reminiscent of spatial updating. Our results suggest that combined EEG and eye tracking, if coupled with appropriate ocular artifact cleaning procedures, provides promising means for addressing fundamental unanswered questions in natural, active vision.

3

The Saccadic Spike Artifact in MEG and EEG (Study 2)

The content of this chapter has been published in Neuroimage: Christine Carl[1,2], Alper Açık[2], Peter König[1,2], Andreas K. Engel[1], Joerg F. Hipp[1,3] (2012) The saccadic spike artifact in MEG.

[1]Department of Neurophysiology and Pathophysiology, University Medical Center Hamburg-Eppendorf, Germany [2]Institute of Cognitive Science, University of Osnabrück, Germany [3]Centre for Integrative Neuroscience, University of Tübingen, Germany

C Carl designed the experiment and performed the experimental recordings and data analysis. J Hipp provided advice for design and analysis and contributed unpublished analytic tools. C Carl and J Hipp wrote the manuscript. A Açık, P König, and AK Engel provided general ideas and contributed to the manuscript.

3.1 Introduction

EEG and MEG are the means for investigating neuronal dynamics non-invasively in the human brain. However, these measures are also sensitive to other physiological sources like heartbeat, muscle activity or the rotation of the eyeball during eye movements. This compound nature of EEG/MEG signals can substantially complicate the interpretation of recorded data. A detailed knowledge of the non-neural sources affecting these measures is thus critical to allow an unequivocal description

of neuronal processes.

The saccadic spike is an important example of such an artifactual signal. It is observed at the onset of even tiny saccadic eye movements. The saccadic spike artifact is characterized by strong electric transients that are believed to reflect the contraction of the extraocular muscles in the orbit (Boylan and Doig, 1989b, Kovach et al., 2011, Moster and Goldberg, 1990, Riemslag et al., 1988, Thickbroom and Mastaglia, 1985, Yuval-Greenberg et al., 2008) although some studies provide evidence for cortical contributions (Balaban and Weinstein, 1985, Brooks-Eidelberg and Adler, 1992, Csibra et al., 1997). In order to account for the effect of the saccadic spike artifact on neurophysiological measurements, one needs to first understand its statistics of occurrence and second characterize its temporal, spectral, and spatial properties.

Under free viewing conditions humans perform approximately three saccadic eye movements per second. Even when attempting to fixate humans execute spontaneous miniature saccades (i.e., microsaccades and saccadic intrusions) with an average rate of one to two saccades per second (Gowen et al., 2007, Martinez-Conde et al., 2009). Importantly, saccade rate, amplitude, and direction are modulated by sensory stimulation and task demands (Engbert, 2006, Engbert and Kliegl, 2003, Gowen et al., 2005, 2007, Laubrock et al., 2005, 2010, Reingold and Stampe, 2002, Rolfs, 2009, Rolfs et al., 2008, Valsecchi et al., 2007, 2009, Yuval-Greenberg et al., 2008) and have been linked to perceptual processes (Laubrock et al., 2008, Troncoso et al., 2008, van Dam and van Ee, 2006). Moreover, the rate of eye movements is altered in clinical populations (Martinez-Conde, 2006). This makes saccades and thus saccadic spikes omnipresent features of the visual system, whose occurrence is often modulated along with experimental contrasts.

The effect of the saccadic spike on EEG and iEEG has been studied in great detail. Both, regular saccades and miniature saccades produce at their onset a biphasic transient artifact of approximately 22 ms duration referred to as the saccadic spike potential (SP; Jerbi et al., 2009, Keren et al., 2010a, Kovach et al., 2011, Riemslag et al., 1988, Yuval-Greenberg et al., 2008). The topography of the SP at its first peak is characterized by a minimum at frontal electrodes and a maximum at posterior electrodes, while the potential gradient is steepest around the eyes. The amplitude values depend on the choice of the EEG reference. For the average reference as used throughout the paper, the SP is characterized by a distribution of negative electrical potential at frontal electrodes and positive potential at parietal and occip-

ital electrodes. This distribution is inverted at the second deflection (Csibra et al., 2000, Keren et al., 2010a, Thickbroom and Mastaglia, 1985, Yuval-Greenberg et al., 2008). In iEEG, the SP is largest at medial and ventral portions of the temporal pole (Jerbi et al., 2009, Kovach et al., 2011). The topography of the SP is lateralized ipsilateral to saccade direction (Keren et al., 2010a, Kovach et al., 2011, Moster et al., 1997, Thickbroom and Mastaglia, 1985) and its amplitude depends on saccade size (Armington, 1978, Boylan and Doig, 1989a, Keren et al., 2010a, Kovach et al., 2011, Riemslag et al., 1988). The power spectrum of the SP is characterized by a broadband peak in the gamma band from roughly 30 to 120 Hz (Jerbi et al., 2009, Yuval-Greenberg et al., 2008).

Due to its spectral properties and statistics of occurrence the SP artifact resembles neuronal gamma band activity (Kovach et al., 2011, Reva and Aftanas, 2004, Schwartzman and Kranczioch, 2011, Trujillo et al., 2005, Yuval-Greenberg et al., 2008). Particularly problematic is the fact that microsaccades and regular saccades follow a characteristic inhibition-enhancement sequence after visual and auditory stimulation that is not precisely time-locked to stimulus onset. The saccadic spike artifact occurring at every saccade onset therefore mimics an induced (non-phase locked) gamma band response to stimulus presentation at parietal EEG sensors. Notably, the effect size depends on the choice of the EEG reference. Since saccade statistics change with sensory stimulation and cognitive demands, the SP's artifact signature is often modulated along with experimental contrasts. Thus, the close resemblance of the SP to neurophysiological activity in combination with stimulation and task dependent saccade statistics constitutes a serious problem for the interpretation of the EEG data. However, the detailed knowledge on the SP's temporal, spectral, and spatial properties provides a good basis to assess confounds of neuronal signals. It is now widely agreed on that any EEG study needs to carefully control for possible SP confounds (Keren et al., 2010a, Schwartzman and Kranczioch, 2011, Yuval-Greenberg et al., 2008).

The currents in neuronal and muscular tissue generating the electrical potential measured with EEG also induce a magnetic field that can be measured with MEG. MEG complements EEG with respect to its high sensitivity for tangential sources and, since magnetic fields are less distorted by the head's tissue properties, provides an excellent basis for source analysis (Hämäläinen et al., 1993). Similarly to the SP in EEG, MEG data should be confounded by a magnetic saccadic spike field (SF). It has been speculated that the saccadic spike artifact is of minor importance for

MEG (Fries et al., 2008, Schwartzman and Kranczioch, 2011) but direct evidence is missing (but see the poster of Keren et al., 2010b, at the HBM 2010 conference). Here, we measure the SF in MEG during a memory-guided delayed saccade task. We provide a detailed temporal, spatial and spectral characterization of the SF both for guided regular as well as spontaneous miniature saccades. We investigate the effects of horizontal saccade directions and saccade sizes on the amplitude and topography of the SF and compare the SF to the SP from concurrent EEG recordings. Furthermore, we estimate the origin of the SF using distributed source analysis.

Our findings demonstrate that the saccadic spike artifact may seriously confound neurophysiological signals in MEG. The detailed characterization of the phenomenon provides a solid basis for assessing possible SF confounds in future MEG experiments. Furthermore, our study constitutes the first step towards developing tools for separating the saccadic spike artifact from MEG data.

3.2 Materials and Methods

3.2.1 Participants

Thirteen healthy volunteers participated in this study (10 female, mean age 27.5). Subjects received monetary compensation for their participation. All participants had normal or corrected-to-normal vision, and had no history of neurological or psychiatric illness. The study was conducted in accordance with the Declaration of Helsinki and informed consent was obtained from all participants prior to recordings.

3.2.2 Behavioral Task and Stimulation

Participants performed a delayed saccade task with horizontal saccades of two different amplitudes (Figure 3.1). At the beginning of each trial, subjects fixated for 800 ms a blue asterisk in the center of the screen. Surrounding the asterisk, 16 Gaussian patches were regularly arranged on an inner and outer circle (distance from the asterisk: 5.5° and 11° respectively). The 4 Gaussian patches on a horizontal line in the center of the screen served as saccade targets corresponding to four experimental conditions: leftwards long and short saccades and rightwards long and short saccades. Following fixation, the central asterisk underwent a 200 ms isoluminant color change to green with a red colored marker. The position of the red marker in-

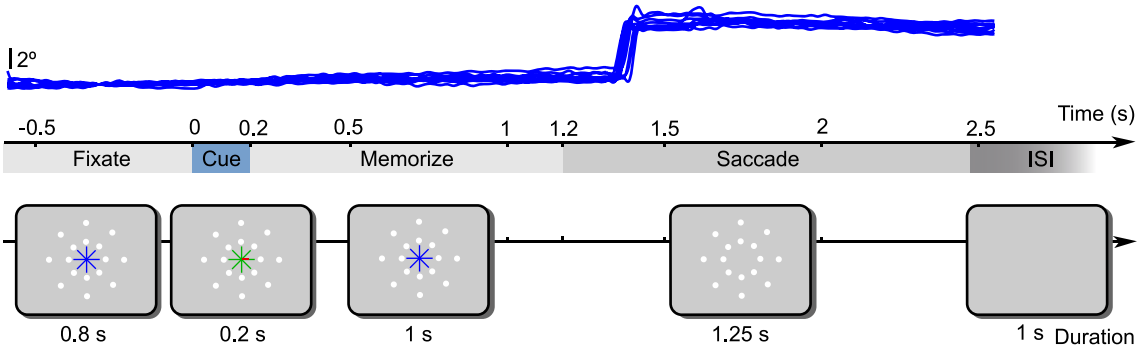

Figure 3.1: Experimental task. Subjects were asked to fixate the blue asterisk in the center of the screen. An intermittent color change to green with a red marker informed about the target location for the saccade. Targets were Gaussian patches located on the horizontal line passing the center. In the depicted example, the subject was instructed to plan a saccade to the inner point on the right side. Subjects waited for 1 s until the asterisk disappeared before executing the saccade. Top: representative eye traces of one participant over the first 10 trials with a saccade to the inner right target.

dicated for each trial one of the four target locations and instructed the participants to prepare a saccade. If the red marker covered the inner part of an asterisk's branch it indicated a small saccade, if it covered the outer part of the asterisk's branch it indicated a large saccade. The side of the marked branch informed the participants of the saccade direction. During the following delay period of 1 s participants had to maintain fixation. Then, the asterisk disappeared. This 'go' signal instructed the subjects to perform the saccade. Subjects should maintain fixation at saccade target until it disappeared after 1.25 s. Between trials, a blank screen was presented for 1 s. In total each subject performed 500 trials (125 for each condition). Trials of all four experimental conditions were randomly presented.

During the experiment, participants were seated in the MEG chamber. Stimuli were back-projected onto the screen at 54 cm distance with a liquid crystal display video projector (Sanyo XP51 Beamer, 60 Hz refresh rate) and a two-mirror system. Stimuli were presented using the software Presentation (Neurobehavioral Systems, Albany, CA).

3.2.3 Analysis Software

All data analyses were performed in Matlab (MathWorks, Natick, MA) with custom software and the open source toolboxes Fieldtrip (Oostenveld et al., 2011) and SPM2 (`http://www.fil.ion.ucl.ac.uk/spm/`).

3.2.4 Data Acquisition and Preprocessing

3.2.4.1 MEG

We recorded MEG continuously with a 275-channel (axial gradiometer) whole-head system (CTF275, VSM MedTech) in a magnetically shielded room. Two sensors were not operating resulting in a total of 273 sensors. MEG data were digitized at 1200 Hz sampling rate (300 Hz low-pass filter). Off-line, we removed line-noise with notch-filters (at 50, 100, 150 Hz), low-pass filtered the data to 170 Hz (zero phase Butterworth IIR filter, filter order 4) and down sampled it to 400 Hz.

3.2.4.2 EEG/EOG

Along with the MEG, we recorded EEG using the EEG channels of the CTF MEG system. Data were collected with an analog passband of $0.16 - 300$ Hz at a sampling rate of 1200 Hz. We used 32 Ag/AgCL sintered flat electrodes (Easycap GmbH, Herrsching, Germany) arranged according to the $10 - 20$ system and two electrodes at the mastoids. Additionally, we recorded a bipolar electrocardiogram and the EOG from 7 electrodes. EOG electrodes were placed over the nose, above and below each eye at the outer canthi and below the left and right eye next to the nose. Data were referenced to an electrode placed at the tip of the nose during the recording. All electrode impedances were below 15 kΩ.

Off-line, the EEG data were re-referenced to the average of the 32 EEG electrodes. The EEG and EOG were low-pass filtered (cut-off 170 Hz, zero phase Butterworth IIR filter, filter order 4). EOG data were re-referenced to the electrode 'Pz'. For three subjects we discarded the right inner infraorbital EOG channel because of poor signal quality. We then derived the radial EOG (REOG; Keren et al., 2010a) as the average of all EOG channels.

3.2.4.3 Structural MRI acquisition

We acquired individual T1-weighted high-resolution structural images (MRIs) of each subject with a 3 T Siemens MAGNETOM Trio Scanner using a coronal magnetization-prepared rapid gradient echo sequence. These MRIs were used to construct individual head models for source analysis (see below).

3.2.4.4 Eye tracker recording

Along with the neurophysiological data we recorded the eye position using an MEG compatible remote eye tracker system (iView X MEG 50 Hz, SMI, Berlin, Germany). The system monitored the right eye with an infrared camera to detect the pupil center and the corneal reflection of the infrared light source. After calibration (9 points) the system determined the gaze direction from the relative position of pupil and the corneal reflection at a rate of 50 Hz. Additionally, digitized eye traces were interpolated to match the MEG/EEG sampling rate (1200 Hz), digital to analog converted and fed to the MEG system on-line. This on-line procedure introduced temporal offsets of the eye tracker signal in relation to the MEG/EEG data. Moreover, the digital to analog conversion produced undesirable ringing artifacts. Therefore, the analog signal recorded along with the MEG/EEG just served as a coarse reference for the first alignment of the eye tracker and MEG/EEG signals.

Off-line, we aligned the digital eye tracking data to the MEG/EEG in a 2-step procedure. First, we interpolated the 50 Hz signal to 400 Hz using cubic smoothing splines and computed the cross-correlation of the interpolated digital eye tracker signal with the analog version recorded with the MEG acquisition system. Then we accounted for the offset identified by the latency of the peak in the cross-correlogram. In a second step, we refined the alignment and corrected for the offset between the EOG and the aligned eye tracker signal. To this end, we smoothed the data with a Savitzky-Golay filter (4^{th} order, 102.5 ms) rectified and averaged all channels of both, the EOG and the eye tracker signals, and estimated the offset from the peak of the cross-correlation.

To improve the quality of the eye tracker signal, we interpolated missing data. We detected periods with loss of eye tracking signal characterized by pupil size and gaze position values close to zero. If these data segments were not identified as blinks (see below), we interpolated the missing data by piecewise constant interpolation.

3.2.4.5 Artifact rejection

Trials contaminated with muscle artifacts, signal jumps or distortions of the magnetic field due to, for example, cars passing in front of the building were rejected off-line using semi-automated threshold procedures applied to the MEG signals. Since eye movements are part of the experimental design, standard EOG based procedures to detect eye blinks fail. We detected eye blinks using a combination of eye

tracker and EOG signals. Data with vanishing pupil diameter and fast changes in the EOG signal were identified as blink artifacts. Finally, we inspected all MEG, EEG and EOG signals manually to ensure good artifact rejection performance. On average $9.5 \pm 3.6\%$ (mean $\pm$ sd) of the trials were rejected.

3.2.5 Data Analysis

3.2.5.1 Behavioral analysis

For detection of regular saccades we employed a velocity threshold based algorithm. If coupled with a minimum saccade duration criterion, this algorithm has very few parameters and is accurate in the face of stereotypical eye-movements such as those analyzed here (Salvucci and Goldberg, 2000). Because the optimal velocity threshold parameter depends on preprocessing and sampling of the recorded data, as well as on saccade amplitudes, we defined the velocity threshold in a data-driven approach. We adapted the thresholds manually for the saccade amplitudes in our task (5.5° and 11°) so that saccades were detected while the number of false positives was minimized. We achieved this by visual inspection of the data, taking into account a priori knowledge on saccade timing. We defined periods as regular saccades in which the eye movement velocity was higher than 28.6°/s for a duration of at least 22.5 ms. Periods where the saccade velocity exceeded 53.7°/s were defined as saccades irrespective of saccade duration. We combined all saccade intervals that were less than 7.5 ms apart from each other into a single saccade interval. All other periods were labeled fixations.

The behavioral analysis revealed that subjects had a considerable variability in saccade onset and also initiated saccades before the 'go' signal. However, since this study focused on the stereotypic saccadic spike, we were not concerned about the exact timing of the saccades in general. We were only interested in ensuring that subjects performed saccades to the cued goal as instructed. To maximize the number of trials to analyze, we accepted trials with saccades that were performed within a broad time window from 500 ms before to 770 ms after the 'go' signal. We excluded trials before 500 ms because they were unlikely to be related to the instruction and saccades later than 770 ms to ensure sufficient data following the saccade for subsequent analysis. In a next step, we rejected all trials with wrong saccade orientation or amplitude. For saccade categorization we applied drift correction at the fixation

period before the cue onset (−300 ms to −100 ms) and ensured that the subjects fixated the asterisk before saccade onset within a tolerance angle of 2.3°. The saccade target was considered correct if the closest location was the cued one. Overall we discarded $13.5 \pm 12.7\%$ (mean ± sd) of the trials because of faulty behavioral performance.

Additionally, we analyzed miniature saccades that occurred within the period from onset of the directional cue and onset of the guided regular saccade. We defined miniature saccades using a threshold procedure applied to the REOG: The $30 - 100$ Hz band-pass filtered REOG signal was convolved with an SP-template (provided by Keren et al., 2010a) and convoluted data segments exceeding 3 standard deviations were detected. Every detected event whose amplitude did not exceed 2° visual angle was defined as a miniature saccade. Miniature saccades occurred at an average rate of 1.45 ± 0.34 per second (mean ± sd) and followed a characteristic inhibition-enhancement sequence after directional cue presentation. Note that the low sampling rate of the eye tracker (50 Hz) did not allow reliable microsaccade detection based on eye tracker recordings.

3.2.5.2 Alignment of trials for saccadic spike characterization

Independent of saccade type or different saccade metrics, the saccadic spike is generated consistently at saccade onset (Keren et al., 2010a). However, saccade detection based on threshold procedures introduces imprecision in the estimated saccade onset and generates jitter in the timing of the saccadic spike over trials. When investigating the average SP or SF over trials we had to correct for this jitter. We aligned each trial to the first trough of the REOG within a time window of ±30 ms from detected saccade onset (Keren et al., 2010a, Kovach et al., 2011). This alignment procedure was applied to miniature and regular saccades for all analyses where we examined the temporal and spatial characteristics of the average saccadic spike.

3.2.5.3 Description of the saccadic spike on sensor level in MEG and EEG

We calculated the time course as well as the topography of the event related average of the saccadic spike for MEG and EEG. For the topographies we provide, in addition to the event related average for MEG and EEG, the root-mean-square of the SP and the planar gradient estimation of the SF for MEG. A baseline of 280 to 180 ms before

saccadic onset was subtracted from the average time course of the MEG/EEG data.

The saccadic spike artifact occurs simultaneously with another eye movement related artifact – the rotation of the corneo-retinal dipole, also known as corneo-retinal potential (CRP) in EEG. This rises slowly and adds to the saccadic spike artifact. It was shown that it heavily distorts the second deflection of the biphasic spike in EEG (Keren et al., 2010a, Riemslag et al., 1988). Therefore, we focused on the first deflection of the saccadic spike to study its topography. We used a baseline directly at saccade onset (7.5 ms before the first saccadic spike peak, onset was defined by the grand average time course of the eye trace). By using this single point baseline, we maximally separate the signal of the saccadic spike artifact from other signals related to saccade generation and preparation like the antecedent potential (Armington, 1978, Jagla et al., 2007, Kurtzberg and Vaughan, 1982), which starts approximately $100 - 150$ ms before saccade onset.

We assessed statistical significance for the event related amplitude of the saccadic spike across subjects (random effects) by applying Student's t-test, ($n = 13$ with n: number of participants) at each sensor. We accounted for multiple comparisons using Bonferroni correction ($\alpha = 0.01$, corrected for the number of sensors).

Next to event related potentials, another commonly used measure in EEG is the root-mean-square. Consequently, we additionally report this measure for the SP. In short, we calculated for each subject individually the root-mean-square of the baseline corrected event related average across the time points of the first peak of the SP (time: $t > 0$ ms, $t < 12.5$ ms, baseline: time $t = 0$). We present the average of the root-mean-square over subjects.

Most MEG systems use either axial or planar gradiometers to record the magnetic fields. The system we used has axial gradiometers. To provide a general description of the SF we additionally computed a planar gradient estimate for our results. To this end, we combined horizontal and vertical estimates of the planar gradient of all sensors for each subject's baseline corrected SF (Bastiaansen and Knösche, 2000). To assess where amplitude deflections of the planar gradient estimate were consistently highest across subjects, we normalized the planar gradient estimation of each subject's SF to a standard normal distribution and tested for statistical significance of the positive deflections with a one-sided Student's t-test over subjects ($\alpha = 0.01$, Bonferroni corrected for the number of sensors).

For visualization we show topographies with the physical quantities (electrical potential and strength of magnetic field). These topographies are statistically

masked such that values that do not reach statistical significance are presented with a semi-opaque white cover.

3.2.5.4 Lateralization of the saccadic spike artifact

We analyzed topographies of the saccadic spike for leftwards and rightward saccades separately. For this purpose we computed the saccadic spike at the time of maximal lateralization, which was derived as the maximal difference in amplitude between ipsi- and contralateral EOGs in relation to saccade direction (5 ms after saccade onset).

3.2.5.5 Spectral characteristics of the SF for regular and miniature saccades in MEG

To investigate the spectral characteristics of the saccadic spike in MEG we derived a time-frequency representation of the SF using Morlet's wavelets (Tallon-Baudry et al., 1996). The characteristic parameter for the wavelet family was, $f/\sigma_f \approx 5.8$ where σ_f is the spectral smoothing and f is the center frequency. We calculated the frequency transform at 25 logarithmically equidistant center frequencies from 16 to 128 Hz. We computed the transform for discrete time points at -100 ms to 100 ms in 10 ms steps (baseline estimated from the average at time $t = -400$ ms to -350 ms, in 10 ms steps, baseline for miniature saccades: $t = -135$ ms to -85 ms in 10 ms steps). For statistical analysis we log-transformed the power estimates to render distributions more normal and computed a Student's t-test on the difference in power relative to baseline over participants. Since the saccadic spike effect size is statistically weaker at a particular point in the time-frequency representation than at the peak in the time domain we used a less conservative method for multiple comparison correction. We controlled for multiple comparisons using false discovery rate (FDR) correction with $q = 0.01$ (Benjamini and Hochberg, 1995, Genovese et al., 2002).

3.2.5.6 Physical forward model for source analysis

To estimate neural activity at the source level, we first derived physical forward models for each subject. To this end, we defined a regular grid (0.7 cm spacing) in MNI space that comprised, in addition to the cortex, the region of the eyeballs and extraocular muscles. We affine transformed this grid into individual head space

using the participants' individual MRI, and aligned the MEG sensors to the head geometry based on 3 fiducial points (nasion, left and right ear, defined in the MEG by 3 head localization coils). To derive the physical relation between sources and sensors we employed a single-shell volume conductor model (Nolte, 2003). On top of the regular grid, we computed leadfields for the center location of the extraocular muscles. The location of the contralateral center of the extraocular muscles was used for suppression in the beamforming source analysis (see below). We defined these positions manually in the MNI template brain (Holmes et al., 1998, $MNI = [-28, 38, -37]$ for left hemisphere, $MNI = [28, 38, -37]$ for right hemisphere).

3.2.5.7 Source analysis of the SF using beamforming

We used adaptive linear spatial filtering (*beamforming*; Gross et al., 2001, Van Veen et al., 1997) with coherent source suppression (Brookes et al., 2007, Dalal et al., 2006) to estimate the amplitude of signals at the source level. The coherent source suppression approach accounts for the highly synchronized electrical activity of the extraocular muscles across the hemispheres (Kovach et al., 2011) that would otherwise lead to signal cancelation in beamforming. In short, for each source location, three orthogonal linear filters (for the three orientations at each source) were computed that pass activity from that location with unit gain and block activity from dipoles of any orientation at the location of the contralateral extraocular muscles, while maximally suppressing activity from any other source. Subsequently, the filters were linearly combined to a single filter that points to the direction of the dominant dipole (Hipp et al., 2011).

Before deriving source estimates of the SF, we band-pass filtered the event related signal by convolution with a 3-point filter to attenuate residual contributions from the corneo-retinal artifact. The 3-point filter was adapted to the temporal structure of the biphasic saccadic spike signal (filter kernel: -0.5 at -7.5 ms; 1 at 0 ms; -0.5 at 5 ms). Then, we estimated the covariance matrix that is needed for the beamforming filter from concatenated data epochs ± 30 ms around the first SF peak of all saccades. The average difference between the first peak of the SF and the baseline at the onset of the SF was then projected into source space. The absolute value served as a source estimate. This source estimate is subject to a positive bias. To account for this problem, we estimated and subtracted the bias. To this end, we randomly permuted the SF peak and SF baseline and estimated the source

distribution for these data 1000 times. The average served as a bias estimate. Finally, we derived the neural activity index (NAI) of the source estimate that accounts for the spatial bias of beamforming for deep sources (Van Veen et al., 1997). For statistical analysis, we computed Student's t-test of the NAI at each voxel across subjects ($\alpha = 0.01$, Bonferroni corrected for the number of voxels). Furthermore, we used a variant of beamforming for frequency domain data (Gross et al., 2001) to estimate the sources at 64 Hz at the time of saccade onset (temporal smoothing = 87 ms, frequency smoothing = 21.96 Hz). We derived a filter estimation from the real part of the cross-spectral-density matrix (cf. Hipp et al., 2011) at the time of saccade onset and baseline ($t = -400$ to -350 ms for regular saccades, $t = -135$ to -85 ms for miniature saccades) and computed the relative change of the signal power. The logarithmic transform of the average power source estimates at saccade onset and at baseline entered the statistical analysis. We tested at each voxel for significance of the difference of those power estimates over subjects using the Student's t-distribution ($q = 0.01$, FDR corrected for the number of voxels).

For visualization we overlaid the functional data onto the structural MRI of the MNI template brain, masked non-significant values and interpolated the source data to 1 mm resolution.

3.2.5.8 Dipole fitting of the SF

To further investigate the sources underlying the lateralization of the saccadic spike of horizontal saccades, we employed dipole fitting in addition to the distributed source analysis. For each subject and saccade direction, we fitted two equivalent current dipoles. We optimized the dipole orientation while dipole position was fixed to the previously defined center of the extraocular muscles (left dipole: $MNI = [-28, 38, -37]$ and right dipole: $MNI = [28, 38, -37]$). Average explained variance of this dipole model was 77.43%. To summarize and visualize the subjects' individual dipole orientations, we projected each subject's normalized dipole onto a common plane. This plane was defined in the MNI template brain by the vector connecting both dipole positions and an orthogonal projection of the average orientation vector of all medial and lateral rectus muscles. We then computed the mean angle between dipoles for leftwards and dipoles for rightwards saccade trials. We tested for significant rotation of dipoles between saccades to the left and to the right using a nonparametric random permutation test (Nichols and Holmes, 2002).

This had the advantage that we did not need to make any assumption about the distribution of the rotation angles. We derived a null-hypothesis distribution by 1000 times randomly permuting saccade labels *right* and *left* and computing the mean angle between dipoles and then determined the p-value.

3.2.5.9 Comparison of the SF and SP for miniature and regular saccades

We quantified the similarity of scalp topographies of the SF for miniature and regular saccades by computing the linear correlation across sensors. To assess differences in SF and SP amplitudes, we computed the absolute SF/SP amplitude for miniature, 5.5°, and 11° saccades at channels of interest (see inset, Figures 3.7C and D) and tested for pairwise amplitude difference across subjects, using Student's t-test (Bonferroni corrected for 2 comparisons).

3.3 Results

3.3.1 The Saccadic Spike Artifact in MEG and EEG

To investigate the effect of the saccadic spike on MEG/EEG signals we performed a delayed saccade experiment with targets at two distances (5.5°/11°) and two directions (left/right). In each trial, a directional cue instructed participants about the saccade target location. Participants memorized the location during a delay period of 1 s before they actually performed the saccade (Figure 3.1).

First, we analyzed the grand average time course of the saccadic spike artifact pooled over both saccade directions and both amplitudes. To this end, we aligned the signals to saccade onset and subtracted a baseline from 280 to 180 ms before the saccade (Figure 3.2A). The average saccade duration was about 50 ms, while the eye movement velocity peaked around 30 ms after saccade onset (Figure 3.2A, first panel). The time course of the REOG (i.e. the average signal of all EOG channels relative to the parietal electrode 'Pz'), the EEG, and the MEG revealed a brief biphasic saccadic spike at saccade onset. The saccadic spike artifact peaked around 7.5 ms after saccade onset, inverted its polarity, and peaked again 15 ms after saccade onset (Figure 3.2A, lower three panels). The second peak of the saccadic spike artifact was overlaid with the concurrent corneo-retinal artifact reflecting the

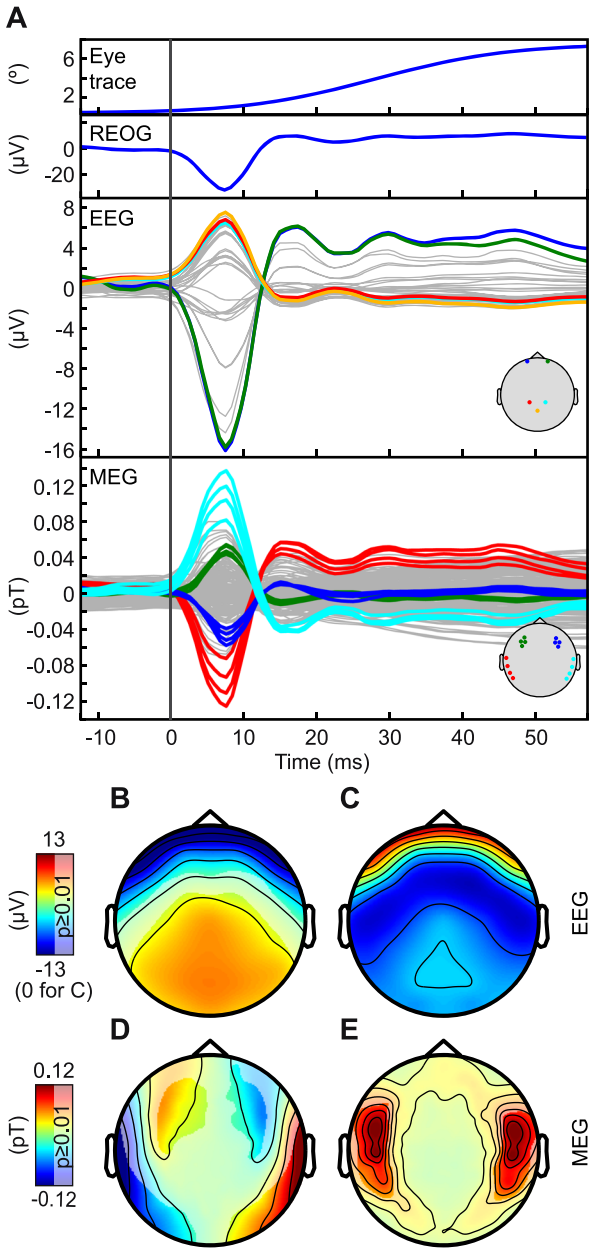

Figure 3.2: SP and SF time course and topography in EEG and MEG sensor space. A. Grand average time course of baseline corrected REOG, EEG and MEG signals pooled over all saccade target locations (baseline from time $t = -280$ ms to -180 ms; saccade onset at time $t = 0$ ms). The eye trace shows the average distance from the fixation point at baseline. Trials were aligned to the first SP peak of the REOG channel (Keren et al., 2010a). Sensors for the highlighted time courses were selected according to the topographic distribution of the SP/SF potential (see B and D) and are illustrated in the insets. Time courses of all other sensors are shown in gray. B to E. Topographies of the SP/SF at the first peak of the saccadic spike (time $t = 7.5$ ms, indicated by the dashed line in A) baseline corrected by the signal at saccade onset (time $t = 0$ ms). Unmasked regions (i.e. intense color scale) in B, D and E denote significant difference to zero (t-test, $p < 0.01$, Bonferroni corrected). B. Event related potential of the EEG. C. Root-mean-square of the EEG. D. Event related field for MEG axial gradiometers. E. Event related field for MEG planar gradiometer estimates.

rotation of the corneo-retinal dipole (Keren et al., 2010a). To isolate the SF or SP, we therefore focused the following analyses on the first deflection of the saccadic spike.

The subjects' average scalp topography of the SP in EEG was characterized by a strong negative potential of up to -16 μV at frontal sensors and a moderate positive potential of up to 8 μV at parietal sensors (Figure 3.2B; average reference; $p < 0.01$, Bonferroni corrected for $n = 32$ sensors). Accordingly, the root-mean-square of the

EEG peaked at similar frontal and parietal sensors (Figure 3.2C). Two sensor types are commonly used in MEG systems, axial gradiometers and planar gradiometers (Hämäläinen et al., 1993, Hämäläinen, 1995). Our MEG setup uses axial gradiometers. However, in the following description of the MEG sensor topographies we also present an estimate of the corresponding planar gradiometer representation (see Section 3.2). The SF in MEG was characterized by increases and decreases at frontal and temporal sensors for axial gradiometers (Figure 3.2D; $p < 0.01$, Bonferroni corrected for $n = 273$ sensors). The average absolute amplitudes across subjects were highest at temporal sensors reaching 14 pT. In the corresponding planar gradient representation the strongest effect of the SF was at the anterior half of the temporal sensors (Figure 3.2E; $p < 0.01$, Bonferroni corrected for $n = 273$ sensors). In conclusion, both MEG and EEG sensors were strongly affected by the saccadic spike. However, the spatial topography differed substantially. In particular, the SF in MEG did not significantly affect parietal sensors.

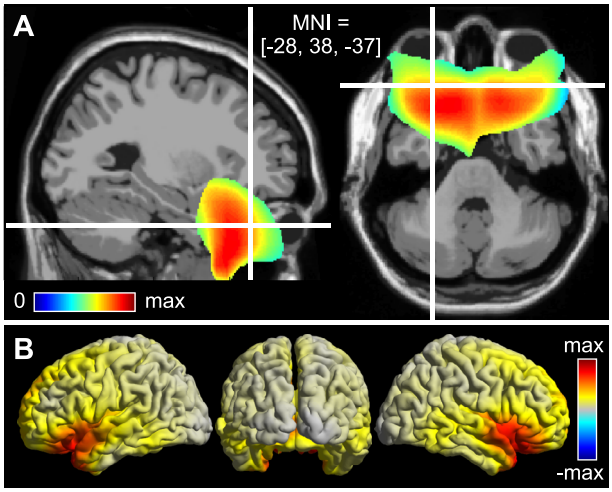

Figure 3.3: SF sources in the extraocular muscles. A. Source analysis using beamforming of the first peak of the SF. The saccadic spike artifact is localized to the region of the extraocular muscles of both eyes. The average neural activity index (NAI) masked by statistics (t-test, $p < 0.01$, Bonferroni corrected) is overlaid on the MNI template brain. B. Surface projection of the SF source without statistical mask.

3.3.2 Source Analysis of the Saccadic Spike

Next, we analyzed the sources of the saccadic spike. We used adaptive linear spatial filtering (beamforming) applied to the broadband SF signal. The sources were

localized to the extraocular muscles of both eyes (Figure 3.3A; $p < 0.01$, Bonferroni corrected for $n = 11,078$ voxels). To elaborate on the spatial specificity of these sources, we omitted statistical thresholds (Figure 3.3B). The activity of the sources of the saccadic spike artifact dropped from the maximum at the extraocular muscles without revealing any other prominent local maxima. Thus, source analysis using beamforming, spatially separated the SF from other neurophysiological signals into the region of the extraocular muscles.

3.3.3 Spectral Signatures of the Saccadic Spike in MEG

We used time-frequency analysis to study the spectral characteristics of the saccadic spike artifact in MEG. The spectro-temporal pattern was characterized by a broadband gamma frequency range increase ($\sim$ 32 to 128 Hz) around the time of saccade onset (Figure 3.4A; $p < 0.01$, FDR corrected for $n = 21 \times 25$ time$\times$frequency points). The strongest power increase at -10 to 30 ms and 64 Hz was at frontal and temporal sensors. The source distribution for this frequency range was highly similar to that of the event related response (Figure 3.4B; $p < 0.01$, FDR corrected for $n = 11,078$ voxels; compare to Figure 3.3). Thus, in line with previous EEG and iEEG studies (Kovach et al., 2011, Yuval-Greenberg et al., 2008) the saccadic spike induced signals that closely resemble neurophysiological gamma range activity in the MEG sensors.

3.3.4 The Topography of SP and SF Reflects Saccade Direction

Many experimental designs involve lateralized covert attention that has been shown to influence the spatial statistics of miniature saccade direction (e.g., Laubrock et al., 2010). It is therefore important to understand potential lateralization of the accompanying SP and SF, since this might induce systematic confounds in such experiments.

As a starting point, we analyzed the time course of the saccadic spike at left, central and right EOGs around saccade onset for leftwards saccades (Figure 3.5A). The latencies of the first saccadic spike peak increased from ipsilateral to contralateral electrodes. However, this shift is unlikely to reflect a change in latency of the saccadic spike itself but likely reflects the corneo-retinal artifact, which adds in a

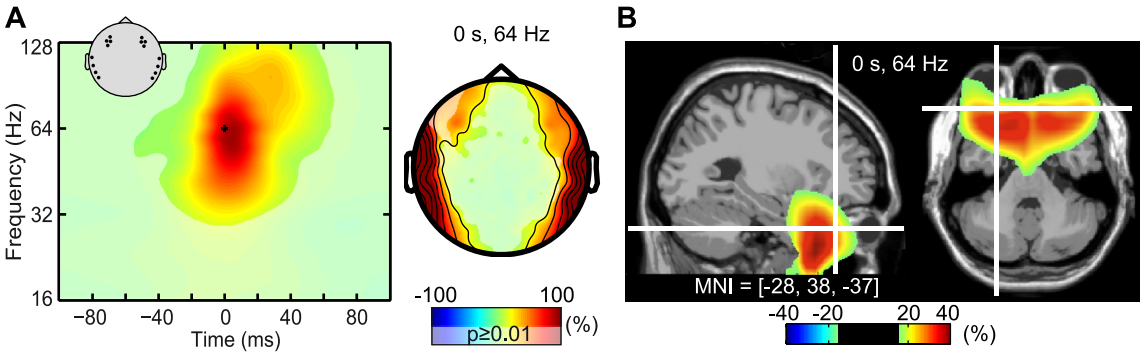

Figure 3.4: Spectral characteristics of the SF. A. Power change at sensor level around the onset of saccades relative to baseline average from 400 ms to 350 ms before saccade onset. Unmasked regions denote significant difference to zero (t-test, $p < 0.01$, FDR corrected). Left: power response resolved in time and frequency for selected regions of interest (indicated in the inset). Right: topography of the relative power changes for 64 Hz at saccade onset (time $t = 0$ ms). Unmasked regions denote significant difference from zero (t-test, $p < 0.01$, FDR corrected). B. Sources for the sensor topography shown in A overlaid on the MNI template brain. Data are masked by statistics (t-test, $p < 0.01$, FDR corrected).

spatially specific manner to the saccadic spike artifact. The CRP with its positive amplitude at ipsilateral and negative amplitude at contralateral EOG electrodes reduces the negative peak of the SP at ipsilateral EOGs and increases the SP at contralateral sites. Thus, while the onset and peak latency of the saccadic spike may actually remain the same, the superposition with the slowly rising CRP appears as a shift of the SP peak dependent on channel location. Consequently, to study the lateralization of the saccadic spike artifact as a function of saccade direction we minimized the influence of the slowly rising corneo-retinal artifact by selecting an early analysis window 2.5 ms before the saccadic spike peak. At this time, the SP topography was lateralized depending on the direction of the saccade (Figure 3.5B). The negative deflection of the SP was higher at ipsilateral frontal electrodes, while the positive peak at posterior electrodes was shifted towards the side contralateral to the saccade direction.

In line with the SP in EEG, the SF in MEG was lateralized. The amplitude of the SF was significantly higher at frontal and temporal sensors ipsilateral to saccade direction (axial gradiometers; Figure 3.5C, upper panel; $p < 0.01$, Bonferroni corrected for $n = 273$ sensors). This finding was paralleled by a planar gradient topography with higher amplitudes at ipsilateral temporal electrodes (Figure 3.5C, lower panel; $p < 0.01$, Bonferroni corrected for $n = 273$ sensors). Thus, for both

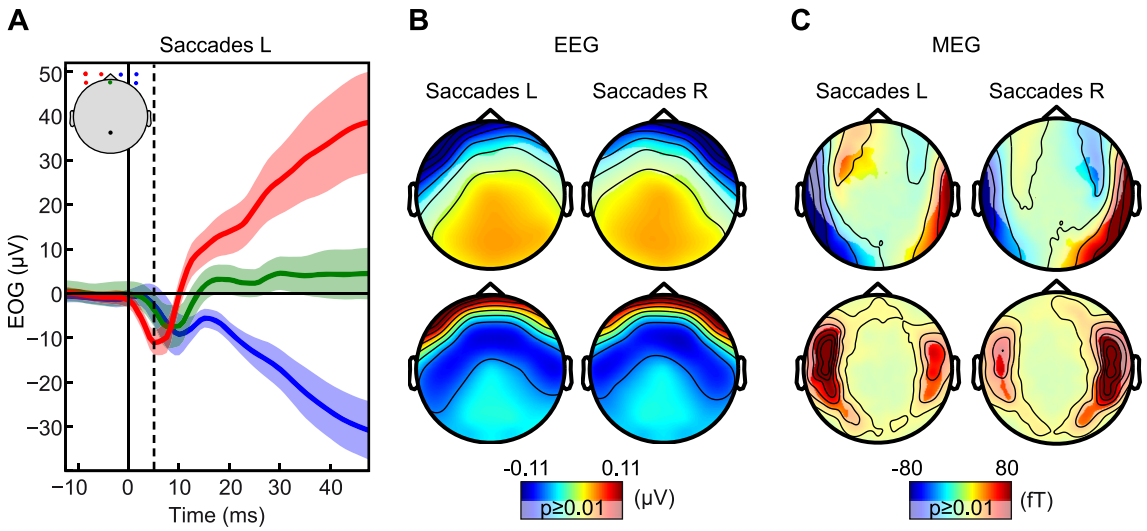

Figure 3.5: Saccade direction reflected in SP and SF lateralization. A. Grand average time course of the SP around onset of leftwards saccades at different EOG sensors. The standard deviation is depicted in transparent shading. The inset shows the locations of EOG electrodes. As reference served electrode 'Pz' (black). B and C. Topographies of the SP/SF for leftwards and rightwards saccades respectively at the time of maximal lateralization (time $t = 5$ ms, dashed line in A). The signal at saccade onset (time $t = 0$ ms) was subtracted as baseline. All topographies except for the root-mean-square (B, lower panel) are statistically masked (t-test, $p < 0.01$, Bonferroni corrected). B. SP in EEG. Top: event related signal. Bottom: root-mean-square. C. SF in MEG. Top: axial gradiometer representation. Bottom: planar gradiometer representation.

EEG and MEG, we found a clearly lateralized saccadic spike artifact. This lateralization may complicate the isolation of signals of neuronal origin.

3.3.5 Orientation of Extraocular Muscle Dipoles Reflects Saccade Direction

We hypothesized that the origin of the lateralized SP/SF sensor topography is related to asymmetrical contraction of the extraocular muscles for left and right saccades. To elaborate on this hypothesis, we fitted the SF with equivalent current dipoles. We placed a dipole in the center of the extraocular muscles of each eye and optimized the orientation of these dipoles for each subject individually. Then we analyzed the orientation of the dipoles in the plane spanned by lateral and medial rectus muscles, the muscles mainly responsible for horizontal movements of the eye. We tested if the orientation of the SF dipoles changed depending on the saccade direction. Dipoles for both saccade directions were on average oriented towards the

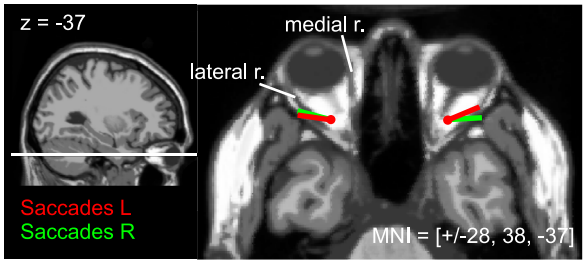

Figure 3.6: Current dipoles for SF of saccades to left and right. Grand average dipole moments for fixed dipole positions at the center of the extraocular muscles rotate depending on the saccade directions. Dipoles were projected onto the nearest horizontal brain slice (MNI coordinate $z = -37$) for illustration. Red: average dipole direction for leftwards saccades. Green: same for rightwards saccades. Lateral r./medial r.: lateral/medial rectus muscle of the left eye.

outer borders of the eyeballs. Contrasting the dipole orientation for leftwards with rightwards saccades revealed a significant rotation of 13.26° towards the ipsilateral side across subjects (Figure 3.6; $p = 0.01$, random permutation test). Consequently, the dipole orientation of a horizontal saccade followed the orientation of the contralateral rectus medialis and ipsilateral rectus lateralis muscle.

3.3.6 Comparison of SF of Miniature and Regular Saccades

Up to this point, we studied the SP and SF at the onset of regular saccades. However, a major problem is the spike artifact related to miniature saccades that occur even under fixation. Thus, we next analyzed the SF and SP induced by miniature saccades. We extracted miniature saccades with a range of less than 2° amplitude from the fixation period of our experiment (see Section 3.2). The SF of miniature saccades had a similar topography as the regular saccades (Figure 3.7A and B). The sensor topographies of the SF of both saccade types were highly correlated ($r = 0.86$). However, the SF of miniature saccades differed in amplitude from that of regular saccades. The average amplitude over frontal and temporal regions of interest was $\sim$ 200% larger for regular saccades compared to miniature saccades (Figure 3.7C; $p = 3.6 \times 10^{-6}$, Bonferroni corrected for $n = 2$ comparisons). In contrast, the SF revealed only small differences in amplitude between saccades of 5.5° and 11° (8% signal increase, $p = 8.2 \times 10^{-4}$, Bonferroni corrected for $n = 2$ comparisons). Similar to the SF, the average SP amplitude at frontal and parietal electrodes of interest was $\sim$ 110% larger for regular compared to miniature saccades

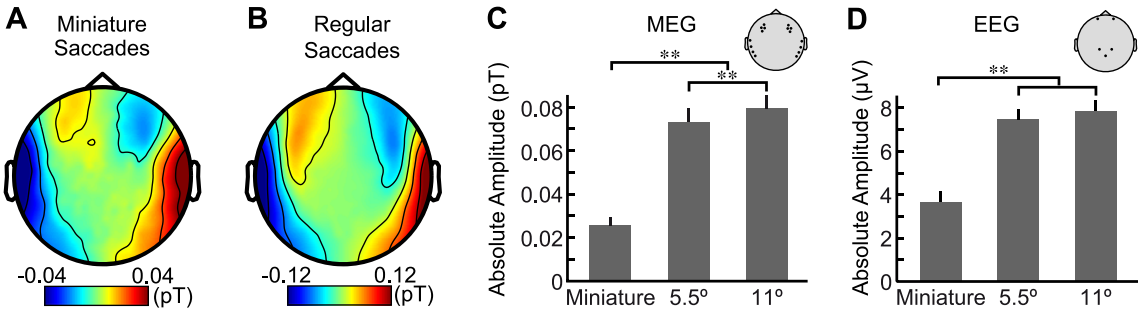

Figure 3.7: The SF of miniature and regular saccades. A. Sensor topography of the SF for miniature saccades of less than 2° amplitude at the first peak of the saccadic spike (relative to baseline at saccade onset, axial gradiometers). B. Equivalent sensor topography for regular saccades (5.5° and 11° amplitude). C. Average absolute amplitude of the SF at sensors of interest (indicated in inset) for different saccade sizes (∗∗: t-test, $p < 0.01$, Bonferroni corrected). Bars indicate the standard error. D. Average absolute amplitude of the SP at sensors of interest (indicated in inset) for different saccade sizes (∗∗: t-test, $p < 0.01$, Bonferroni corrected).

(Figure 3.7D; $p = 2.1 \times 10^{-5}$, Bonferroni corrected for $n = 2$ comparisons). The difference in average SP amplitude between 11° and 5.5° saccades was not significant (5% signal increase for 11° saccades, $p = 8.6 \times 10^{-2}$, Bonferroni corrected for $n = 2$ comparisons).

Source analysis of the SF from miniature saccades revealed the strongest power changes at 64 Hz at the extraocular muscles behind the eyes (Figure 3.8; $p < 0.01$, FDR corrected). Thus, the source distribution of the SF from miniature saccades resembled the source distribution that we derived for regular saccades but with reduced amplitude (cf. Figure 3.4B). In summary, the amplitude of the SF was modulated nonlinearly with saccade size but the spatial distribution at source and sensor level remained constant.

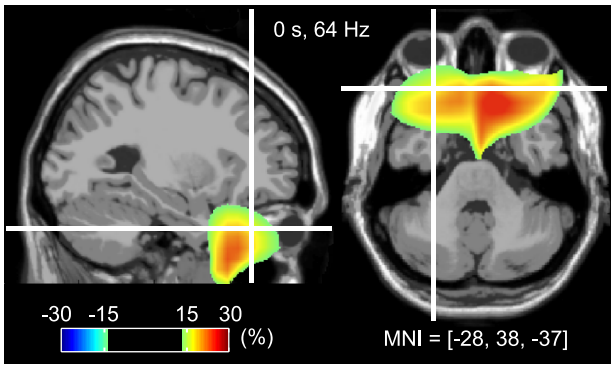

Figure 3.8: Source analysis of SF from miniature saccades. Source of the relative change in signal power at 64 Hz at saccade onset compared to average baseline at 135 ms to 85 ms before miniature saccade onset. Functional data are overlaid on the MNI template brain and statistically masked (t-test, $p < 0.01$, FDR corrected).

3.4 Discussion

We provide the first characterization of the SF, the saccadic spike artifact in MEG. Our results show that the saccadic spike artifact affects MEG signals mainly at frontal and temporal sensors. We observed that the topography of the SF is modulated with saccade direction while the SF amplitude depends on saccade size. Furthermore, our source analysis localizes the origin of the SF to the extraocular muscles. Because of its close resemblance to neural gamma band activity and its modulations in appearance and rate with experimental manipulations the saccadic spike artifact is prone to confusion with true neuronal activity in any EEG/MEG experiment. The detailed characterization of the SF in this study constitutes a solid basis for assessing possible saccadic spike related contamination in MEG experiments.

3.4.1 The Saccadic Spike in MEG and EEG

We found that the SF is a biphasic transient signal of $\sim$ 24 ms duration and a peak-to-peak response of $\sim$ 8 ms occurring at saccade onset. Its power spectrum is dominated by energy in the gamma frequency range ($\sim 32 - 128$ Hz). With these properties it is consistent with the well-known SP in EEG (Keren et al., 2010a, Yuval-Greenberg et al., 2008). However, a crucial issue of great practical importance for the interpretation of the data is the difference in sensor topography. While the SF affects frontal and temporal MEG sensors, the SP has an impact on frontal and posterior EEG sensors. Both SF and SP are the measurement specific signatures of the saccadic spike produced with saccade initiation.

3.4.2 Source Localization Confirms Extraocular Muscles as Saccadic Spike Generator

Our results provide the first distributed source estimation of the saccadic spike field in MEG. We reliably localized the saccadic spike artifact of the miniature and regular saccades in the centers of the extraocular muscles of each eye. The source localization is robust with respect to different saccade types (miniature or regular saccades) and different signal representations (frequency or time domain). In accordance with the spatial resolution of MEG, the source reconstruction does not resolve individual muscles in the periorbital space but locates the source into the region spanned by the

extraocular muscles of each eye. Nevertheless, the source estimation provides strong evidence for the muscular origin of the saccadic spike artifact arguing against any cortical contribution (Balaban and Weinstein, 1985, Brooks-Eidelberg and Adler, 1992, Csibra et al., 1997, 2000, Parks and Corballis, 2008). Our results substantiate previous EEG studies that suggested the myogenic origin of the saccadic spike artifact based on patient data and sensor characteristics of the saccadic spike (Becker et al., 1972, Blinn, 1955, Boylan and Doig, 1989a, Dimigen et al., 2009, Keren et al., 2010a, Moster and Goldberg, 1990, Picton et al., 2000a, Riemslag et al., 1988, Thickbroom and Mastaglia, 1985, 1987) or provided constrained source models of the SP (Hassler et al., 2011, Picton et al., 2000a, Thickbroom and Mastaglia, 1985, Yuval-Greenberg et al., 2008). Our findings further agree with evidence from intracranial recordings that observed the highest saccadic spike amplitudes in the temporal pole near the extraocular muscles (Jerbi et al., 2009, Kovach et al., 2011). In summary, our source estimation confirms that the saccadic spike reflects the engagement of the extraocular muscles at saccade onset. Furthermore, we show that the artifact can be reliably identified by distributed source analysis.

3.4.3 Modulation of SF with Saccade Metrics

Even in experiments demanding steady fixation, experimental stimulus and task parameters can influence the size (Gowen et al., 2005, Yuval-Greenberg et al., 2008) and direction (Engbert and Kliegl, 2003, Gowen et al., 2007, Laubrock et al., 2010, Rolfs et al., 2004, Turatto et al., 2007) of fixational eye movements. Consequently, understanding the modulation of SF with saccade metrics is necessary to assess the effect of SF artifacts in experiments with asymmetric saccade statistics.

Our results show that the SF in MEG is enhanced ipsilateral to saccade direction. The effect is strongest at temporal sensors. These findings are consistent with the lateralized topography of the saccadic spike that we and others observed in EEG (Keren et al., 2010a, Kovach et al., 2011, Moster and Goldberg, 1990, Moster et al., 1997, Thickbroom and Mastaglia, 1985, 1986). It has been suggested that the saccadic spike reflects the summation potential of synchronously recruited motor units of the extraocular muscles (Blinn, 1955, Moster and Goldberg, 1990, Picton et al., 2000a, Thickbroom and Mastaglia, 1985). Building on our beamforming results, we demonstrate that a dipole model of the lateralized SF is indeed compatible with the asymmetrical contraction pattern of the predominantly engaged muscles during

horizontal saccades, namely, the ipsilateral rectus lateralis and contralateral rectus medialis muscle.

We expect similar saccadic spike topographies for horizontal saccades that are performed from peripheral locations of the visual field towards the center. These saccades engage the same muscles as the centrifugal saccades we observed but with a different contraction level before saccade onset, affecting probably the amplitude of the saccadic spike. Saccades in directions other than the horizontal plane require the participation of different extraocular muscles, which presumably slightly changes the topography of the SF as indicated by previous EEG studies (Keren et al., 2010a, Thickbroom and Mastaglia, 1986).

The SF for saccades of different amplitudes did not differ in sensor topography or the distribution of sources. However, we found strongly reduced SF amplitudes for miniature saccades compared to the 5.5° and 11° saccades, but only minor amplitude differences between both types of regular saccades. We found a similar relation for EEG except that the difference between both types of regular saccades did not reach significance. These results are in line with previous EEG studies, supporting a nonlinear dependence of saccade size on saccadic spike amplitude (Armington, 1978, Boylan and Doig, 1989a, Keren et al., 2010a, Kovach et al., 2011, Riemslag et al., 1988, Thickbroom and Mastaglia, 1985). These studies observed an amplitude dependence for saccades up to 10° while the amplitude of the saccadic spike remained constant for larger saccades. Most probably, the maximal recruitment of motor units is already reached for these large saccades (Thickbroom and Mastaglia, 1987). The similarity of the sensor topography and source localization of the SF for spontaneous miniature and guided regular saccades suggests that both types of saccades have the same muscular recruitment pattern and thus the same sources underlying their saccadic spike artifact.

In summary, our results show that saccade metrics affect the topography and amplitude of both the SF and the SP in a characteristic manner. Any experimental comparisons that may be accompanied by asymmetric saccade patterns could therefore be subject to a potential confound with metric specific changes of the saccadic spike artifact and should be carefully controlled.

3.4.4 Practical Implications for MEG Experiments

In contrast to EEG, the saccadic spike artifact in MEG does not affect posterior sensors. Consequently, the SF is not prone to misinterpretations as gamma activity reflecting higher visual processes in parietal and occipital areas, as it is the case for EEG (Yuval-Greenberg et al., 2008). However, the SF may be confused with neuronal activity originating from frontal and temporal brain regions. For example, the response to auditory stimulation at the MEG sensor level might be contaminated by saccadic spike induced gamma band responses in the temporal cortex. The miniature saccade rate is characteristically modulated by auditory stimulation and additionally depends on experimental manipulations. Consequently, auditory stimulation can lead to task modulated gamma band responses due to the saccadic spike artifact (Yuval-Greenberg and Deouell, 2011). For auditory MEG experiments, the SF artifact could then confound genuine neural responses within the auditory processing stream since both map to overlapping temporal MEG sensors. Similarly, any neural activity reflecting higher cognitive processing in temporal and prefrontal cortex that maps to similar sensors as the SF might be subject to artifact contamination from the saccadic spike. Thus, unlike the SP in EEG, the SF in MEG is not prone to confusion with neuronal activity in parietal and occipital cortex, but putative frontal and temporal neuronal processes need to be carefully controlled for the saccadic spike artifact. It should be further noted that for some analyses artifacts could have consequences far beyond their topographical maximum. For example when computing measures of neuronal interactions such as phase synchronization between sensors the saccadic spike artifact may be problematic for a large part of all sensors.

To control for saccadic spike artifacts the first step is to investigate the modulation of the saccadic spike rate along with the experimental contrast at hand. Saccades and miniature saccades can be measured via video based eye tracking along with MEG/EEG but this is technically challenging and often the equipment is not available. An efficient and practical alternative is to follow the procedure described by Keren et al. (2010a) that detects SPs in the REOG. Importantly, to apply this approach in MEG experiments a parietal reference electrode is needed to measure the REOG. We highly recommend adapting this as a standard procedure in MEG experiments. If the saccadic spike rate is indeed modulated along with the experimental contrast, putative effects of neuronal origin need to be critically

evaluated. Our characterization of the SF provides a reference for this purpose. The precise comparison of the temporal, spatial and spectral characteristics of the signal of interest with the characteristics of the saccadic spike artifact may help to clarify the origin.

If the saccadic spike artifact covers potential neural signatures artifact cleaning and separation procedures are required. Our investigations provide a starting point for future studies exploring artifact cleaning procedures on the removal of the saccadic spike artifact in MEG. Promising candidates are independent component analysis or linear regression techniques that have successfully been applied in EEG to remove saccadic spike artifacts (Hassler et al., 2011, Keren et al., 2010a, Kovach et al., 2011, Nottage, 2010).

However, most cleaning procedures only augment the signal-to-noise ratio without perfectly separating noise from genuine neural signals (Keren et al., 2010a, Nottage, 2010, Shackman et al., 2010) and should therefore not replace a careful identification and visualization of the artifact. As an alternative to these procedures, we suggest an analysis in source space. Beamforming is especially well suited for separating artifacts from cortical sources, because it does not rely on inverse solutions. Hence, beamforming does not assume cortical sources for the entire sensor signal containing putative artifacts (Baillet et al., 2001). We showed that beamforming reliably locates the SF in the extraorbital region. While neuronal activity in the orbitofrontal cortex or the temporal pole may still be difficult to disentangle from the artifact, our results provide evidence that beamforming is suitable for spatially separating the saccadic spike artifact from neuronal signals if the latter is sufficiently distant from the former.

4

Spectral Signatures of Action Selection (Study 3)

The content of this chapter has been encouraged to resubmission in the Journal of Neuroscience: Christine Carl[1,2], Joerg F. Hipp[1,3,4], Peter König[1,2], Andreas K. Engel[1]: Spectral Signatures of Action Selection.

[1]Department of Neurophysiology and Pathophysiology, University Medical Center Hamburg-Eppendorf, Germany [2]Institute of Cognitive Science, University of Osnabrück, Germany [3]Centre for Integrative Neuroscience, University of Tübingen, Germany [4]MEG-Center, University of Tübingen, Germany

C Carl designed the experiment, performed the experimental recordings and data analysis, and wrote the paper. J Hipp designed the experiment, contributed analytic tools and contributed to writing the manuscript. P König and A K Engel designed the experiment and contributed to writing the manuscript.

4.1 Introduction

In everyday live we constantly face the challenge of selecting between several action alternatives. For example, a player in a soccer game acquiring the ball could either pass it on to a team member or take a shot at the goal. Also he has to re-adjust his choices both rapidly and flexibly to account for the continuously changing player constellations due to his own movements and those of the others. Increasing evidence

suggests that this form of action selection is not a sequential process where first the sensory input is acquired, followed by a decision and subsequent planning of an action. Rather, dynamic goal-oriented behavior might be achieved by continuously encoding, updating, and weighting sensory evidence, action goals and plans for potential movements in parallel, so that different action alternatives are continuously at hand (Cisek and Kalaska, 2010, Engel et al., 2013, Shadlen and Newsome, 2001). These simultaneously evolving and competing action plans may form an integral part of a distributed and emergent decision process that integrates perceptual, cognitive and motor functions (Cisek and Kalaska, 2010). In support of this view, neural correlates of decision variables have been observed in various cortical and subcortical regions distributed across the brain, particularly including those structures that are specific for sensorimotor processing (Andersen and Cui, 2009, Cisek, 2007, Cui and Andersen, 2007, Glimcher, 2003, Gold and Shadlen, 2007, Hoshi and Tanji, 2007, Pesaran et al., 2008, Shadlen and Newsome, 2001).

Physiological signatures of action selection have been studied extensively in non-human primates and implicate various areas of fronto-parietal sensorimotor association cortex in voluntary action selection in the presence of competing options (Cisek and Kalaska, 2010, Haggard, 2008, Kable and Glimcher, 2009). These areas include effector specific regions in posterior parietal cortex and frontal premotor areas (Andersen and Cui, 2009, Cui and Andersen, 2007, Lawrence and Snyder, 2006), which engage in oscillatory coupling during internally motivated choices (Pesaran et al., 2008). In humans, fMRI, transcranial magnetic stimulation (TMS), or lesion studies have provided evidence for distributed cortical substrates of action selection including parietal and premotor areas (Beudel and de Jong, 2009, Coulthard et al., 2008, de Jong, 2011, Hare et al., 2011, Milea et al., 2007, Oliveira et al., 2010). However, while investigations of perceptual decisions have emphasized the importance of oscillatory population activity in sensorimotor areas (Donner et al., 2009, Gould et al., 2012, Siegel et al., 2011, Wyart et al., 2012), the role of oscillatory dynamics in human voluntary action selection independent of sensory evidence or expected rewards has not yet been addressed.

Studying the oscillatory dynamics of distributed and fast-changing networks of action selection in humans requires measuring brain activity during active behavior with high temporal resolution. While fMRI and lesion studies have revealed relevant cortical substrates of action selection, they do not provide access to fast neuronal dynamics. Here, we used MEG and source analysis to investigate the physiological

processes of action selection in human subjects. To study voluntary action selection we compared spectral signatures for selecting a saccade target among equally valuable alternatives with externally cued delayed saccades. We dissociated fast selection processes of actions instructed by sensory cues from longer lasting competitive processes where a decision about an action emerges intrinsically independent from sensory input. We found that oscillatory population activity of a fronto-parietal network within gamma and alpha to beta frequency range is associated with internally driven action selection between competing behavioral alternatives.

4.2 Materials and Methods

4.2.1 Participants

Fifteen healthy volunteers participated in this study (7 female, mean age 25.7 ± 3.3). Participants received monetary compensation for their participation. All participants had normal or corrected-to-normal vision and had no history of neurological or psychiatric illness. The study was conducted in accordance with the Declaration of Helsinki and informed consent was obtained from all participants prior to recordings.

4.2.2 Stimulation and Behavioral Task

Participants performed a delayed saccade task with saccades of two different amplitudes and 8 different directions (16 targets, Figure 4.1). The delayed saccade task consisted of two experimental task conditions: In the memory-guided saccade condition, participants were asked to perform a guided saccade to one of the 16 targets indicated by a brief visual cue before the delay period. In the decision condition subjects could freely chose a saccade target out of the same 16 target positions (we will refer to these conditions as *guided* and *free* saccades, respectively).

At the beginning of each trial, subjects fixated for 800 ms a blue asterisk presented in the center of the screen. Surrounding the asterisk, 16 Gaussian patches were regularly arranged (width: 0.34° sd) on an inner and outer circle (distance from the asterisk: 5° and 10° respectively) serving as saccade targets. The background was gray, the peak of the Gaussian patches was white. Following fixation, the asterisk underwent a 200 ms isoluminant color change to either green (*free* saccades)

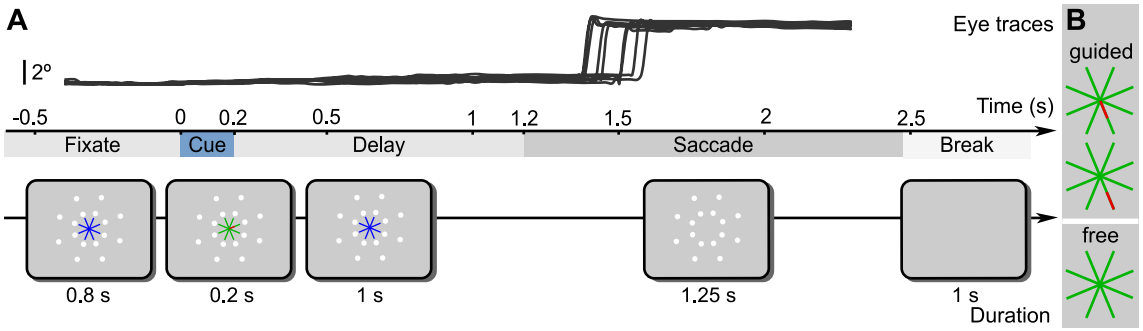

Figure 4.1: Experimental task. A. At trial onset subjects fixated a blue asterisk presented in the center of the screen. After a delay of 800 ms an isoluminant color change to green with a red marker instructed the target location of guided saccade trials. In half of the trials, a change to green without red marker instructed the subjects to freely choose one of the 16 targets. In the displayed example, the red marker instructed the subject to plan a short saccade to the right. After a delay of 1 s the asterisk disappeared and instructed the subject to execute the saccade. Top: Representative eye traces of one participant over the first 9 trials. B. Cue examples for *guided* and *free* saccade trials.

or green with a red marker (*guided* saccades) that indicated the task for each trial and served as a spatial cue. In the *guided* saccade condition the position of the red marker defined the direction of saccade target and instructed participants to prepare a saccade to this location. Moreover, the marker indicated a small saccade or a large saccade by being displayed at the inner or the outer part of the asterisk's branch, respectively. In the free decision task, a color change to a fully green asterisk instructed subjects to immediately choose one out of the 16 target alternatives and prepare a saccade to the freely chosen location. In both conditions participants had to maintain fixation during the following delay period of 1 s. Then, the asterisk disappeared instructing the subjects to perform the saccade. Subjects were told to maintain fixation at saccade target until it disappeared after 1.25 s. In between trials, a blank screen was presented for 1 s. In total each subject performed 702 trials (352 for *free* decision and *guided* saccade task, respectively, for the guided saccade task all 16 targets were cued equally often). Trials of all experimental conditions (*guided* and *free* saccades, as well as saccade targets in the *guided* saccade condition) were randomly presented.

During the experiment, participants were seated in the MEG chamber. Stimuli were back-projected onto a screen at 60 cm distance with an LCD video projector (Sanyo Pro Xtrax PLC-XP51) and a two-mirror system. Stimuli were presented using the software Presentation (Neurobehavioral Systems, Albany, CA).

4.2.3 Analysis Software

All data analyses were performed in Matlab (MathWorks, Natick, MA) with custom implementations and the open source toolboxes Fieldtrip (Oostenveld et al., 2011), and SPM2 (`http://www.fil.ion.ucl.ac.uk/spm/`).

4.2.4 MEG Data Acquisition

We recorded MEG continuously with a 275-channel (axial gradiometer) whole-head system (Omega 2000, CTF Systems) in a magnetically shielded room. MEG data were digitized at 1200 Hz sampling rate (300 Hz low-pass filter). Off-line, we removed line-noise with notch-filters (at 50, 100, 150 Hz), high- and low-pass filtered the data to 1 Hz and 170 Hz respectively (zero phase Butterworth IIR filter, filter order 4), and down sampled it to 400 Hz.

4.2.5 EOG recordings

Along with the MEG, we recorded the EOG using the EEG channels of the CTF MEG system. Data were collected from AG/AGCL sintered flat electrodes (Easycap GmbH, Herrsching, Germany) with an analog passband of $0.16 - 300$ Hz at a sampling rate of 1200 Hz. 7 EOG electrodes were placed over the nose, above and below each eye at the outer canthi, and below the left and right eye next to the nose. Data were referenced to an electrode placed at the tip of the nose during the recording. All electrode impedances were below 10 kΩ. Off-line, the EOG were high- and low-pass filtered (cut-off 1 Hz and 170 Hz respectively, zero phase Butterworth IIR filter, filter order 4) and down-sampled to 400 Hz.

4.2.6 Structural MRI Acquisition

We acquired individual T1-weighted 1 mm^3 high-resolution structural images (MRIs) of each subject with a 3T Siemens MAGNETOM Trio Scanner using a coronal magnetization-prepared rapid gradient echo sequence. These MRIs were used to construct individual head models for source analysis.

4.2.7 Eye Tracker Recording

Along with the neurophysiological data we recorded the eye position using an MEG compatible remote eye tracker system (iView X MEG 50Hz, SMI, Berlin, Germany). The system monitored the right eye with an infrared camera to detect the pupil center and the corneal reflection of the infrared light source. After calibration (9 points) the system determined the gaze direction from the relative position of pupil and the corneal reflection at a rate of 50 Hz. Additionally, eye traces were digital to analog converted and fed to the MEG system on-line. This on-line procedure introduced temporal offsets on the order of 10^{th} of milliseconds between eye tracker signal and MEG/EOG data and was characterized by undesirable ringing artifacts but served as a coarse reference for the first alignment of the eye tracker and MEG/EOG signals.

Off-line, we aligned the digital eye tracking data to the MEG/EOG in a 2-step procedure: First, we interpolated the 50 Hz signal to 400 Hz using cubic smoothing splines and computed the cross-correlation of the interpolated digital eye tracker signal with the analog version recorded with the MEG acquisition system. Then, we accounted for the offset identified by the latency of the peak in the cross-correlogram. In a second step, we refined the alignment and corrected for the offset between the EOG and the aligned eye tracker signal. To this end, we smoothed the data with a Savitzky-Golay filter (4^{th} order, 102.5 ms), rectified and averaged all channels of both the EOG and the eye tracker signals, and estimated the offset from the peak of the cross-correlation.

To improve the range of validity of the eye tracker signal, we interpolated missing data. We detected periods with loss of eye tracking signal characterized by pupil size and gaze positions values close to zero. If these data segments were not identified as blinks (see below), we interpolated the missing data by piecewise constant interpolation.

4.2.8 Artifact Rejection

Trials contaminated with muscle artifacts, signal jumps, or distortions of the magnetic field due to, for example, cars passing in front of the building were rejected off-line using semi-automated threshold procedures applied to the MEG signals. Since eye movements are part of the experimental design standard EOG based procedures to detect eye blinks fail. We detected eye blinks using a combination of eye

tracker and EOG signals. Data with vanishing pupil diameter and fast changes in the EOG signal were identified as blink artifacts. Finally, we inspected all MEG, EEG, and EOG signals manually to ensure good artifact rejection performance. On average across subjects, $17.0 \pm 9.2\%$ (mean $\pm$ sd) of the trials were rejected.

4.2.9 Cleaning of Eye Movement Artifacts

Saccades induce two major kinds of eye movement artifacts: the corneo-retinal artifact, resulting from the rotation of the eyeball, and the saccadic spike artifact, which originates from the contraction of the extraocular muscles at saccade onset. Since we investigated MEG signals during the execution of regular saccades it is especially important to account for these artifacts. However, even during fixation periods eye movements occur in form of microsaccades and related artifacts can distort the EEG or MEG signal seriously (Carl et al., 2012, Yuval-Greenberg et al., 2008).

To clean the MEG signal from eye movement artifacts, while preserving all neuronal activity, we performed a two-step process. First, corneo-retinal artifacts were removed by linear regression based on the EOG. Second, we attenuated the saccadic spike artifact and possibly remaining eye movement related artifacts using ICA. Note that by applying these cleaning procedures throughout all analyzed data periods, we did not only suppress the artifacts originating from regular saccades but also those from microsaccades during fixation periods.

In order to remove corneo-retinal artifacts we used an EOG based linear regression technique (Croft and Barry, 2000b, Gratton et al., 1983, Schlögl et al., 2007). To obtain the appropriate regression coefficients, we recorded 3 min of voluntary eye movements on a gray screen before and after the main experiment. These signals were cleaned from non-saccadic artifacts, preprocessed, and then served to compute the linear relation between the EOG sensors (7 EOG electrodes referenced against an electrode at the nose, and reduced to 3 dimensions using principal component analysis) and each MEG channel (cf. Schlögl et al., 2007). MEG data were then cleaned by subtracting the weighted EOG signal.

EOG based regression without a radial component with posterior reference - although otherwise superior in performance to regressions based on such a component - performs weak in removing the saccadic spike artifact (cf. Plöchl et al., 2012). Because ICA has been shown to be especially suited to attenuate the saccadic spike artifact for EEG (Hassler et al., 2011, Hipp and Siegel, 2013, Keren et al., 2010a,

Kovach et al., 2011, Plöchl et al., 2012), we subsequently applied ICA on the cleaned data. ICA aims at finding a linear transformation of the sensor signal that separates the putative underlying sources by maximizing their statistical independence. Because the number of sources that can be separated by ICA is limited to the number of sensor channels, its performance for artifact suppression depends strongly on the data selection used for computation: To better isolate the saccadic spike artifact from the cerebral sources, it was proposed to augment it's contribution to the overall variance of the signal by restricting the signal to the dominant spectral range of the artifact (Kovach et al., 2011), selecting relevant data periods that emphasize the artifact but still include all cerebral sources of interest (Keren et al., 2010a), or including additional 'virtual' channels that focus on the saccadic spike artifact (Hassler et al., 2011).

A clear separation of eye movement artifacts from any other cortical signal related to the saccade is especially important when studying the cortical signals of saccade generation themselves. In the present study, we therefore maximized this separation by combining approaches of the above-cited EEG studies to our ICA analysis.

In detail, we computed a two-step ICA separately for each subject using the extended infomax algorithm (Lee et al., 1999). In order to remove saccadic spike artifacts, we computed an ICA on the band limited data of $24 - 160$ Hz, a spectral band that includes the characteristic spectral range of the saccadic spike artifact (Carl et al., 2012, Jerbi et al., 2009, Keren et al., 2010a, Kovach et al., 2011). The ICA was computed for each subject on the concatenated data of the trial periods and additional perisaccadic time intervals of each trial (50 ms before and after the saccade onset). Artifact components were selected based on visual inspection of their topography, the spectral power and the single trial saccade related response of the independent components (for the spatial distribution of the saccadic spike artifact in MEG see Carl et al., 2012). To further reduce cardiac artifact components and possibly remaining eye movement artifacts we rerun the ICA analysis on the broadband cleaned signal including EOG channels normalized to the standard deviation of the MEG channels. With this 2-step approach, we found on average one saccadic spike component per subject and $1 - 2$ other artifactual components.

4.2.10 Behavioral Analysis

For detection of regular saccades we employed a velocity threshold based algorithm on the eye tracker data. If coupled with a minimum saccade duration criterion, this algorithm has very few parameters and is accurate in the face of stereotypical eye movements such as those analyzed here (Salvucci and Goldberg, 2000). Because the optimal velocity threshold parameter depends on preprocessing and sampling of the recorded data, as well as on saccade amplitudes, we defined the velocity threshold in a data-driven approach. We adapted the thresholds manually for the saccade amplitudes in our task (5° and 10°) so that saccades were detected while the number of false positives was minimized. We achieved this by visual inspection of the data, taking into account a priori knowledge on saccade timing. We defined periods as regular saccades in which the eye movement velocity was higher than 26.9°/s for a duration of at least 22.5 ms. Periods where the saccade velocity exceeded 67.1°/s were defined as saccades irrespective of saccade duration. We combined all saccade intervals that were less than 7.5 ms apart from each other into a single saccade interval. All other periods were labeled fixations.

We aligned all trials either to the cue or to saccade onset. Precise alignment to saccade onset relied on the EOG signal with higher temporal resolution than the eye tracker signal.

The behavioral analysis revealed that subjects showed a considerable variability in saccade onset and also initiated saccades before the 'go' signal. To maximize the number of trials for analysis and at the same time ensure sufficient data length of the saccade planning and re-fixation period, we accepted trials with saccades that were performed within a broad time window from 250 ms before to 450 ms after the 'go' signal. In a next step, we rejected all trials with incorrect saccade orientation or amplitude. For saccade categorization we applied drift correction at the fixation period before the cue onset (−300 ms to −100 ms) and ensured that the subjects fixated the asterisk before saccade onset within a tolerance angle of 2.5°. In the *guided* saccade condition saccade target was considered correct if the closest location was the cued one, for *free* decision trials chosen saccade target was defined as the closest of the 16 target points if it was maximally 2.5° away from it. Overall we discarded $15.8 \pm 9.2\%$ (mean ± sd) of the trials because of faulty behavioral performance.

For the decision contrast we had to modify the definition of valid trials. Neuronal

signatures of free target selection can occur within the whole delay period since the task does not impose an explicit constraint on when exactly to perform the decision within the delay period. Consequently, for all decision related contrasts (*free* vs. *guided* saccades, *free* or *guided* saccades vs. baseline respectively) we analyzed the entire delay period of 1.2 s. For these analyses, we rejected all premature saccades that were performed before the 'go' signal. For 2 out of the 15 subjects less than 25% of the trials remained after rejecting these premature saccades. We excluded these two subjects in the analyses of decision processes.

4.2.11 Spectral Analysis

We estimated spectral power using the multi-taper method based on discrete prolate spheroidal (slepian) sequences (Mitra and Pesaran, 1999, Thomson, 1982). Spectral estimates were computed across 19 logarithmically scaled equidistant frequencies from 5.7 to 128 Hz (in 0.25 octave steps) and up to 34 points in time from -1.25 s to 0.4 s for the saccade-aligned data (-0.05 s to 1.6 s for the cue-aligned data, 0.05 s steps). We adjusted the temporal and spectral smoothing using the multi-taper method so that it matched approximately 250 ms and 3/4 octaves, respectively. For frequencies $\geq$ 16 Hz we used temporal windows of 250 ms and adjusted the number of slepian tapers accordingly to the spectral smoothing of 3/4 octaves. For frequencies $<$ 16 Hz we adjusted the time window to yield a frequency smoothing of 3/4 octaves with a single taper. To estimate signal power, we multiplied the complex spectrum with its complex conjugate and averaged this across trials and tapers. We characterized the power response relative to the pre-stimulus baseline at 54 ms before cue onset.

4.2.12 Source Analysis

Estimating the neural activity at the source level requires a physical forward model or leadfield that describes the electromagnetic relations between sources and sensors. To derive this physical relation we employed a single-shell volume conductor model (Nolte, 2003). We computed two physical forward models for each subject that differed in spatial resolution and distribution of source locations. Sources of one model covered the whole brain with a regular grid in MNI space of 1 cm resolution resulting in 3648 sources. Sources of the second model were distributed with a

spacing of 1 cm on a shell lying 1 cm beneath the skull (for a detailed description of the source grid see Hipp et al., 2011). This model comprises only 400 source locations and samples the source space more sparsely than the first model. However, the second model still ensures homogeneous coverage across the cortex. To derive the individual physical forward models for each subject, we affine transformed source locations into individual head space using the participants' individual T1-weighted structural MRI and aligned the MEG sensors to the head geometry based on 3 fiducial points (nasion, left and right ear, defined in the MEG by 3 head localization coils).

We used adaptive linear spatial filtering (*beamforming*; Gross et al., 2001, Van Veen et al., 1997) to estimate the amplitude of neural population signals at cortical source level. In short, for each source location, three orthogonal linear filters (for the three orientations at each source) were computed that pass activity from that location with unit gain, while maximally suppressing activity from any other source. Subsequently, the filters were linearly combined to a single filter that points to the direction of the dominant dipole. For each experimental contrast (e.g., activation versus baseline or left versus right saccades), we derived a separate filter estimation from the real part of the cross-spectral-density matrix at each point in time and frequency. To avoid a bias of the filter, we randomly choose trials to equalize the trial number between the experimental contrasts at hand before computing the filter. To derive the complex source estimates, the complex frequency domain data were then multiplied with the real-valued filter. To estimate power in source space we multiplied the complex spectral estimate with its conjugate and averaged across all trials and tapers.

For illustration of the sources we overlaid the functional data onto the structural MRI of the segmented surface or cut surface of the *colin27* MRI T1 average (Holmes et al., 1998), masked non-significant values (see Section 4.2.14), and interpolated the source data to 1 mm resolution. We express changes of spectral power either as percentage change (relative to baseline), as contrast, or as z-scores (cf. Medendorp et al., 2007).

4.2.13 Definition of Regions of Interest

We defined regions of interest (ROIs) based on coordinates of areas identified in an fMRI study that examined cortical areas involved in saccade planning and execution

in a similar delayed saccade task (Kagan et al., 2010). We adapted the selection and labeling of ROIs to better suit the spatially coarser resolution of MEG. We defined 3 regions along the intraparietal sulcus: posterior intraparietal sulcus (pIPS; V7 in Kagan et al., 2010), medial intraparietal sulcus (mIPS; union of areas IPS2 and retIPS in Kagan et al., 2010), and anterior intraparietal sulcus (aIPS). The ROI for the frontal eye fields (FEF) was defined as the union of lateral and medial frontal eye fields (cf. Kagan et al., 2010). We further defined a ROI for the supplementary eye fields (SEF) and the dorsolateral prefrontal cortex (dLPFC). Furthermore, we created a ROI for the primary visual cortex (V1).

For defining the frontal and parietal ROIs we transformed Talairach coordinates of ROI centers reported in Kagan et al. (2010) into MNI space using the transform functions suggested by Lancaster et al. (2007) and identified nearest neighbors of this MNI coordinate to the source location of the used leadfield (1 nearest neighbor for the single shell leadfield and 7 nearest neighbors for the fine grained leadfield covering the whole cortex). V1 was defined as all nearest neighbors of the source locations of the used leadfield to the template of Brodman area 17 provided by MRIcroN.

4.2.14 Statistical Analysis

For statistical testing of differences in spectral power between conditions, we first log-transformed the power values to render the distributions more normal. For each subject, we then computed a 2-sided paired t-test of spectral power between conditions for each source or ROI at each time and frequency window, transformed t-values into z-scores, averaged across subjects, and multiplied with the square root of the number of subjects to obtain a fixed-effects measure of the significance for each time-frequency-voxel volume.

In order to analyze spectral power signatures with little a priori restrictions about cortical locations of interest or specific time or frequency windows we estimated differences in local neural population activity between conditions throughout the cortex resolved in time and frequency. We investigated power differences at 5 continuous frequency ranges corresponding approximately to the classical frequency bands known from EEG and MEG (theta $5.7 - 8$ Hz, alpha $8 - 16$ Hz, beta $16 - 32$ Hz, low gamma $32 - 64$ Hz, and high gamma $64 - 128$ Hz) and time intervals of 100 ms length in 100 ms steps if not indicated otherwise. The high dimensional

time-frequency-voxel space induces many separate statistical tests that reduce sensitivity of statistical analysis when accounting for multiple comparisons. To adapt the sensitivity of analysis to the effect size of the experimental contrast at hand we used two physical forward models differing in their spatial distribution and number of sources (see Section 4.2.12) and employed two different methods for multiple comparison correction across the whole time-frequency-voxel space. In this way, we were able to investigate the cortical network of saccade related activity as detailed as possible across the whole time, frequency, and cortical space while we still ensured the necessary statistical power of the analysis.

Since the comparison of activation against baseline generally yields strong effects, we computed these power differences on the more detailed regular source grid covering the whole cortex (3648 sources) and accounted for multiple comparisons across the time-frequency-voxel space using FDR correction (Benjamini and Hochberg, 1995, Genovese et al., 2002) with $q = 0.05$.

For comparing the smaller signal differences between *free* versus *guided* saccades or between horizontal saccade directions we employed the forward model that covers the cortex in a single shell at 1 cm below the skull's surface comprising 400 sources or an adapted subset thereof. We accounted for multiple comparison correction within this 4 dimensional time-frequency-voxel space (2 dimensions for space because of the planar geometry of the source grid) by a cluster based random permutation approach. In particular, we identified bins in the time-frequency-voxel space whose t-statistic exceeded a threshold corresponding to a significance level of $p < 0.05$, resulting in a binary matrix with values of 1 for bins larger than the threshold. For each time and frequency bin separately, we identified clusters in voxels of this binary matrix that are linked through direct neighborhood relations (neighboring voxels with 1). Such a cluster corresponds to a network of cortical regions with different spectral power between conditions that is continuous across space. For each cluster, we defined its size as the integral of the statistical z-scores of the power differences between conditions across the volume of the cluster and tested its statistical significance using a random permutation statistic: For each separate time and frequency bin, we repeated the cluster identification 1000 times (starting with the t-statistic between conditions) with shuffled condition labels to create an empirical distribution of cluster sizes under the null-hypothesis of no difference between conditions. The null-distribution was constructed from the largest clusters (two-tailed) of each resample across all time and frequency bins, therefore accounting for multiple

comparisons across space, time, and frequency bins (Nichols and Holmes, 2002).

To further elucidate the spectro-temporal evolution of signal power at a finer scale, we show time-frequency spectra at selected ROIs across all time-frequency points computed in the source analysis (see Section 4.2.11). In order to visualize the extent of important spectral changes in frequency bands and latencies, we mask spectra statistically, using an uncorrected threshold at a significance level of $p < 0.05$. Direction specific neuronal activity for saccades to the left and the right can be assumed to be largely mirror symmetric and lateralized to the contralateral hemisphere. Therefore, we combined data for the direction specific contrast by subtracting power of right from left homologous ROIs and dividing this by 2. In order to illustrate the directional specificity for *free* and *guided* saccades separately, we computed the Michelson contrast: We subtracted average of left from average of right saccades divided by the mean sum of the power of both conditions and subsequently averaged mirrored left and right ROIs. For all other investigations, where lateralization of direction independent saccade related activity was weak, we averaged homologous ROIs in the two hemispheres.

4.3 Results

We investigated neuronal activity related to human saccade target selection, planning, and execution by measuring MEG and gaze position in a delayed saccade task (see Figure 4.1). In each experimental trial, subjects either performed a cued saccade to one of 16 targets or were free to choose a target. First, we studied general signatures of saccade planning and execution. Then, by contrasting *free* and *guided* saccades we differentiated voluntary action selection processes from saccade preparation.

4.3.1 Oscillatory Signatures during Saccade Planning and Execution

We pooled data of *guided* and *free* saccades across all directions and amplitudes, to investigate changes in local population activity relative to a pre-cue baseline reflecting processes of saccade planning and execution. In particular, we analyzed changes in spectral power of saccade-aligned signals in 6 time windows ranging from

600 ms before to 400 ms after saccade onset and in 5 frequency bands from the theta to the high gamma range (Figure 4.2).

We found sustained and spatially widespread changes in spectral power during saccade planning and execution in fronto-parietal areas (t-test, $p < 0.05$, FDR corrected for number of sources, time, and frequency windows, $n = 3648 \times 6 \times 5$). During the delay period, before saccade execution, we identified a sustained increase in high gamma power ($64 - 128$ Hz) in posterior and medial parietal areas along the intraparietal sulcus and precuneus. Shortly before the upcoming saccade the activity extended to anterior regions of intraparietal sulcus and to the frontal and supplementary eye fields. Following the saccade, gamma power further increased in posterior and medial parietal areas. In the beta frequency range ($16 - 32$ Hz), spectral power was reduced around superior portions of the parietal cortex during the delay period. Shortly before saccade execution the decrease in beta power extended to frontal regions around the frontal eye fields and the supramarginal gyrus, where it persisted during re-fixation. After saccade execution, also power in the alpha frequency band ($8 - 16$ Hz window) reduced in posterior portions of the parietal and occipital cortex. After saccade onset a transient broadband spectral power increase (all frequency windows up to 64 Hz) originated from early visual areas.

To resolve the time courses and bandwidth of the observed spectral power changes, we computed time-frequency spectrograms with a high resolution for selected ROIs of the fronto-parietal saccade related network (see Section 4.2, Figure 4.3). Increases in the gamma band in the fronto-parietal regions (FEF, aIPS, mIPS, and pIPS) were sustained throughout the delay period (from time $t = -600$ to 0 ms) and ranged from 45 to 128 Hz. Increases intensified after saccade onset in all these ROIs and persisted in parietal ROIs and early visual cortex (V1) during the whole re-fixation period that was analyzed (up to 400 ms after saccade onset). The decrease in beta power, strongest at 16 to 23 Hz, was sustained in parietal ROIs (mIPS, pIPS, and aIPS) throughout the analysis window (starting 600 ms before saccade onset) and appeared in frontal regions (FEF and SEF) approximately 300 ms before the saccade. pIPS and V1 showed strong spectral changes during re-fixation: The transient broadband increase with a peak around 32 Hz approximately 100 ms after saccade onset was followed 50 ms later by a decrease in intermediate frequency range at $8 - 23$ Hz. Power in the low frequency range of theta below 8 Hz was increased and probably reflected visual evoked event related responses.

In summary, these results revealed a dichotomy of oscillatory activity, with in-

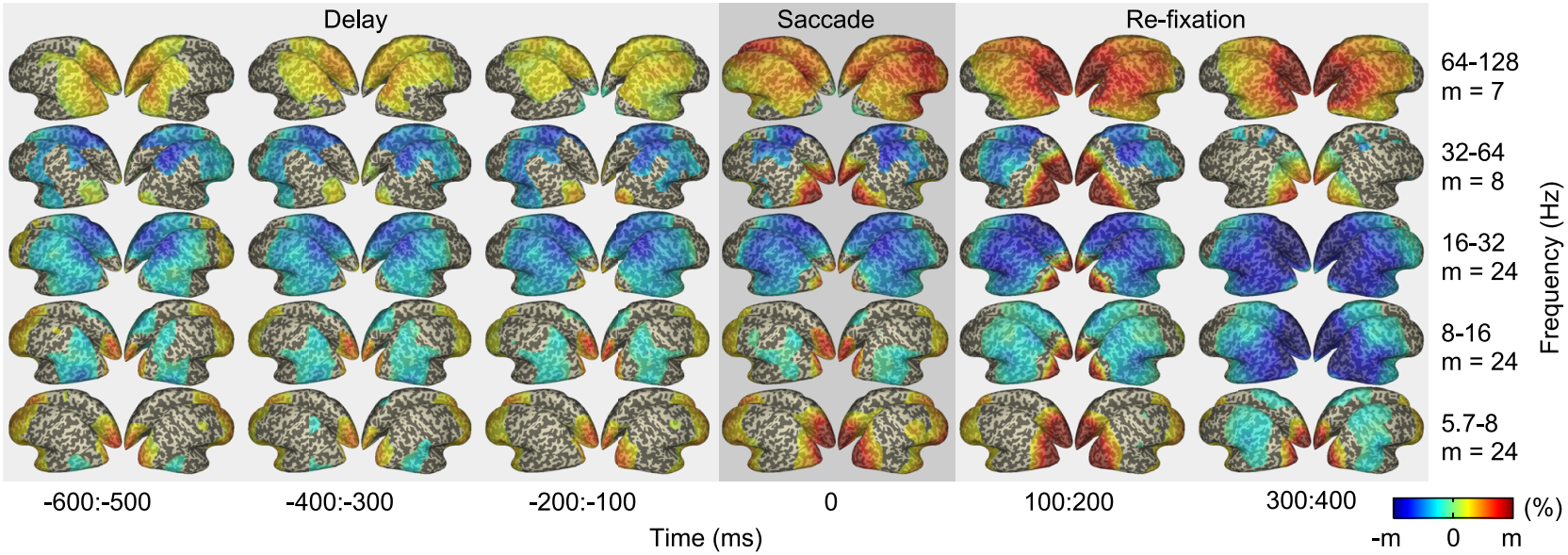

Figure 4.2: Spectral power changes during saccade planning and execution. Change in spectral power relative to pre-cue baseline (54 ms before cue onset) for different points in time and frequency resolved in cortical space. Data are aligned to saccade onset (at time $t = 0$ ms). The color maps are adapted to the range of power changes for each frequency. Power changes are statistically masked for significant difference from zero (t-test, $p < 0.05$, FDR corrected).

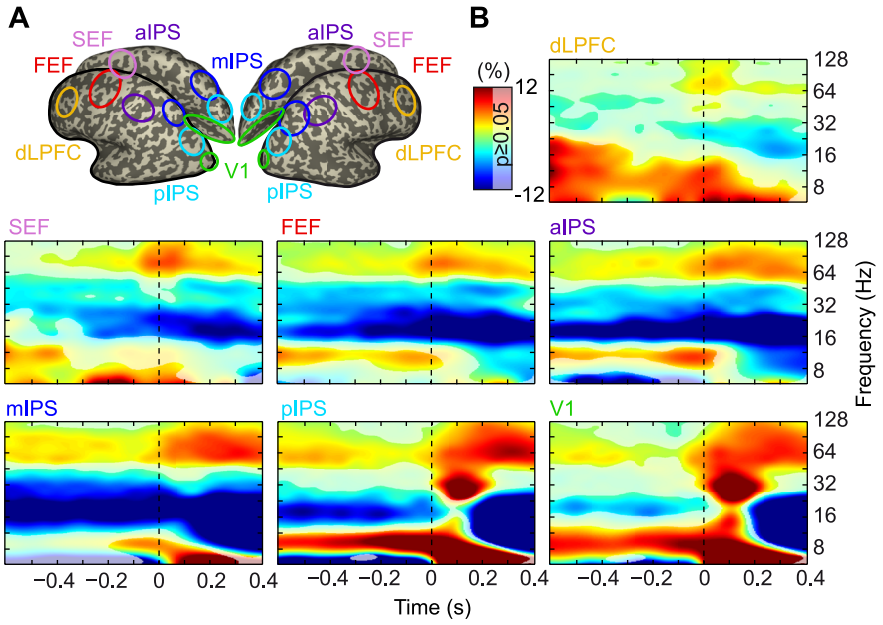

Figure 4.3: Spectral power changes during saccade planning and execution in selected ROIs. A. Circled areas specify the spatial location of each ROI on the inflated template brain (dLPFC: dorsal lateral prefrontal cortex; SEF: putative human homologue of supplementary eye fields; FEF: putative human homologue of lateral and medial frontal eye fields; aIPS, mIPS, pIPS: anterior, medial and posterior intraparietal sulcus; V1: primary visual cortex). B. Relative spectral power changes of saccade-aligned data (saccade onset at time $t = 0$ ms, dotted line) for the ROIs relative to baseline (54 ms before cue onset). Data are pooled across homologous areas in the two hemispheres. Unmasked regions denote significant difference from zero (t-test, $p < 0.05$, uncorrected for multiple comparisons).

creases of high frequency (gamma) activity and decreases of low frequency (beta) activity that was associated with delayed saccades in a widespread fronto-parietal network. Furthermore, visual areas were characterized by strong and broadband power changes during and after saccade execution.

4.3.2 Oscillatory Signatures of Saccade Target Selection

Next, we investigated oscillatory activity specifically related to the selection of saccade targets. To this end, we contrasted spectral power between *free* and *guided* saccade trials. The reasoning was that, in *guided* trials, the spatial cue immediately leads to the selection of a specific motor plan while in *free* saccade trials subjects were required to choose between 16 possible targets. Consequently, early cue-related activity should capture the instructed selection of a specific motor action in *guided*

trials, while we expected a prolonged signature of the action selection process for *free* trials.

Therefore, we analyzed power differences between *free* and *guided* trials for cue (Figure 4.4A) as well as saccade-aligned data (Figure 4.4B) across the whole delay phase in 10 time windows starting 50 ms before cue onset until 400 ms after the go signal for the cue-aligned data (time windows for saccade-aligned data were chosen equivalently, we only show a relevant subset from both alignments).

In response to the cue, we found more gamma ($64 - 128$ Hz) and theta power ($5.7-8$ Hz) in occipital and posterior parietal cortex for *guided* compared to *free* saccade trials (cluster based random permutation test, $p < 0.05$, corrected for multiple comparisons of number of sources, time, and frequency windows, $n = 400 \times 10 \times 5$, Figure 4.4A). In the delay phase before saccade initiation until re-fixation (from 600 ms before to 200 ms after saccade onset) high gamma power was stronger in a fronto-parietal network when freely choosing saccade targets compared to *guided* saccade trials (cluster based random permutation test, $p < 0.05$, corrected for multiple comparisons of number of sources, time, and frequency windows, $n = 400 \times 10 \times 5$, Figure 4.4B). This network comprised frontal and supplementary eye fields as well as parietal areas around precuneus and along the intraparietal sulcus from its medial to posterior parts. For lower frequencies in the alpha and beta frequency range ($8-16$ Hz and $16-32$ Hz) we found a significant reduction of power during the delay period in widespread regions of posterior parietal cortex for *free* saccades compared to *guided* saccades. During execution and re-fixation this reduction was strongest at infero-temporal areas.

To understand the origin of the differences between *free* and *guided* saccades we analyzed power changes relative to pre-cue baseline separately for both conditions at several locations within the fronto-parietal network (Figure 4.5). The analysis revealed that the difference in gamma power in the fronto-parietal network during the delay interval before saccade onset (starting approximately 600 ms before saccade onset) was caused by an increase in *free* saccade trials relative to baseline rather than a decrease in *guided* saccade trials. The decrease in alpha and beta power relative to pre-cue baseline appeared to be stronger in the *free* saccade compared to the *guided* saccade condition.

These findings suggest sustained increased gamma power accompanied by decreased alpha to beta power in a fronto-parietal network during the delay reflecting the selection between different possible motor plans in *free* saccade trials. However,

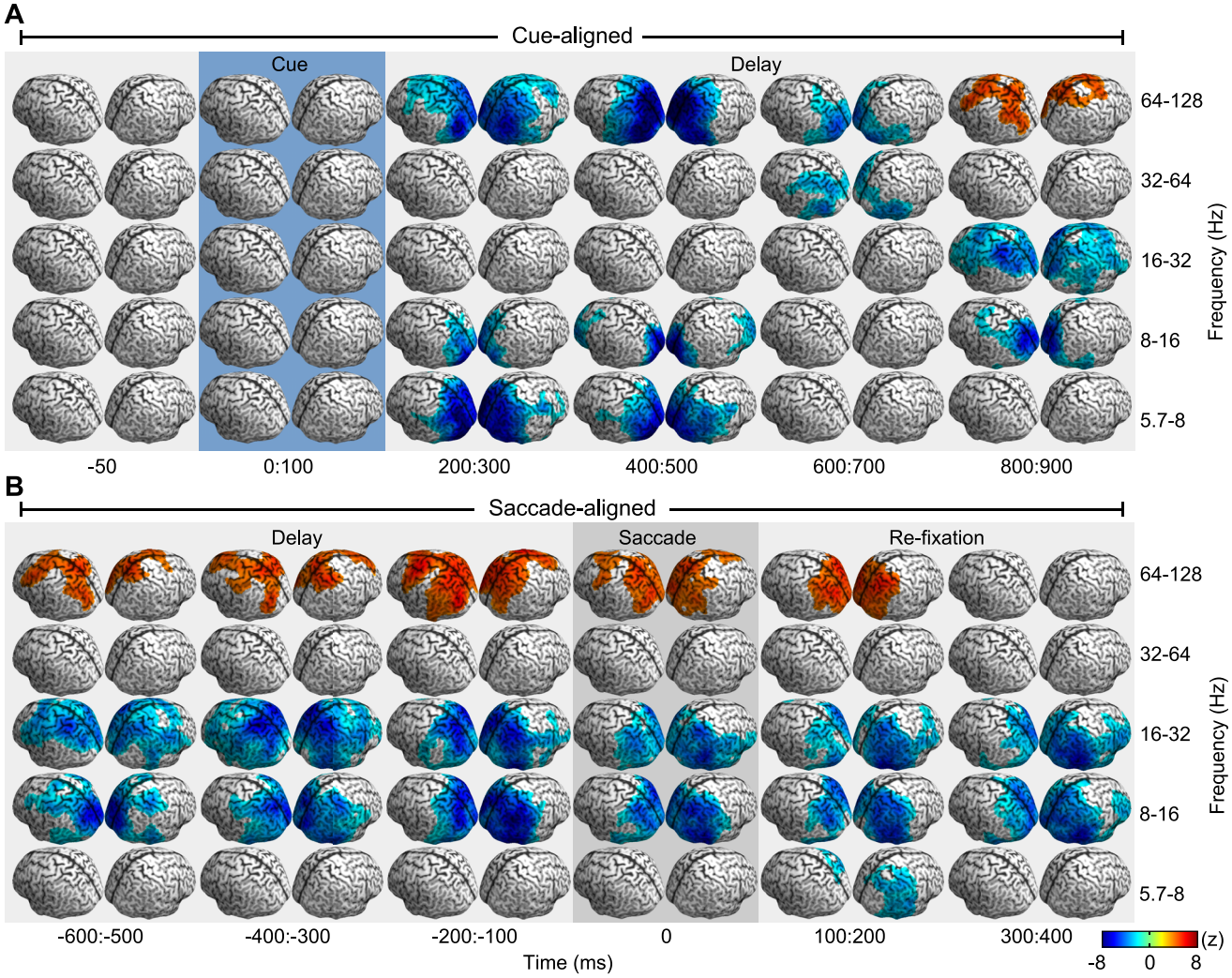

Figure 4.4: Saccade target selection. A and B. Spatio-temporal evolution of differences in spectral power between *free* and *guided* saccades ($free - guided$). Differences from zero were statistically assessed for the time period from cue presentation until re-fixation by cluster based random permutation correcting for multiple comparisons of number of voxels, time and frequency windows ($p < 0.05$, we show a relevant subset of comparisons). Functional maps are masked by the extent of the identified clusters and are illustrated on a 3D cortical slice. Response to cue is shown with cue-aligned data (A), activity during delay and subsequent saccade is shown in alignment to saccade onset (B). Time windows during delay are partly overlapping for A and B.

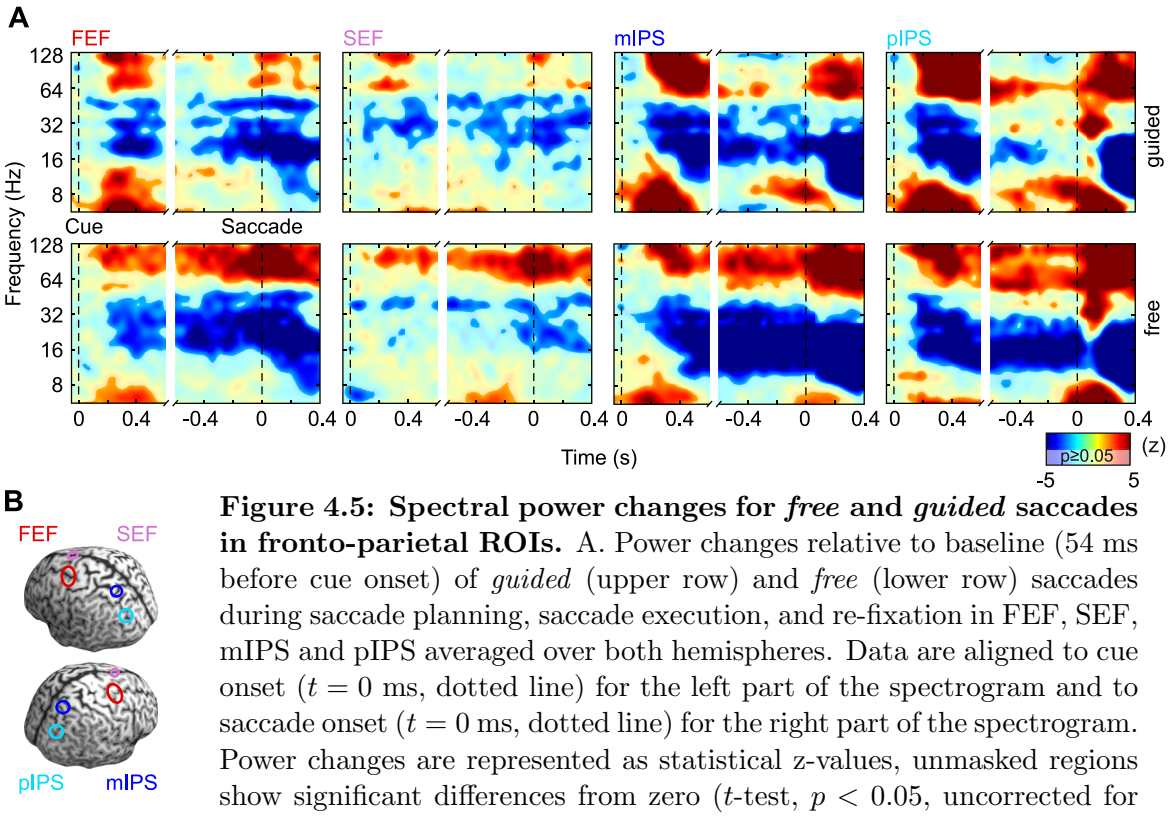

Figure 4.5: Spectral power changes for *free* and *guided* saccades in fronto-parietal ROIs. A. Power changes relative to baseline (54 ms before cue onset) of *guided* (upper row) and *free* (lower row) saccades during saccade planning, saccade execution, and re-fixation in FEF, SEF, mIPS and pIPS averaged over both hemispheres. Data are aligned to cue onset ($t = 0$ ms, dotted line) for the left part of the spectrogram and to saccade onset ($t = 0$ ms, dotted line) for the right part of the spectrogram. Power changes are represented as statistical z-values, unmasked regions show significant differences from zero (t-test, $p < 0.05$, uncorrected for multiple comparisons). B. ROIs.

a possible alternative explanation may be differences in saccade statistics between *free* and *guided* saccades. To test for this possible confound, we compared saccade metrics between conditions. A 1-way ANOVA of frequency of choice of the 16 targets across subjects showed no significant effect of preferred target selection ($F = 1.3$; $p = 0.2053$). Also, the difference in target frequencies between *free* and *guided* saccades showed no significant preference of any saccade target ($F = 1.33$; $p = 0.1865$), suggesting that observed selection specific differences in power are independent of saccade metrics.

4.3.3 Encoding of Saccade Direction

In the above analysis, we pooled the data for saccades to different spatial locations. This identifies processes involved in selection, planning, and execution of saccades independent of the saccade metrics. Despite its limited spatial resolution, hemispheric specificity to the left and right visual hemifields is accessible with MEG. In order to study neuronal processes encoding saccade metrics, we exploited this

property and compared the difference in neuronal activity between left and right hemispheres for trials of left- and rightwards saccades closest to the midline of the monitor. We restricted the analysis to fronto-parietal and visual sources that we found to be related to saccade preparation (Figure 4.6A, cf. Figure 4.2). We averaged hemispheres by mirroring homologous sources across the midline (cf. Statistical analysis in Methods). We pooled *free* and *guided* saccades and analyzed spectral power of the difference between left and right saccades at 3 time windows. These separated the delay phase from 600 ms to 100 ms before saccade onset from the saccade execution at time t = 0 ms and re-fixation from 100 ms to 400 ms after saccade onset. We employed cluster based random permutation tests ($p < 0.05$, corrected for multiple comparisons of number of sources, time, and frequency windows, $n = 95 \times 3 \times 5$, Figure 4.6A).

During preparation of saccades, we found significantly stronger power in the low gamma frequency range ($32 - 64$ Hz window) for sites in pIPS contralateral to saccade direction. During re-fixation low gamma power was stronger contralateral to saccade direction at extrastriate regions around the junctions of lateral occipital sulcus and inferior temporal sulcus and around pIPS. During saccade execution we did not find significant lateralization effects in the gamma range. Power in all lower frequency windows (theta $5.7 - 8$ Hz, alpha $8 - 16$ Hz, beta $16 - 31$ Hz) was significantly lower at the contralateral compared to the ipsilateral site of saccade direction during delay, execution, and re-fixation at extended regions of the posterior cortex. This difference was largest in the alpha range around pIPS during delay and at extrastriate areas at the junctions of lateral occipital sulcus and inferior temporal sulcus during re-fixation.

To resolve the time courses and bandwidth of the observed differences in spectral power, we computed a time-frequency spectrogram with a high resolution for pIPS (Figure 4.6B). The lateralized change in gamma power extended into higher gamma frequencies above 64 Hz.

In a next step we investigated if the identified saccade-metric specific signatures in pIPS differed between *guided* and *free* saccades (Figure 4.6C). There was a significant difference in alpha power between hemifields contra- and ipsilateral to saccade direction for *free* as well as *guided* saccade trials during delay and saccade execution. This saccade direction specific effect was stronger for *guided* than *free* saccades during the delay period (t-test, $p < 0.05$, FDR corrected for conditions, time, and frequency windows, $n = 3 \times 3 \times 2$). Only *guided* saccades showed significant stronger

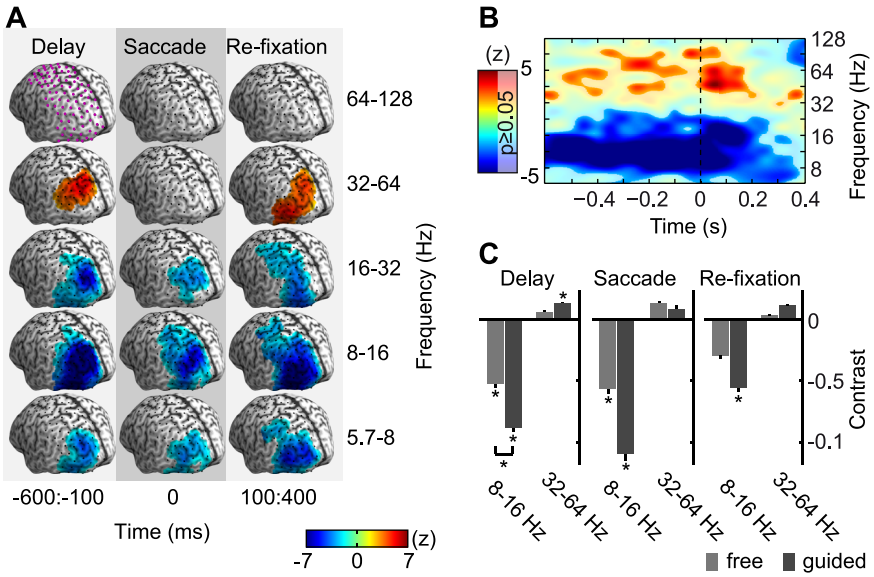

Figure 4.6: Lateralized spectral signatures for horizontal saccades. A. Differences in spectral power between contralateral and ipsilateral sites of saccade direction for horizontal saccades pooled over *free* and *guided* condition (*contralateral* − *ipsilateral*). Statistical comparisons were restricted to 95 source locations in frontal, parietal and occipital areas (indicated by purple dots in the upper left). Difference from zero was statistically assessed by a cluster based random permutation test correcting for multiple comparisons of number of voxels, time windows, and frequency windows ($p < 0.05$). Functional maps are masked by the extent of the identified clusters and illustrated on a 3D cortical slice. B. Time-frequency resolved differences in spectral power for contralateral versus ipsilateral parts of pIPS for horizontal saccades. The plot depicts statistically masked z-scores (t-test, $p < 0.05$, uncorrected for multiple comparisons). C. Differentiation of lateralization effects for *free* and *guided* saccades in selected frequency bands (alpha and low gamma) in pIPS. Lateralization is shown as the average contrast of spectral power of contra versus ipsilateral parts of pIPS (mean over subjects ± sem) for *free* (light gray bars) and *guided* (dark gray bars) saccades separately. Lateralization was tested against zero for both saccade types separately as well as for the difference between both conditions (t-test, $* : p < 0.05$, FDR corrected).

gamma power in contralateral versus ipsilateral sites of the pIPS in the delay period.

In summary, horizontal saccade direction was reflected in lateralized power changes in low gamma and alpha around the posterior parietal cortex. These lateralization effects were strongest during the delay period and stronger for *guided* trials.

4.4 Discussion

The goal of this study was to shed light on the spatiotemporal dynamics of action selection. To this end, we investigated the neuronal signatures of preparation, execution, and target selection for freely chosen and visually guided saccades. We found a fronto-parietal network exhibiting sustained power changes within gamma and alpha to beta frequency bands that reflect the process of action selection between competing alternatives.

In the first analysis combining *free* and *guided* saccades we identified significant changes of local oscillatory population activity related to general saccade planning and execution. Specifically, we identified a fronto-parietal network including the intraparietal sulcus, the frontal and supplementary eye fields, as well as visual areas that exhibited an antagonistic signature of increased gamma band activity and suppressed beta band activity. These findings are in line with previous electrophysiological studies on sensorimotor transformations of guided saccades (Gregoriou et al., 2012, Hinkley et al., 2011, Lachaux et al., 2006, Medendorp et al., 2007, Pesaran et al., 2002).

The neuronal activity we found for the combined analysis of *free* and *guided* saccades likely reflects different concurrently active processes including motor preparation, action selection, spatial attention, and working memory operations that are part of an integrated process towards goal-oriented behavior. In order to unravel the mechanisms specific for action selection, we compared the neuronal activity for instructed action (*guided* saccades) with action selection between competing behavioral alternatives (*free* saccades). *Guided* saccade trials exhibited a stronger fast and transient gamma band response to the instructional cue than *free* saccade trials in extrastriate and posterior parietal cortex. In contrast, freely selecting saccade targets between equally valuable alternatives was associated with subsequent sustained enhancements of fronto-parietal gamma power during the late preparation phase of the saccade.

Activity in the gamma frequency range is thought to reflect local excitatory-inhibitory interactions and can be regarded as a signature of enhanced cortical processing (Bartos et al., 2007, Cardin et al., 2009, Donner and Siegel, 2011, Fries, 2009, Hasenstaub et al., 2005). In this context, the fast transient and late persistent increases in gamma band in the contrast of *guided* and *free* saccades may reflect

two distinct cortical processes associated with different aspects of action selection: While stronger gamma power for *guided* saccades directly after the cue may reflect fast selection of the one, cued action, the protracted increase of gamma band activity in *free* choice trials might reflect action selection between competing alternatives with equal rewarding outcomes that only evolves over time (cf. Cisek and Kalaska, 2010). In particular, the sustained nature of the free selection specific enhancement of gamma power in combination with its localization in areas of sensorimotor transformation provides supporting evidence for the assumption that the selection of actions emerges in a distributed way through mutual competition between neural representations of parallel evolving motor plans (Cisek and Kalaska, 2005, Coulthard et al., 2008, Cui and Andersen, 2007, Oliveira et al., 2010, Pastor-Bernier and Cisek, 2011, Pastor-Bernier et al., 2012, Platt and Glimcher, 1999, Shadlen and Newsome, 2001). Integrated models of action selection claim that this form of decision making is a general mechanism for all decisions resulting in a movement (Cisek, 2006, 2007, Cisek and Kalaska, 2010, Shadlen et al., 2008).

How is this mutual competition between different action plans realized within the sensorimotor areas? Physiological measurements of single neuron activity in parietal cortex suggest that competition between multiple actions is encoded as relative rate code, reflecting the number of available options and the subjective desirability of each action alternative (Dorris and Glimcher, 2004, Klaes et al., 2012, Sugrue et al., 2004). On the population level, we observed a global enhancement of gamma power in fronto-parietal association cortex associated with the presence of multiple action alternatives. Our observations suggest that in addition to spike rates, precise timing – reflected in synchronization – plays a role in the competition between cell assemblies representing different available action alternatives.

Because all choices in the *free* saccade trials were behaviorally equally valuable in our experiment, subjects were free to choose and had to motivate their choice internally. Interpreting this as a form of voluntary choice, our findings corroborate studies that have attributed aspects of voluntariness of action selection to the fronto-parietal network. Human fMRI, TMS, and lesion studies suggested that parietal and premotor areas are involved in the process of voluntary or free action selection (Beudel and de Jong, 2009, Milea et al., 2007, Oliveira et al., 2010, Soon et al., 2008). Furthermore, the fronto-parietal network was proposed to specifically implement the choice of an action when maximally competing alternatives are present (de Jong, 2011, Haggard, 2008, Kable and Glimcher, 2009). This assumption is supported by

electrophysiological studies in non-human primates that found single unit activity in lateral intraparietal area and oscillatory coupling between premotor and parietal areas representing the specific outcome of a chosen movement amongst competing alternatives (Gold and Shadlen, 2007, Pesaran et al., 2008). Our findings of enhanced fronto-parietal gamma activity during saccade target selection provides evidence for a similar choice network in humans and suggests an important role of oscillatory activity for implementing voluntary action selection.

Various cerebral structures have been associated with the origin of voluntary decisions. While e.g. Bode et al. (2012), Soon et al. (2008) suggested that frontopolar cortex implements the initial step in generating decisions, other evidence points to medial frontal cortex as a key player in intentional action selection in humans (Cunnington et al., 2002, Fried et al., 2011, Libet et al., 1983, Rowe et al., 2010). If voluntary decision is a cooperative distributed process (Cisek, 2012, Cisek and Kalaska, 2010), the question where a decision first originates from is less relevant. We do not exclude that other structures like medial frontal cortex including the supplementary eye fields might modulate the here identified fronto-parietal structures in order to mediate saccade target selection (cf. Coe et al., 2002). Instead, we assume that decisions might be implemented in a network of concurrently active brain areas operating in a parallel manner (Ledberg et al., 2007). We found sustained and concurrent fronto-parietal oscillatory activity associated with free action selection supporting the model of decision formation emerging from a network of distributed brain areas.

An important question is to what degree attentional mechanisms might contribute to the selection specific differences in gamma power between *free* and *guided* saccades. Since spatial orienting implicates spatial attention, choosing spatial saccade targets is correlated to some degree with attentional shifts (cf. Andersen and Cui, 2009), and there is good evidence that overt orienting and covert attention are mediated partly by the same networks (Corbetta et al., 1998, Kustov and Robinson, 1996, Rizzolatti et al., 1987). Therefore, all selection specific effects observed here are likely to include attentional contributions. We understand decision towards action as an emergent phenomenon that is necessarily composed of several sub-functions. If intention and attention signals are part of a common process of action selection, dissociating attentional and decision processes might even be misleading. In line with this argument, Bisley and Goldberg (2010) proposed the concept of priority maps that highlight behavioral salient information to bias sensorimotor systems for

appropriate action selections. The lateral intraparietal area was suggested as a neural substrate of such a priority map in monkeys. Our data support the hypothesis of a similar priority map in humans (cf. also Jerde et al., 2012).

In addition to the selection specific changes in gamma power, we found that power was reduced within alpha and beta band during free saccade target selection compared to *guided* saccade trials. These lower frequency changes spatially overlapped with the changes in the gamma band but were more widespread. Beta band activity has been related to signaling the status quo of sensorimotor or cognitive states (Engel and Fries, 2010). Its suppression has been associated with general motor preparation and reflects the formation of a decision as a preparatory motor signal based on the integrated evidence in perceptual decisions (Donner et al., 2009, Wyart et al., 2012). Oscillations in the alpha band have been implicated in a gating mechanism that inhibits task irrelevant areas and by release of inhibition enhances the general excitability of task relevant areas (Jensen and Mazaheri, 2010, Klimesch et al., 2007), a mechanism often associated with spatial attentional allocation (Siegel et al., 2008, Thut et al., 2006, Wyart and Tallon-Baudry, 2008). In our data, effects in the alpha and beta frequency bands are not clearly separable. The observed reduction in these frequency ranges during action selection trials may therefore reflect engagement in movement preparation for multiple actions plans as well as stronger attentional load, or a combination of both effects.

To further pinpoint the functional role of the spectral signatures of saccade target selection we investigated their directional specificity. In line with previous reports on guided saccades (Buchholz et al., 2011, Medendorp et al., 2007, Van Der Werf et al., 2013, 2008, 2010), we found lateralized gamma band activity in pIPS and lateralized alpha modulations in posterior parietal cortex. However, directional specificity in pIPS was much less pronounced for *free* compared to *guided* saccades. A possible explanation is that lateralization effects gradually build up with the evolvement of a decision for the *free* saccade trials, resulting in overall weaker spectral lateralization. Further studies are needed to elaborate on the direction specific dynamics of the selection process in presence of competing alternatives.

In conclusion, our data show that action selection for instructed behavior dissociates from internally motivated action selection in spatiotemporal dynamics, with fast transient gamma band responses for instructed and later sustained gamma band activity for freely selected saccades in a fronto-parietal network. These spectrotemporal characteristics strongly suggest an integrated and parallelized process of

action selection when selection between competing movements is required.

5

General Discussion

In this thesis, we have provided crucial groundwork for studying active vision in EEG/MEG. In contrast to previous concerns raised in the literature, we have demonstrated that EOG regression for CRP removal is not especially susceptible to removing neural activity in MEG (Study 1). By providing a detailed spectral and topographic characterization of the saccadic spike artifact in MEG (Study 2), we have shown that the saccadic spike artifact indeed affects MEG recordings for regular and miniature saccades. Both studies were prerequisites to later unravel cortical mechanisms during eye movements in MEG. In particular, knowledge on the topographic distribution of the SF and the insight that source reconstruction aids in reducing artifactual confounds enabled us to establish a procedure for ocular artifact handling. This procedure combined EOG regression as well as an ICA tailored to SF removal with an analysis in source space. Applying this approach, we have revealed cortical signatures of eye movement control and voluntary saccade selection in MEG (Study 3). More specifically, we found saccade related areas showing a dichotomy of oscillatory activity with high gamma band increases and beta band deceases during saccade planning and execution. Within a network comprising fronto-parietal areas, we could disentangle a fast process of stronger transient gamma band activity in response to the sensory cue for *guided* saccades from a later sustained increase in gamma band activity associated with selecting a saccade target among competing behavioral alternatives.

Here, we would like to discuss the impact and limitations of the presented studies

and provide an outlook on future work addressing fundamental principles of active vision.

Results from Study 1 and 2 support that we have found a suitable procedure for separating artifactual from cortical components related to saccades. Still, it might be desirable to systematically compare performance of the applied approach of artifact removal to a one-time ICA of the broadband MEG/EEG signal, as it has been suggested by Plöchl et al. (2012) for removing all ocular artifacts in EEG. In case of comparable performance, such a procedure would be preferable given its simplicity and the fact, that this is currently the most common way for removing ocular artifacts with ICA. However, although we did not statistically compare performance of approaches, our unpublished observations indicate an inferior performance of an ICA on the broadband data at least for the removal of the SF in MEG: For the majority of subjects, the algorithm applied to the broadband MEG data was not able to separate any SF component and hence could not clean the data from this artifact for these subjects.

Furthermore, we focused on cleaning saccade related artifacts with our cleaning procedure and rejected periods containing blinks before artifact cleaning with EOG regression and ICA. Since blink occurrence can correlate with cognitive factors, rejecting these periods can induce systematic confounds in the experimental data (Oh et al., 2012, Siegle et al., 2008, Smilek et al., 2010). Consequently, especially when investigating unrestricted viewing behavior, where subjects are not instructed to refrain from blinking during experimental trials, an ocular artifact cleaning procedure should address the removal of the blinks as well.

Separation between artifacts and cortical correlates of eye movements is hard to validate and potentially incomplete. Therefore, it is important to have a good knowledge about the characteristics of the artifacts as well as about the cortical components of gaze control in order to proceed towards neural correlates of unrestricted viewing behavior. This thesis provides contributions in both directions. Apart from characterizing the saccadic spike in MEG, we have shown in Study 3 that eye movement related neuronal signals include spectrally specific changes in power especially in fronto-parietal and visual areas.

Real-world behavior does not only imply frequent and regular eye movements but also continuously imposes the need to select actions from many behavioral alternatives. In order to focus on internal selection mechanisms independent from direct sensory or value guidance, we contrasted spectral power of sensory-guided

saccades with saccades where a target could be freely chosen out of 16 equally valuable behavioral alternatives. Such a contrast might include confounding differences between conditions apart from the action selection specific processes we discussed in Section 4.4.

First, *guided* saccade trials were indicated to the subjects by an isoluminant but nevertheless different sensory cue compared to the free target selection trials. This difference between sensory cues may have, in principle, induced a stronger sensory response directly after cue presentation for the *guided* saccade condition. However, evidence from monkey literature questions that a response such as the strong transient gamma band increase after cue presentation is purely sensory driven, especially since even salient but overtly ignored stimuli do not elicit a strong neuronal response in parietal areas (Ipata et al., 2006, for a discussion see Andersen and Cui, 2009). In addition, an MEG study in humans has suggested that only luminance but not isoluminant color contrasts cause gamma band responses in primary visual cortex (Adjamian et al., 2008). These findings support our assumption that the stronger transient response of *guided* compared to *free* saccades is likely not only driven by different sensory stimulation but might also relate to processes of sensory-guided saccade target selection.

Second, *free* and *guided* saccade trials might differentially engage working memory: In particular, maintaining the spatial cueing in memory in the *guided* condition might specifically engage working memory for this condition. Indeed, the spatial and spectral appearance of the transient cortical response to cue presentation with stronger theta and gamma band activity for *guided* saccade trials is compatible with neural signatures of working memory (cf. Jensen et al., 2007, for a review on spectral signatures of working memory). Also, persistent activity during the delay in memory-guided delayed saccade tasks in distributed regions including parietal areas has often been attributed to working memory engagement (Brignani et al., 2010, Curtis, 2006, Pesaran et al., 2002, Raabe et al., 2013). However, the transient nature of the stronger response for *guided* saccade trials argues against ascribing this effect to working memory processes, since a characteristic feature of working memory is the persistent activity throughout the memory period (cf. Curtis and Lee, 2010).

Third, neural correlates of voluntary decisions are also susceptible to be mixed with supposedly distinct mental functions like memory processes or attentional allocation (we addressed the latter confound in Section 4.4). More specifically, saccade selection might have been guided by strategies exploiting target selection history.

Such a strategy of selection would activate processes involved in recalling past target selections with the onset of the cue presentation. Consequently, the gamma band increases we attributed to competitive selection mechanisms during *free* saccade target trials might - to an extent - be attributed to neural processes associated with recall or working memory.

The concern that voluntary actions are often associated with processes of action-monitoring like response inhibition of the last action taken has been raised by a number of studies (e.g., Baddeley et al., 1998, Haggard, 2008, Jahanshahi and Dirnberger, 1999, Rowe et al., 2010, Silvis and Van der Stigchel, 2013, Zhang et al., 2012). One line of research (Rowe et al., 2010, Zhang et al., 2012) suggests that higher BOLD responses in fronto-parietal areas when contrasting free and guided button presses may be related to processing response history. In particular, the authors suggested that activations in inferior frontal cortex (Zhang et al., 2012) and lateral prefrontal cortex (Rowe et al., 2010) were specific for action monitoring of previous selections. In contrast to these activations, the medial frontal cortex was specifically engaged in the process of a selection competition between equally rewarding actions. However, the regions Zhang et al. (2012) and Rowe et al. (2010) report are not consistent across studies. In addition, the decision tasks presented in these studies differ in effector and decision type from the task presented in this thesis (choice of finger for button press versus selection of saccade target). As a consequence, the results of Zhang et al. (2012) and Rowe et al. (2010) are not directly transferable to our work. Nevertheless, the large difference in BOLD activation pattern Rowe and colleagues found when controlling for action monitoring effects suggests that it is advisable to investigate such possible confounds when contrasting *free* and *guided* conditions in future studies.

The discussion about possible confounds related to memory processes or attention when measuring voluntary selection processes is based on the assumption that the brain is largely organized in a modular fashion where these mental processes are assumed to be clearly distinct from one another on the neural level. However, from an embodied perspective, these mental processes might be interdependent, and their separation on the functional and neural level might be an oversimplifying assumption (cf. Cisek and Kalaska, 2010). If this is the case, the ongoing discussion about the differentiation of the functional role of persistent activity that has been related to working memory, decision processes, or anticipation of future motor plans would be more readily explainable (for a review see Curtis and Lee, 2010).

For fronto-parietal areas, evidence points against a functionally clear differentiation between subsumed distinct processes of (saccade) motor planning, action selection, attentional allocation, and working memory (Cisek and Kalaska, 2005, Jerde et al., 2012). Rather than delimiting a specific mental function by clever experimental design, an embodied approach would instead inquire what neural activities are related to a specific ecologically valid task context, in our case the selection of saccade targets. If working memory and action monitoring processes are indeed an integral part in selecting saccade targets in the real world, then these processes are of considerable interest for understanding decision processes in free viewing behavior rather than being mere confounds.

In any case, working memory and action monitoring processes should be considered in future studies of saccade target selection, and we should be careful about naming a mental function if it might actually be a mix of different interacting processes. Of course, if neural activities related to action monitoring are the mere result of the specific experimental design with its trial structure and task instruction, this is clearly a confound that we have to control for and should address in future investigations. For estimating the extent of action monitoring and working memory processes in the employed experimental paradigm, we should – as a first step – investigate if a strategy based on previous saccade selections has indeed been employed. This could be revealed by searching for systematic correlations between each actual selected target with saccade target history.

Another possible confound for the selection related signatures we identified is the timing of internal decisions. Although participants were instructed to select a target as soon as the spatial cue indicated a free selection, the decision for a specific saccade target could have been made anytime within the delay period. This might lead to a temporal jitter in decision formation over the trials that is absent in the *guided* condition, thus contributing to the observed pattern of immediate and transient increase in gamma band power for *guided* but sustained and delayed increase for *free* saccades. If this is indeed the case, the observed conditional effect might reflect a condition specific different *timing* of, for example, spatial orienting (cf. Jerde et al., 2012) rather than reflect differential processes related to sensory-guided and free action selection.

It is questionable if such temporal jitter between trials in selecting a motor plan for *free* saccades would indeed yield a fronto-parietal gamma band increase that is sustained throughout the delay and seems to strengthen towards saccade

execution in frontal and supplementary eye fields (see Section 4.3.2). Also, the spatial distributions of the transient and sustained gamma band signatures do not completely match, thus making temporal jitter unlikely to be the sole source of such a differentiation between *free* and *guided* saccade selection. However, in order to clearly disentangle both processes, further investigations are needed. Studies that have opted for precisely estimating the timing of internal decisions (Soon et al., 2008) require highly artificial experimental designs. Alternatively, assuming that the timing of decisions is associated with saccade latencies, a comparison of saccade latencies within and between conditions might clarify if decision trials show stronger temporal jitter (cf. Pesaran et al., 2008). Ideally, one could try to identify the latency of gamma power increases on single trial level and correlate this with saccade reaction time.

As we mentioned in Section 1.2, it has been suggested that embodied cognition might arise by distributed processes mediated by large-scale frequency specific correlations (Engel, 2010, cf. Siegel et al., 2012, for a review on large-scale oscillatory interactions). In this thesis we did not directly analyze large-scale oscillatory interactions, rather we have presented changes in local oscillatory population activity that were distributed over mainly fronto-parietal and extrastriate areas. Especially for the gamma band, increases in local power are supposed to reflect local excitatory-inhibitory interactions and can be regarded as a signature of enhanced local cortical processing (Bartos et al., 2007, Cardin et al., 2009, Donner and Siegel, 2011, Fries, 2009, Hasenstaub et al., 2005). These local oscillatory dynamics likely form an basis for large-scale frequency specific correlations although local power changes and oscillatory large-scale interactions can be dissociated (as reviewed in Fries, 2009, Siegel et al., 2012). As a consequence, we can only suspect that the fronto-parietal activity we observed during free action selection is associated with large-scale oscillatory interactions establishing a fronto-parietal choice circuit.

Evidence for oscillatory long-range interactions between dorsal premotor area and parietal reach region associated with free decision of reach sequences originates from a non-human primate study (Pesaran et al., 2008). In that study, coherent oscillations in the beta frequency range were attributed to mediate selection between competitive movement goals with the dorsal premotor area being the driving force. In contrast to the sustained gamma signature we found, Pesaran et al. report an increase in coherence as transient activity appearing early after target presentation. Irrespective of these differences, their results suggest that a tight communication,

established by oscillatory couplings between fronto-parietal areas, arises during competitive action selection and that these large-scale couplings might be important also for competitive saccadic target selection. Frequency specific oscillatory couplings between frontal and parietal eye fields and along the dorsal visual pathway during spatially guided orienting further highlight the possible role of oscillations in setting up a functional pathway for communication between these distant areas (Buschman and Miller, 2007, Gregoriou et al., 2009, Siegel et al., 2008). Along these lines there is evidence for task-dependent top-down modulations of local gamma band oscillations in LIP by microstimulation in the frontal eye fields in a delayed saccade task (Premereur et al., 2012).

These observations suggest that oscillatory processes establish distributed fronto-parietal circuits mediating visually guided behavior. Consequently, investigating the role of large-scale frequency couplings of such presumed fronto-parietal interactions specific for saccadic action selection could be a promising subject of future studies. Recent publications have presented various approaches that enable researchers to uncover such large-scale oscillatory networks from EEG/MEG measurements in humans (e.g., Hipp et al., 2011, 2012).

The experimental setup we have presented in this thesis is still restricting free viewing behavior in many ways. First, we did not allow subjects to freely look at every aspect of the scene at any point in time. Such free viewing experiments have only rarely been performed in EEG/MEG. Some studies restricted their analysis of free viewing behavior on effects related to fixation after each eye movement: Ossandón et al. (2010) revealed a superposition of ongoing oscillations and visually evoked responses at fixation onset in occipital areas. Kamienkowski et al. (2012) found that fixation related potentials indicate an interaction of visual responses and eye movements. These fixation locked analyses are one way to study free viewing behavior, and their results encourage proceeding into this direction.

Second, we have focused on internal selection mechanisms since, next to stimulus-guided behavior, internal motivations or expectations are an important part of real-world behavior. In order to maximize competition between action alternatives and drive internally motivated action selection, we presented artificial gaussian patches as saccade targets that were equally looking and behaviorally equally valuable. In contrast, freely deciding where and when to look in real-world behavior underlies various influences that we eliminated in our experimental paradigm. It is strongly depending on the current task at hand (e.g., Betz et al., 2010, Einhäuser et al.,

2008a), on local features of the sensory input (e.g., Engmann et al., 2009, Jansen et al., 2009, Kienzle et al., 2009), as well as on the presence of objects in the current environment (e.g., Drewes et al., 2011, Einhäuser et al., 2008b, but see also Borji et al., 2013). Although directing gaze in natural settings is not immediately associated with reward, there is evidence for indirect value and intrinsic reward related to saccade selections: Since selecting a certain gaze position means that we see things more detailed and colorful at the fixation point, an indirect value of saccadic eye movements is the information gained by directing gaze to a location. Indeed, one line of research has shown that viewing behavior is similar to that of an ideal observer maximizing information gain (Najemnik and Geisler, 2005, 2008, but see Araujo et al., 2001, for contradicting evidence). Deaner et al. (2005) further suggested that eye movement selections might follow intrinsic rewards. They have shown that monkeys value specific visual information about their social group more than direct liquid rewards.

In contrast to these studies, we instructed subjects to choose one out of 16 saccade targets with choice options of presumably equal indirect values. Consequently, the selection mechanisms we investigated were not set into the context of real-world behavioral relevance and thus cannot reveal how indirect rewards might bias action selection. To do so, future studies on saccade target selection should incorporate real-world behavioral tasks or naturalistic stimuli, where selecting gaze position determines the amount of information gain.

Finally, for advancing ecologically relevant investigations of neural activities in MEG/EEG, further progress besides reliable artifact cleaning is required. For instance, studying real-world behavior including limb and head movements imposes significant technical problems of recording and integrating of neural activities together with information about bodily dynamics. An example for an experimental platform that allows recording EEG and muscle activity while monitoring the point of regard and the bodily movements in 3-D space is the setup developed recently by Makeig and colleagues (Gramann et al., 2011, Makeig et al., 2009).

Additionally, given the high variance in neural activity depending of the metrics of the (eye) movement and resulting visual changes, the need of many common analysis methods to average over a large number of trials becomes highly problematic. For example, stimulus contrast can be different from one saccade to the next in free viewing paradigms, thus influencing visual responses. Similarly, as we have shown, saccade directions may impose differently lateralized spectral changes. For active

paradigms allowing movements, analysis approaches investigating single-trial data (Müller et al., 2008, Sajda et al., 2009) should be considered. Regarding the presented work in this thesis, a prediction of selected saccade target based on single trial analysis would contribute towards better understanding how selection mechanisms are implemented in the observed fronto-parietal structures.

To conclude, although we focused on specific and simplified aspects of active vision that are still very different from real-world unrestricted behavior, the presented work on artifact correction and investigation of saccade related cortical signatures provide an important step for future studies into this direction. Our results show that saccade preparation and execution, as well as selection specific processes impose strong characteristic changes in spectral power. Such signatures will possibly form a large part of the neural activity one will encounter in free viewing behavior. Knowing about these signatures is therefore important in order to proceed towards real-world unrestricted behavior.

Bibliography

Adjamian, P., Hadjipapas, A., Barnes, G. R., Hillebrand, A., and Holliday, I. E. (2008). Induced Gamma activity in primary visual cortex is related to luminance and not color contrast: An MEG study. *J Vis*, 8(7):4.1–7.

Agre, P. (1997). *Computation and human experience*. Learning in doing: Social, cognitive and computational perspectives. Cambridge University Press, New York.

Amedi, A., Stern, W. M., Camprodon, J. A., Bermpohl, F., Merabet, L., Rotman, S., Hemond, C., Meijer, P., and Pascual-Leone, A. (2007). Shape conveyed by visual-to-auditory sensory substitution activates the lateral occipital complex. *Nat Neurosci*, 10(6):687–689.

Andersen, R. A. and Cui, H. (2009). Intention, action planning, and decision making in parietal-frontal circuits. *Neuron*, 63(5):568–583.

Antervo, A., Hari, R., Katila, T., Ryhänen, T., and Seppänen, M. (1985). Magnetic fields produced by eye blinking. *Electroencephalogr Clin Neurophysiol*, 61(4):247–253.

Araujo, C., Kowler, E., and Pavel, M. (2001). Eye movements during visual search: the costs of choosing the optimal path. *Vision Res*, 41(25-26):3613–3625.

Arden, G. B. and Constable, P. A. (2006). The electro-oculogram. *Prog Retin Eye Res*, 25(2):207–248.

Arend, L. E. (1973). Spatial differential and integral operations in human vision: implications of stabilized retinal image fading. *Psychol Rev*, 80(5):374–395.

Armington, J. C. (1978). Potentials that precede small saccades. In Armington, J. C., Krauskopf, J., and Wooten, B. R., editors, *Visual psychophysics and physiology: A volume dedicated to Lorrin Riggs*, pages 363–372. Academic Press, New York.

Bach-y Rita, P. (1972). *Brain mechanisms in sensory substitution.* Academic Press, New York.

Bach-y Rita, P. (1984). The relationship between motor processes and cognition in tactile vision substitution. In Prinz, W. and Sanders, A. F., editors, *Cognition and motor processes*, pages 149–160. Springer, Berlin, Heidelberg.

Bach-y Rita, P., Collins, C. C., Saunders, F. A., White, B., and Scadden, L. (1969). Vision substitution by tactile image projection. *Nature*, 221(5184):963–964.

Bach-y Rita, P., Tyler, M. E., and Kaczmarek, K. A. (2003). Seeing with the brain. *International Journal of Human-Computer Interaction*, 15(2):285–295.

Baddeley, A. A., Emslie, H. H., Kolodny, J. J., and Duncan, J. J. (1998). Random generation and the executive control of working memory. *Q J Exp Psychol A*, 51(4):819–852.

Baillet, S., Mosher, J. C., and Leahy, R. M. (2001). Electromagnetic brain mapping. *IEEE Signal Process. Mag.*, 18(6):14–30.

Balaban, C. D. and Weinstein, J. M. (1985). The human pre-saccadic spike potential: influences of a visual target, saccade direction, electrode laterality and instructions to perform saccades. *Brain Res*, 347(1):49–57.

Ballard, D. H., Hayhoe, M. M., and Pelz, J. B. (1995). Memory representations in natural tasks. *J Cogn Neurosci*, 7(1):66–80.

Ballard, D. H., Hayhoe, M. M., Pook, P. K., and Rao, R. P. (1997). Deictic codes for the embodiment of cognition. *Behav Brain Sci*, 20(4):723–42– discussion 743–67.

Barbati, G., Porcaro, C., Zappasodi, F., Rossini, P. M., and Tecchio, F. (2004). Optimization of an independent component analysis approach for artifact identification and removal in magnetoencephalographic signals. *Neurophysiol Clin*, 115(5):1220–1232.

Barrett, L. (2010). Distributed cognition. In *Encyclopedia of animal behavior*, pages 543–547. Elsevier, Amsterdam.

Barrett, L. (2011). *Beyond the brain: How body and environment shape animal and human minds*. Princeton University Press, Princeton, NJ.

Barry, W. and Jones, G. M. (1965). Influence of eye lid movement upon electro-oculographic recording of vertical eye movements. *Aerosp Med*, 36:855–858.

Barsalou, L. W. (2008). Grounded cognition. *Annu Rev Psychol*, 59:617–645.

Bartlett, A. M., Ovaysikia, S., Logothetis, N. K., and Hoffman, K. L. (2011). Saccades during object viewing modulate oscillatory phase in the superior temporal sulcus. *J Neurosci*, 31(50):18423–18432.

Bartos, M., Vida, I., and Jonas, P. (2007). Synaptic mechanisms of synchronized gamma oscillations in inhibitory interneuron networks. *Nat Rev Neurosci*, 8(1):45–56.

Basso, M. A. and Wurtz, R. H. (1998). Modulation of neuronal activity in superior colliculus by changes in target probability. *J Neurosci*, 18(18):7519–7534.

Bastiaansen, M. C. and Knösche, T. R. (2000). Tangential derivative mapping of axial MEG applied to event-related desynchronization research. *Neurophysiol Clin*, 111(7):1300–1305.

Beauchamp, M. S. and Martin, A. (2007). Grounding object concepts in perception and action: evidence from fMRI studies of tools. *Cortex*, 43(3):461–468.

Becker, W., Hoehne, O., Iwase, K., and Kornhuber, H. (1972). Bereitschaftspotential, prämotorische Positivierung und andere Hirnpotentiale bei sakkadischen Augenbewegungen [Readinesspotential, antecedent potential and other cortical potentials related to saccades]. *Vision Res*, 12:421–436.

Bell, A. J. and Sejnowski, T. J. (1995). An information-maximization approach to blind separation and blind deconvolution. *Neural Comput*, 7(6):1129–1159.

Bellebaum, C. and Daum, I. (2006). Time course of cross-hemispheric spatial updating in the human parietal cortex. *Behav Brain Res*, 169(1):150–161.

Bellebaum, C., Hoffmann, K.-P., and Daum, I. (2005). Post-saccadic updating of visual space in the posterior parietal cortex in humans. *Behav Brain Res*, 163(2):194–203.

Belouchrani, A. and Cichocki, A. (2000). Robust whitening procedure in blind source separation context. *Electronics Letters*, 36(24):2050.

Belyusar, D., Snyder, A. C., Frey, H.-P., Harwood, M. R., Wallman, J., and Foxe, J. J. (2013). Oscillatory alpha-band suppression mechanisms during the rapid attentional shifts required to perform an anti-saccade task. *Neuroimage*, 65:395–407.

Benjamini, Y. and Hochberg, Y. (1995). Controlling the false discovery rate: A practical and powerful approach to multiple testing. *J R Statistic Soc Series B (Methodological)*, 57(1):289–300.

Berg, P. and Scherg, M. (1991). Dipole modelling of eye activity and its application to the removal of eye artefacts from the EEG and MEG. *Clin Phys Physiol Meas*, 12 Suppl A:49–54.

Berg, P. and Scherg, M. (1994). A multiple source approach to the correction of eye artifacts. *Electroencephalogr Clin Neurophysiol*, 90(3):229–241.

Betz, T., Kietzmann, T. C., Wilming, N., and König, P. (2010). Investigating task-dependent top-down effects on overt visual attention. *J Vis*, 10(3):15.1–14.

Beudel, M. and de Jong, B. M. (2009). Overlap and segregation in predorsal premotor cortex activations related to free selection of self-referenced and target-based finger movements. *Cereb Cortex*, 19(10):2361–2371.

Bisley, J. W. and Goldberg, M. E. (2010). Attention, intention, and priority in the parietal lobe. *Annu Rev Neurosci*, 33:1–21.

Blinn, K. A. (1955). Focal anterior temporal spikes from external rectus muscle. *Electroencephalogr Clin Neurophysiol*, 7(2):299–302.

Bode, S., Bogler, C., Soon, C. S., and Haynes, J.-D. (2012). The neural encoding of guesses in the human brain. *Neuroimage*, 59(2):1924–1931.

Borji, A., Sihite, D. N., and Itti, L. (2013). Objects do not predict fixations better than early saliency: A re-analysis of Einhäuser et al.'s data. *J Vis*, 13(10):18.1–4.

Bosman, C. A., Schoffelen, J.-M., Brunet, N., Oostenveld, R., Bastos, A. M., Womelsdorf, T., Rubehn, B., Stieglitz, T., De Weerd, P., and Fries, P. (2012). Attentional stimulus selection through selective synchronization between monkey visual areas. *Neuron*, 75(5):875–888.

Bosman, C. A., Womelsdorf, T., Desimone, R., and Fries, P. (2009). A microsaccadic rhythm modulates gamma-band synchronization and behavior. *J Neurosci*, 29(30):9471–9480.

Boylan, C. and Doig, H. R. (1989a). Effect of saccade size on presaccadic spike potential amplitude. *Invest Ophthalmol Vis Sci*, 30(12):2521–2527.

Boylan, C. and Doig, H. R. (1989b). Presaccadic spike potential with congenital lateral rectus palsy. *Electroencephalogr Clin Neurophysiol*, 73(3):264–267.

Brignani, D., Bortoletto, M., Miniussi, C., and Maioli, C. (2010). The when and where of spatial storage in memory-guided saccades. *Neuroimage*, 52(4):1611–1620.

Brignani, D., Maioli, C., Maria Rossini, P., and Miniussi, C. (2007). Event-related power modulations of brain activity preceding visually guided saccades. *Brain Res*, 1136:122–131.

Brookes, M. J., Stevenson, C. M., Barnes, G. R., Hillebrand, A., Simpson, M. I. G., Francis, S. T., and Morris, P. G. (2007). Beamformer reconstruction of correlated sources using a modified source model. *Neuroimage*, 34(4):1454–1465.

Brooks-Eidelberg, B. A. and Adler, G. (1992). A frontal cortical potential associated with saccades in humans. *Exp Brain Res*, 89(2):441–446.

Bruce, C. J. and Goldberg, M. E. (1985). Primate frontal eye fields. I. Single neurons discharging before saccades. *J Neurophysiol*, 53(3):603–635.

Buchholz, V. N., Jensen, O., and Medendorp, W. P. (2011). Multiple reference frames in cortical oscillatory activity during tactile remapping for saccades. *J Neurosci*, 31(46):16864–16871.

Bunge, S. A., Wallis, J. D., Parker, A., Brass, M., Crone, E. A., Hoshi, E., and Sakai, K. (2005). Neural circuitry underlying rule use in humans and nonhuman primates. *J Neurosci*, 25(45):10347–10350.

Buschman, T. J. and Miller, E. K. (2007). Top-down versus bottom-up control of attention in the prefrontal and posterior parietal cortices. *Science*, 315(5820):1860–1862.

Buswell, G. T. (1935). *How People Look at Pictures*. A Study of the Psychology of Perception in Art. Univ Chicago Press, Oxford, UK.

Cardin, J. A., Carlén, M., Meletis, K., Knoblich, U., Zhang, F., Deisseroth, K., Tsai, L.-H., and Moore, C. I. (2009). Driving fast-spiking cells induces gamma rhythm and controls sensory responses. *Nature*, 459(7247):663–667.

Carl, C., Açık, A., König, P., Engel, A. K., and Hipp, J. F. (2012). The saccadic spike artifact in MEG. *Neuroimage*, 59(2):1657–1667.

Casile, A. (2013). Mirror neurons (and beyond) in the macaque brain: An overview of 20 years of research. *Neurosci Lett*, 540:3–14.

Chapman, C. S., Gallivan, J. P., Wood, D. K., Milne, J. L., Culham, J. C., and Goodale, M. A. (2010). Reaching for the unknown: multiple target encoding and real-time decision-making in a rapid reach task. *Cognition*, 116(2):168–176.

Chapman, S. (1968). Catching a Baseball. *American Journal of Physics*, 36(10):868.

Cisek, P. (2006). Integrated neural processes for defining potential actions and deciding between them: a computational model. *J Neurosci*, 26(38):9761–9770.

Cisek, P. (2007). Cortical mechanisms of action selection: the affordance competition hypothesis. *Philos Trans R Soc Lond B Biol Sci*, 362(1485):1585–1599.

Cisek, P. (2012). Making decisions through a distributed consensus. *Curr Opin Neurobiol*, 22(6):927–936.

Cisek, P. and Kalaska, J. F. (2005). Neural correlates of reaching decisions in dorsal premotor cortex: specification of multiple direction choices and final selection of action. *Neuron*, 45(5):801–814.

Cisek, P. and Kalaska, J. F. (2010). Neural mechanisms for interacting with a world full of action choices. *Annu Rev Neurosci*, 33:269–298.

Clancey, W. J. (1997). *Situated cognition: On human knowledge and computer representations*. Cambridge University Press, New York.

Clark, A. (1997). *Being there: Putting brain, body, and world together again*. MIT Press, Cambridge, MA, 2nd edition.

Clark, A. (1999). An embodied cognitive science? *Trends Cogn Sci*, 3(9):345–351.

Coe, B., Tomihara, K., Matsuzawa, M., and Hikosaka, O. (2002). Visual and anticipatory bias in three cortical eye fields of the monkey during an adaptive decision-making task. *J Neurosci*, 22(12):5081–5090.

Corbetta, M., Akbudak, E., Conturo, T. E., Snyder, A. Z., Ollinger, J. M., Drury, H. A., Linenweber, M. R., Petersen, S. E., Raichle, M. E., Van Essen, D. C., and Shulman, G. L. (1998). A common network of functional areas for attention and eye movements. *Neuron*, 21(4):761–773.

Cordones, I., Gómez, C. M., and Escudero, M. (2013). Cortical dynamics during the preparation of antisaccadic and prosaccadic eye movements in humans in a gap paradigm. *PLoS ONE*, 8(5):e63751.1–11.

Coulthard, E. J., Nachev, P., and Husain, M. (2008). Control over conflict during movement preparation: role of posterior parietal cortex. *Neuron*, 58(1):144–157.

Craighero, L., Carta, A., and Fadiga, L. (2001). Peripheral oculomotor palsy affects orienting of visuospatial attention. *Neuroreport*, 12(15):3283–3286.

Crapse, T. B. and Sommer, M. A. (2008). Corollary discharge across the animal kingdom. *Nat Rev Neurosci*, 9(8):587–600.

Croft, R. J. and Barry, R. J. (2000a). EOG correction of blinks with saccade coefficients: a test and revision of the aligned-artefact average solution. *Neurophysiol Clin*, 111(3):444–451.

Croft, R. J. and Barry, R. J. (2000b). Removal of ocular artifact from the EEG: a review. *Neurophysiol Clin*, 30(1):5–19.

Croft, R. J. and Barry, R. J. (2002). Issues relating to the subtraction phase in EOG artefact correction of the EEG. *Int J Psychophysiol*, 44(3):187–195.

Croft, R. J., Chandler, J. S., Barry, R. J., Cooper, N. R., and Clarke, A. R. (2005). EOG correction: a comparison of four methods. *Psychophysiology*, 42(1):16–24.

Csibra, G., Johnson, M. H., and Tucker, L. A. (1997). Attention and oculomotor control: a high-density ERP study of the gap effect. *Neuropsychologia*, 35(6):855–865.

Csibra, G., Tucker, L. A., Volein, A., and Johnson, M. H. (2000). Cortical development and saccade planning: the ontogeny of the spike potential. *Neuroreport*, 11(5):1069–1073.

Cui, H. and Andersen, R. A. (2007). Posterior parietal cortex encodes autonomously selected motor plans. *Neuron*, 56(3):552–559.

Cunnington, R., Windischberger, C., Deecke, L., and Moser, E. (2002). The preparation and execution of self-initiated and externally-triggered movement: a study of event-related fMRI. *Neuroimage*, 15(2):373–385.

Curtis, C. E. (2006). Prefrontal and parietal contributions to spatial working memory. *Neuroscience*, 139(1):173–180.

Curtis, C. E. and Connolly, J. D. (2008). Saccade preparation signals in the human frontal and parietal cortices. *J Neurophysiol*, 99(1):133–145.

Curtis, C. E. and D'Esposito, M. (2006). Selection and maintenance of saccade goals in the human frontal eye fields. *J Neurophysiol*, 95(6):3923–3927.

Curtis, C. E. and Lee, D. (2010). Beyond working memory: the role of persistent activity in decision making. *Trends Cogn Sci*, 14(5):216–222.

Dalal, S. S., Sekihara, K., and Nagarajan, S. S. (2006). Modified beamformers for coherent source region suppression. *IEEE Trans Biomed Eng*, 53(7):1357–1363.

de Jong, B. M. (2011). Neurology of widely embedded free will. *Cortex*, 47(10):1160–1165.

Deaner, R. O., Khera, A. V., and Platt, M. L. (2005). Monkeys pay per view: adaptive valuation of social images by rhesus macaques. *Curr Biol*, 15(6):543–548.

Debener, S., Thorne, J., Schneider, T. R., and Viola, F. C. (2011). Using ICA for the analysis of multi-channel EEG data. In Ullsperger, M. and Debener, S., editors, *Simultaneous EEG and fMRI: Recording, analysis, and application*, pages 121–133. Oxford University Press, New York.

Delorme, A., Palmer, J., Onton, J., Oostenveld, R., and Makeig, S. (2012). Independent EEG sources are dipolar. *PLoS ONE*, 7(2):e30135.1–14.

Dewey, J. (1896). The reflex arc concept in psychology. *Psychol Rev*, 3(4):357–370.

di Pellegrino, G., Fadiga, L., Fogassi, L., Gallese, V., and Rizzolatti, G. (1992). Understanding motor events: a neurophysiological study. *Exp Brain Res*, 91(1):176–180.

Dias, E. C. and Segraves, M. A. (1999). Muscimol-induced inactivation of monkey frontal eye field: effects on visually and memory-guided saccades. *J Neurophysiol*, 81:2191–2214.

Dimigen, O., Valsecchi, M., Sommer, W., and Kliegl, R. (2009). Human Microsaccade-Related Visual Brain Responses. *J Neurosci*, 29(39):12321–12331.

Ditchburn, R. W. and Ginsborg, B. L. (1952). Vision with a stabilized retinal image. *Nature*, 170(4314):36–37.

Dodge, R. (1900). Visual perception during eye movement. *Psychol Rev*, 7(5):454–465.

Donner, T. H. and Siegel, M. (2011). A framework for local cortical oscillation patterns. *Trends Cogn Sci*, 15(5):191–199.

Donner, T. H., Siegel, M., Fries, P., and Engel, A. K. (2009). Buildup of choice-predictive activity in human motor cortex during perceptual decision making. *Curr Biol*, 19(18):1581–1585.

Dorr, M. and Bex, P. J. (2013). Peri-saccadic natural vision. *J Neurosci*, 33(3):1211–1217.

Dorris, M. C. and Glimcher, P. W. (2004). Activity in posterior parietal cortex is correlated with the relative subjective desirability of action. *Neuron*, 44(2):365–378.

Drewes, J., Trommershauser, J., and Gegenfurtner, K. R. (2011). Parallel visual search and rapid animal detection in natural scenes. *J Vis*, 11(2):20.1–21.

Drewes, J. and VanRullen, R. (2011). This is the rhythm of your eyes: the phase of ongoing electroencephalogram oscillations modulates saccadic reaction time. *J Neurosci*, 31(12):4698–4708.

Duhamel, Colby, C., and Goldberg, M. (1992). The updating of the representation of visual space in parietal cortex by intended eye movements. *Science*, 255(5040):90–92.

Einhäuser, W. and König, P. (2010). Getting real—sensory processing of natural stimuli. *Curr Opin Neurobiol*, 20(3):389–395.

Einhäuser, W., Rutishauser, U., and Koch, C. (2008a). Task-demands can immediately reverse the effects of sensory-driven saliency in complex visual stimuli. *J Vis*, 8(2):2.1–19.

Einhäuser, W., Spain, M., and Perona, P. (2008b). Objects predict fixations better than early saliency. *J Vis*, 8(14):18.1–26.

Elbert, T., Lutzenberger, W., Rockstroh, B., and Birbaumer, N. (1985). Removal of ocular artifacts from the EEG–a biophysical approach to the EOG. *Electroencephalogr Clin Neurophysiol*, 60(5):455–463.

Engbert, R. (2006). Microsaccades: A microcosm for research on oculomotor control, attention, and visual perception. *Prog Brain Res*, 154:177–192.

Engbert, R. and Kliegl, R. (2003). Microsaccades uncover the orientation of covert attention. *Vision Res*, 43(9):1035–1045.

Engel, A. K. (2010). Directive minds: how dynamics shapes cognition. In Stewart, J. R., Gapenne, O., and Di Paolo, E. A., editors, *Enaction: Towards a new paradigm for cognitive science*, pages 219–243. MIT Press, Cambridge, MA.

Engel, A. K. and Fries, P. (2010). Beta-band oscillations - signalling the status quo? *Curr Opin Neurobiol*, 20(2):156–165.

Engel, A. K., Fries, P., and Singer, W. (2001). Dynamic predictions: oscillations and synchrony in top-down processing. *Nat Rev Neurosci*, 2(10):704–716.

Engel, A. K., Maye, A., Kurthen, M., and König, P. (2013). Where's the action? The pragmatic turn in cognitive science. *Trends Cogn Sci*, 17(5):202–209.

Engmann, S., 't Hart, B. M., Sieren, T., Onat, S., König, P., and Einhäuser, W. (2009). Saliency on a natural scene background: effects of color and luminance contrast add linearly. *Atten Percept Psychophys*, 71(6):1337–1352.

Everling, S., Spantekow, A., Krappmann, P., and Flohr, H. (1998). Event-related potentials associated with correct and incorrect responses in a cued antisaccade task. *Exp Brain Res*, 118(1):27–34.

Fatima, Z., Quraan, M. A., Kovacevic, N., and McIntosh, A. R. (2013). ICA-based artifact correction improves spatial localization of adaptive spatial filters in MEG. *Neuroimage*, 78:284–294.

Fink, P. W., Foo, P. S., and Warren, W. H. (2009). Catching fly balls in virtual reality: A critical test of the outfielder problem. *J Vis*, 9(13):14.1–8.

Flusberg, S. J., Thibodeau, P. H., Sternberg, D. A., and Glick, J. J. (2010). A Connectionist Approach to Embodied Conceptual Metaphor. *Front Psychol*, 1:197.1–11.

Fodor, J. A. (1981). *Representations: philosophical essays on the foundations of cognitive science.* MIT Press, Cambridge, MA, 2nd print edition.

Fodor, J. A. (2000). *The mind doesn't work that way: The scope and limits of computational psychology.* MIT Press, Cambridge, MA.

Fox, P. T. and Friston, K. J. (2012). Distributed processing; distributed functions? *Neuroimage*, 61(2):407–426.

Fried, I., Mukamel, R., and Kreiman, G. (2011). Internally generated preactivation of single neurons in human medial frontal cortex predicts volition. *Neuron*, 69(3):548–562.

Fries, P. (2005). A mechanism for cognitive dynamics: neuronal communication through neuronal coherence. *Trends Cogn Sci*, 9(10):474–480.

Fries, P. (2009). Neuronal gamma-band synchronization as a fundamental process in cortical computation. *Annu Rev Neurosci*, 32(1):209–224.

Fries, P., Scheeringa, R., and Oostenveld, R. (2008). Finding gamma. *Neuron*, 58(3):303–305.

Fujiwara, Y., Yamashita, O., Kawawaki, D., Doya, K., Kawato, M., Toyama, K., and Sato, M.-a. (2009). A hierarchical Bayesian method to resolve an inverse problem of MEG contaminated with eye movement artifacts. *Neuroimage*, 45(2):393–409.

Gallivan, J. P., McLean, D. A., Smith, F. W., and Culham, J. C. (2011). Decoding effector-dependent and effector-independent movement intentions from human parieto-frontal brain activity. *J Neurosci*, 31(47):17149–17168.

Genovese, C. R., Lazar, N. A., and Nichols, T. (2002). Thresholding of statistical maps in functional neuroimaging using the false discovery rate. *Neuroimage*, 15(4):870–878.

Gibson, J. J. (1966). *The senses considered as perceptual systems*. Houghton Mifflin, Boston.

Gibson, J. J. (1979). *The ecological approach to visual perception*. Houghton Mifflin, Boston.

Gilchrist, I. D., Brown, V., and Findlay, J. (1997). Saccades without eye movements. *Nature*, 390(6656):130–131.

Gilchrist, I. D., Brown, V., Findlay, J., and Clarke, M. P. (1998). Using the eye-movement system to control the head. *Proc. Biol. Sci.*, 265(1408):1831–1836.

Glimcher, P. W. (2003). The neurobiology of visual-saccadic decision making. *Annu Rev Neurosci*, 26:133–179.

Glimcher, P. W. (2009). Choice: Towards a standard back-pocket model. In Glimcher, P. W., Camerer, C. F., Fehr, E., and Poldrack, R. A., editors, *Neuroeconomics: Decision making and the brain*, pages 503–521. Academic Press, Amsterdam, 1st edition.

Glimcher, P. W. (2011). *Foundations of neuroeconomic analysis*. Oxford University Press, Oxford.

Gold, J. I. and Shadlen, M. N. (2007). The neural basis of decision making. *Annu Rev Neurosci*, 30:535–574.

Görgen, K. (2010). Combining Eyetracking and EEG. *PICS - Publications of the Institute of Cognitive Science*, 15:1–65.

Gould, I. C., Nobre, A. C., Wyart, V., and Rushworth, M. F. S. (2012). Effects of decision variables and intraparietal stimulation on sensorimotor oscillatory activity in the human brain. *J Neurosci*, 32(40):13805–13818.

Gowen, E., Abadi, R. V., and Poliakoff, E. (2005). Paying attention to saccadic intrusions. *Cogn Brain Res*, 25(3):810–825.

Gowen, E., Abadi, R. V., Poliakoff, E., Hansen, P. C., and Miall, R. C. (2007). Modulation of saccadic intrusions by exogenous and endogenous attention. *Brain Res*, 1141:154–167.

Gramann, K., Gwin, J. T., Ferris, D. P., Oie, K., Jung, T.-P., Lin, C.-T., Liao, L.-D., and Makeig, S. (2011). Cognition in action: imaging brain/body dynamics in mobile humans. *Rev Neurosci*, 22(6):593–608.

Gratton, G. (1998). Dealing with artifacts: The EOG contamination of the event-related brain potential. *Behavior Research Methods, Instruments, & Computers*, 30(1):44–53.

Gratton, G., Coles, M. G., and Donchin, E. (1983). A new method for off-line removal of ocular artifact. *Electroencephalogr Clin Neurophysiol*, 55(4):468–484.

Gregoriou, G. G., Gotts, S. J., and Desimone, R. (2012). Cell-type-specific synchronization of neural activity in FEF with V4 during attention. *Neuron*, 73(3):581–594.

Gregoriou, G. G., Gotts, S. J., Zhou, H., and Desimone, R. (2009). High-frequency, long-range coupling between prefrontal and visual cortex during attention. *Science*, 324(5931):1207–1210.

Gross, J., Kujala, J., Hämäläinen, M., Timmermann, L., Schnitzler, A., and Salmelin, R. (2001). Dynamic imaging of coherent sources: studying neural interactions in the human brain. *Proc. Natl. Acad. Sci. U.S.A.*, 98(2):694–699.

Gutteling, T. P., van Ettinger-Veenstra, H. M., Kenemans, J. L., and Neggers, S. F. W. (2010). Lateralized frontal eye field activity precedes occipital activity shortly before saccades: evidence for cortico-cortical feedback as a mechanism underlying covert attention shifts. *J Cogn Neurosci*, 22(9):1931–1943.

Haarmeier, T., Thier, P., Repnow, M., and Petersen, D. (1997). False perception of motion in a patient who cannot compensate for eye movements. *Nature*, 389(6653):849–852.

Haegens, S., Nácher, V., Luna, R., Romo, R., and Jensen, O. (2011). α-Oscillations in the monkey sensorimotor network influence discrimination performance by rhythmical inhibition of neuronal spiking. *Proc Natl Acad Sci USA*, 108(48):19377–19382.

Hafed, Z. M. and Clark, J. J. (2002). Microsaccades as an overt measure of covert attention shifts. *Vision Res*, 42(22):2533–2545.

Hafed, Z. M. and Krauzlis, R. J. (2006). Ongoing eye movements constrain visual perception. *Nat Neurosci*, 9(11):1449–1457.

Haggard, P. (2008). Human volition: towards a neuroscience of will. *Nat Rev Neurosci*, 9(12):934–946.

Hämäläinen, M., Hari, R., Ilmoniemi, R. J., Knuutila, J., and Lounasmaa, O. V. (1993). Magnetoencephalographytheory, instrumentation, and applications to noninvasive studies of the working human brain. *Reviews of Modern Physics*, 65(2):413–497.

Hämäläinen, M. S. (1995). Functional localization based on measurements with a whole-head magnetometer system. *Brain Topogr*, 7(4):283–289.

Hamm, J. P., Dyckman, K. A., Ethridge, L. E., McDowell, J. E., and Clementz, B. A. (2010). Preparatory activations across a distributed cortical network determine production of express saccades in humans. *J Neurosci*, 30(21):7350–7357.

Hamm, J. P., Maldonado, P., Dyckman, K. A., Grün, S., McDowell, J. E., and Clementz, B. A. (2012). Pre-cue fronto-occipital alpha phase and distributed cortical oscillations predict failures of cognitive control. *J Neurosci*, 32(20):7034–7041.

Hare, T. A., Schultz, W., Camerer, C. F., O'Doherty, J. P., and Rangel, A. (2011). Transformation of stimulus value signals into motor commands during simple choice. *Proc Natl Acad Sci USA*, 108(44):18120–18125.

Harnad, S. (1990). The symbol grounding problem. *Physica D: Nonlinear Phenomena*, 42(1):335–346.

Hasenstaub, A., Shu, Y., Haider, B., Kraushaar, U., Duque, A., and McCormick, D. A. (2005). Inhibitory postsynaptic potentials carry synchronized frequency information in active cortical networks. *Neuron*, 47(3):423–435.

Hassler, U., Barreto, N. T., and Gruber, T. (2011). Induced gamma band responses in human EEG after the control of miniature saccadic artifacts. *Neuroimage*, 57(4):1411–1421.

Hassler, U., Friese, U., Martens, U., Trujillo-Barreto, N., and Gruber, T. (2013). Repetition priming effects dissociate between miniature eye movements and induced gamma-band responses in the human electroencephalogram. *Eur J Neurosci*, 38(3):2425–2433.

Hayden, B. Y. and Platt, M. L. (2010). Neurons in Anterior Cingulate Cortex Multiplex Information about Reward and Action. *J Neurosci*, 30(9):3339–3346.

Hayhoe, M. M. and Rothkopf, C. A. (2011). Vision in the natural world. *WIREs Cogn Sci*, 2(2):158–166.

Hayhoe, M. M., Shrivastava, A., Mruczek, R., and Pelz, J. B. (2003). Visual memory and motor planning in a natural task. *J Vis*, 3(1):49–63.

Held, R. and Hein, A. (1963). Movement-produced stimulation in the development of visually guided behavior. *Journal of Comparative and Physiological Psychology*, 56(5):872–876.

Herdman, A. T. and Ryan, J. D. (2007). Spatio-temporal brain dynamics underlying saccade execution, suppression, and error-related feedback. *J Cogn Neurosci*, 19(3):420–432.

Hillyard, S. A. and Galambos, R. (1970). Eye movement artifact in the CNV. *Electroencephalogr Clin Neurophysiol*, 28(2):173–182.

Hinkley, L. B. N., Nagarajan, S. S., Dalal, S. S., Guggisberg, A. G., and Disbrow, E. A. (2011). Cortical temporal dynamics of visually guided behavior. *Cereb Cortex*, 21(3):519–529.

Hipp, J. F., Engel, A. K., and Siegel, M. (2011). Oscillatory synchronization in large-scale cortical networks predicts perception. *Neuron*, 69(2):387–396.

Hipp, J. F., Hawellek, D. J., Corbetta, M., Siegel, M., and Engel, A. K. (2012). Large-scale cortical correlation structure of spontaneous oscillatory activity. *Nat Neurosci*, 15(6):884–890.

Hipp, J. F. and Siegel, M. (2013). Dissociating neuronal gamma-band activity from cranial and ocular muscle activity in EEG. *Front Hum Neurosci*, 7:338.1–11.

Hoffmann, S. and Falkenstein, M. (2008). The correction of eye blink artefacts in the EEG: a comparison of two prominent methods. *PLoS ONE*, 3(8):e3004.1–11.

Holmes, C. J., Hoge, R., Collins, L., Woods, R., Toga, A. W., and Evans, A. C. (1998). Enhancement of MR images using registration for signal averaging. *J Comput Assist Tomogr*, 22(2):324–333.

Hoshi, E. and Tanji, J. (2007). Distinctions between dorsal and ventral premotor areas: anatomical connectivity and functional properties. *Curr Opin Neurobiol*, 17(2):234–242.

Hyvärinen, A. (1999). Fast and robust fixed-point algorithms for independent component analysis. *IEEE Trans Neural Netw*, 10(3):626–634.

Hyvärinen, A. and Oja, E. (2000). Independent component analysis: algorithms and applications. *Neural Netw*, 13(4-5):411–430.

Iacono, W. G. and Lykken, D. T. (1981). Two-year retest stability of eye tracking performance and a comparison of electro-oculographic and infrared recording techniques: evidence of EEG in the electro-oculogram. *Psychophysiology*, 18(1):49–55.

Ibbotson, M. and Krekelberg, B. (2011). Visual perception and saccadic eye movements. *Curr Opin Neurobiol*, 21(4):553–558.

Ibbotson, M. R., Crowder, N. A., Cloherty, S. L., Price, N. S. C., and Mustari, M. J. (2008). Saccadic modulation of neural responses: possible roles in saccadic suppression, enhancement, and time compression. *J Neurosci*, 28(43):10952–10960.

Ille, N., Berg, P., and Scherg, M. (2002). Artifact correction of the ongoing EEG using spatial filters based on artifact and brain signal topographies. *J Clin Neurophysiol*, 19(2):113–124.

Ipata, A. E., Gee, A. L., Gottlieb, J., Bisley, J. W., and Goldberg, M. E. (2006). LIP responses to a popout stimulus are reduced if it is overtly ignored. *Nat Neurosci*, 9(8):1071–1076.

Iriki, A., Tanaka, M., and Iwamura, Y. (1996). Coding of modified body schema during tool use by macaque postcentral neurones. *Neuroreport*, 7(14):2325–2330.

Ito, J., Maldonado, P., Singer, W., and Grün, S. (2011). Saccade-related modulations of neuronal excitability support synchrony of visually elicited spikes. *Cereb Cortex*, 21(11):2482–2497.

Jagla, F., Jergelová, M., and Riecanský, I. (2007). Saccadic eye movement related potentials. *Physiol Res*, 56(6):707–713.

Jahanshahi, M. and Dirnberger, G. (1999). The left dorsolateral prefrontal cortex and random generation of responses: studies with transcranial magnetic stimulation. *Neuropsychologia*, 37(2):181–190.

James, C. J. and Hesse, C. W. (2004). Independent component analysis for biomedical signals. *Physiol Meas*, 26(1):R15–R39.

Jansen, L., Onat, S., and König, P. (2009). Influence of disparity on fixation and saccades in free viewing of natural scenes. *J Vis*, 9(1):29.1–19.

Jensen, O., Kaiser, J., and Lachaux, J.-P. (2007). Human gamma-frequency oscillations associated with attention and memory. *Trends Neurosci*, 30(7):317–324.

Jensen, O. and Mazaheri, A. (2010). Shaping functional architecture by oscillatory alpha activity: gating by inhibition. *Front Hum Neurosci*, 4:186.1–8.

Jerbi, K., Freyermuth, S., Dalal, S., Kahane, P., Bertrand, O., Berthoz, A., and Lachaux, J.-P. (2009). Saccade related gamma-band activity in intracerebral EEG: dissociating neural from ocular muscle activity. *Brain Topogr*, 22(1):18–23.

Jerde, T. A., Merriam, E. P., Riggall, A. C., Hedges, J. H., and Curtis, C. E. (2012). Prioritized Maps of Space in Human Frontoparietal Cortex. *J Neurosci*, 32(48):17382–17390.

Johnston, K. and Everling, S. (2008). Neurophysiology and neuroanatomy of reflexive and voluntary saccades in non-human primates. *Brain Cogn*, 68(3):271–283.

Joyce, C. A., Gorodnitsky, I. F., and Kutas, M. (2004). Automatic removal of eye movement and blink artifacts from EEG data using blind component separation. *Psychophysiology*, 41(2):313–325.

Jung, T. P., Makeig, S., Humphries, C., Lee, T. W., McKeown, M. J., Iragui, V., and Sejnowski, T. J. (2000a). Removing electroencephalographic artifacts by blind source separation. *Psychophysiology*, 37(2):163–178.

Jung, T. P., Makeig, S., Westerfield, M., Townsend, J., Courchesne, E., and Sejnowski, T. J. (2000b). Removal of eye activity artifacts from visual event-related potentials in normal and clinical subjects. *Neurophysiol Clin*, 111(10):1745–1758.

Jutras, M. J., Fries, P., and Buffalo, E. A. (2013). Oscillatory activity in the monkey hippocampus during visual exploration and memory formation. *Proc Natl Acad Sci USA*, 110(32):13144–13149.

Kable, J. W. and Glimcher, P. W. (2009). The neurobiology of decision: consensus and controversy. *Neuron*, 63(6):733–745.

Kagan, I., Iyer, A., Lindner, A., and Andersen, R. A. (2010). Space representation for eye movements is more contralateral in monkeys than in humans. *Proc Natl Acad Sci USA*, 107(17):7933–7938.

Kamienkowski, J. E., Ison, M. J., Quiroga, R. Q., and Sigman, M. (2012). Fixation-related potentials in visual search: A combined EEG and eye tracking study. *J Vis*, 12(7):4.1–20.

Kazai, K. and Yagi, A. (2003). Comparison between the lambda response of eye-fixation-related potentials and the P100 component of pattern-reversal visual evoked potentials. *Cognitive, Affective, & Behavioral Neuroscience*, 3(1):46–56.

Kelly, D. H. (1981). Disappearance of stabilized chromatic gratings. *Science*, 214(4526):1257–1258.

Kennerley, S. W., Walton, M. E., Behrens, T. E. J., Buckley, M. J., and Rushworth, M. F. S. (2006). Optimal decision making and the anterior cingulate cortex. *Nat Neurosci*, 9(7):940–947.

Keren, A. S., Yuval-Greenberg, S., and Deouell, L. Y. (2010a). Saccadic spike potentials in gamma-band EEG: characterization, detection and suppression. *Neuroimage*, 49(3):2248–2263.

Keren, A. S., Yuval-Greenberg, S., Gao, Z., Gerber, E., Bentinand, S., and Deouell, L. Y. (2010b). Saccadic spike potentials in gamma-band EEG and MEG: characterization, detection and suppression. In *Human Brain Mapping Annual Meeting, abstract no 1014 WTh-PM*, Barcelona, ES.

Kienzle, W., Franz, M. O., Schölkopf, B., and Wichmann, F. A. (2009). Center-surround patterns emerge as optimal predictors for human saccade targets. *J Vis*, 9(5):7.1–15.

Kierkels, J. J. M., Riani, J., Bergmans, J. W. M., and van Boxtel, G. J. M. (2007). Using an eye tracker for accurate eye movement artifact correction. *IEEE Trans Biomed Eng*, 54(7):1256–1267.

Kietzmann, T. C., Geuter, S., and König, P. (2011). Overt visual attention as a causal factor of perceptual awareness. *PLoS ONE*, 6(7):e22614.1–9.

Klaes, C., Schneegans, S., Schöner, G., and Gail, A. (2012). Sensorimotor learning biases choice behavior: a learning neural field model for decision making. *PLoS Comp Biol*, 8(11):e1002774.1–19.

Klaes, C., Westendorff, S., Chakrabarti, S., and Gail, A. (2011). Choosing goals, not rules: deciding among rule-based action plans. *Neuron*, 70(3):536–548.

Kleiser, R. and Skrandies, W. (2000). Neural correlates of reafference: evoked brain activity during motion perception and saccadic eye movements. *Exp Brain Res*, 133(3):312–320.

Klimesch, W., Sauseng, P., and Hanslmayr, S. (2007). EEG alpha oscillations: the inhibition-timing hypothesis. *Brain Res Rev*, 53(1):63–88.

Kovach, C. K., Tsuchiya, N., Kawasaki, H., Oya, H., Howard, M. A., and Adolphs, R. (2011). Manifestation of ocular-muscle EMG contamination in human intracranial recordings. *Neuroimage*, 54(1):213–233.

Kowler, E. (1990). The role of visual and cognitive processes in the control of eye movement. *Rev Oculomot Res*, 4:1–70.

Kurtzberg, D. and Vaughan, H. G. (1982). Topographic analysis of human cortical potentials preceding self-initiated and visually triggered saccades. *Brain Res*, 243(1):1–9.

Kustov, A. A. and Robinson, D. L. (1996). Shared neural control of attentional shifts and eye movements. *Nature*, 384(6604):74–77.

Lachaux, J.-P., Hoffmann, D., Minotti, L., Berthoz, A., and Kahane, P. (2006). Intracerebral dynamics of saccade generation in the human frontal eye field and supplementary eye field. *Neuroimage*, 30(4):1302–1312.

Lancaster, J. L., TordesillasGutiérrez, D., Martinez, M., Salinas, F., Evans, A., Zilles, K., Mazziotta, J. C., and Fox, P. T. (2007). Bias between MNI and Talairach coordinates analyzed using the ICBM152 brain template. *Hum Brain Mapp*, 28(11):1194–1205.

Land, M., Mennie, N., and Rusted, J. (1999). The roles of vision and eye movements in the control of activities of daily living. *Perception*, 28(11):1311–1328.

Land, M. F. (2006). Eye movements and the control of actions in everyday life. *Prog Retin Eye Res*, 25(3):296–324.

Laubrock, J., Engbert, R., and Kliegl, R. (2005). Microsaccade dynamics during covert attention. *Vision Res*, 45(6):721–730.

Laubrock, J., Engbert, R., and Kliegl, R. (2008). Fixational eye movements predict the perceived direction of ambiguous apparent motion. *J Vis*, 8(14):13.1–17.

Laubrock, J., Kliegl, R., Rolfs, M., and Engbert, R. (2010). When do microsaccades follow spatial attention? *Atten Percept Psychophys*, 72(3):683–694.

Lawrence, B. M. and Snyder, L. H. (2006). Comparison of effector-specific signals in frontal and parietal cortices. *J Neurophysiol*, 96(3):1393–1400.

Lebedev, M. A. and Wise, S. P. (2002). Insights into seeing and grasping: distinguishing the neural correlates of perception and action. *Behav Cogn Neurosci Rev*, 1(2):108–129.

Ledberg, A., Bressler, S. L., Ding, M., Coppola, R., and Nakamura, R. (2007). Large-scale visuomotor integration in the cerebral cortex. *Cereb Cortex*, 17(1):44–62.

Lee, A. K. C., Hämäläinen, M. S., Dyckman, K. A., Barton, J. J. S., and Manoach, D. S. (2011). Saccadic preparation in the frontal eye field is modulated by distinct trial history effects as revealed by magnetoencephalography. *Cereb Cortex*, 21(2):245–253.

Lee, T. W., Girolami, M., and Sejnowski, T. J. (1999). Independent component analysis using an extended infomax algorithm for mixed subgaussian and supergaussian sources. *Neural Comput*, 11(2):417–441.

Lehmann, D. and Skrandies, W. (1980). Reference-free identification of components of checkerboard-evoked multichannel potential fields. *Electroencephalogr Clin Neurophysiol*, 48(6):609–621.

LeVan, P., Urrestarazu, E., and Gotman, J. (2006). A system for automatic artifact removal in ictal scalp EEG based on independent component analysis and Bayesian classification. *Neurophysiol Clin*, 117(4):912–927.

Libet, B., Gleason, C. A., Wright, E. W., and Pearl, D. K. (1983). Time of conscious intention to act in relation to onset of cerebral activity (readiness-potential). The unconscious initiation of a freely voluntary act. *Brain*, 106 (Pt 3):623–642.

Lins, O. G., Picton, T. W., Berg, P., and Scherg, M. (1993a). Ocular artifacts in EEG and event-related potentials. I: Scalp topography. *Brain Topogr*, 6(1):51–63.

Lins, O. G., Picton, T. W., Berg, P., and Scherg, M. (1993b). Ocular artifacts in recording EEGs and event-related potentials. II: Source dipoles and source components. *Brain Topogr*, 6(1):65–78.

Low, M. D., Borda, R. P., Frost, J. D., and Kellaway, P. (1966). Surface-negative slow potential shift associated with conditioning in man. *Neurology (Minneap.)*, 16:771–782.

Ma, J., Bayram, S., Tao, P., and Svetnik, V. (2011). High-throughput ocular artifact reduction in multichannel electroencephalography (EEG) using component subspace projection. *J Neurosci Methods*, 196(1):131–140.

Maimon, G., Straw, A. D., and Dickinson, M. H. (2010). Active flight increases the gain of visual motion processing in Drosophila. *Nat Neurosci*, 13(3):393–399.

Makeig, S., Gramann, K., Jung, T.-P., Sejnowski, T. J., and Poizner, H. (2009). Linking brain, mind and behavior. *Int J Psychophysiol*, 73(2):95–100.

Maldonado, P. (2007). What we see is how we are: New paradigms in visual research. *Biol Res*, 40(4):439–450.

Maldonado, P. E., Ossandón, J. P., and Flores, F. J. (2009). Attention and neurodynamical correlates of natural vision. In Aboitiz, F. and Cosmelli, D., editors, *From attention to goal-directed behavior: Neurodynamical, methodological and clinical trends*, pages 67–82. Springer Verlag, s.l., online ed.

Malmivuo, J. and Plonsey, R. (1995). *Bioelectromagnetism*. Principles and Applications of Bioelectric and Biomagnetic Fields. Oxford University Press, New York.

Marr, D. (1982). *Vision: A computational investigation into the human representation and processing of visual information*. Freeman, San Francisco.

Martinez-Conde, S. (2006). Fixational eye movements in normal and pathological vision. In Martinez-Conde, S., Macknik, S. L., Martinez, L. M., Alonso, J.-M., and Tse, P. U., editors, *Perception (Part 1): Fundamentals of vision : low and mid-level processes in perception. Volume 154 of Progress in Brain Research*, pages 151–176. Elsevier, Amsterdam.

Martinez-Conde, S., Macknik, S. L., Troncoso, X. G., and Dyar, T. A. (2006). Microsaccades counteract visual fading during fixation. *Neuron*, 49(2):297–305.

Martinez-Conde, S., Macknik, S. L., Troncoso, X. G., and Hubel, D. H. (2009). Microsaccades: a neurophysiological analysis. *Trends Neurosci*, 32(9):463–475.

Martinez-Conde, S., Otero-Millan, J., and Macknik, S. L. (2013). The impact of microsaccades on vision: towards a unified theory of saccadic function. *Nat Rev Neurosci*, 14(2):83–96.

Mathewson, K. E., Lleras, A., Beck, D. M., Fabiani, M., Ro, T., and Gratton, G. (2011). Pulsed out of awareness: EEG alpha oscillations represent a pulsed-inhibition of ongoing cortical processing. *Front Psychol*, 2:99.1–15.

Matsuo, F., Peters, J. F., and Reilly, E. L. (1975). Electrical phenomena associated with movements of the eyelid. *Electroencephalogr Clin Neurophysiol*, 38(5):507–511.

Maye, A. and Engel, A. K. (2011). A discrete computational model of sensorimotor contingencies for object perception and control of behavior. In *2011 IEEE International Conference on Robotics and Automation (ICRA)*, pages 3810–3815. IEEE.

McBeath, M. K., Shaffer, D. M., and Kaiser, M. K. (1995). How baseball outfielders determine where to run to catch fly balls. *Science*, 268(5210):569–573.

McCamy, M. B., Otero-Millan, J., Macknik, S. L., Yang, Y., Troncoso, X. G., Baer, S. M., Crook, S. M., and Martinez-Conde, S. (2012). Microsaccadic efficacy and contribution to foveal and peripheral vision. *J Neurosci*, 32(27):9194–9204.

McDowell, J. E., Dyckman, K. A., Austin, B. P., and Clementz, B. A. (2008). Neurophysiology and neuroanatomy of reflexive and volitional saccades: Evidence from studies of humans. *Brain Cogn*, 68(3):255–270.

McPeek, R. M., Han, J. H., and Keller, E. L. (2003). Competition between saccade goals in the superior colliculus produces saccade curvature. *J Neurophysiol*, 89(5):2577–2590.

Medendorp, W. P., Buchholz, V. N., Van Der Werf, J., and Leoné, F. T. M. (2011). Parietofrontal circuits in goal-oriented behaviour. *Eur J Neurosci*, 33(11):2017–2027.

Medendorp, W. P., Kramer, G. F. I., Jensen, O., Oostenveld, R., Schoffelen, J.-M., and Fries, P. (2007). Oscillatory activity in human parietal and occipital cortex shows hemispheric lateralization and memory effects in a delayed double-step saccade task. *Cereb Cortex*, 17(10):2364–2374.

Meier, T., Rosburg, T., Arnold, M., Kreitschmann-Andermahr, I., Sauer, H., Nowak, H., and Witte, H. (1998). Quantification and rejection of ocular artifacts in auditory evoked fields in schizophrenics. *Electroencephalogr Clin Neurophysiol*, 108(6):526–535.

Melcher, D. and Colby, C. L. (2008). Trans-saccadic perception. *Trends Cogn Sci*, 12(12):466–473.

Merleau-Ponty, M. (1963). *The Structure of Behavior*. (Fisher, A., translator) Beacon Press, Boston, 1942 original edition.

Merriam, E. P., Genovese, C. R., and Colby, C. L. (2003). Spatial updating in human parietal cortex. *Neuron*, 39(2):361–373.

Milea, D., Lobel, E., Lehéricy, S., Leboucher, P., Pochon, J.-B., Pierrot-Deseilligny, C., and Berthoz, A. (2007). Prefrontal cortex is involved in internal decision of forthcoming saccades. *Neuroreport*, 18(12):1221–1224.

Mitra, P. P. and Pesaran, B. (1999). Analysis of dynamic brain imaging data. *Biophys J*, 76(2):691–708.

Moon, S. Y., Barton, J. J. S., Mikulski, S., Polli, F. E., Cain, M. S., Vangel, M., Hämäläinen, M. S., and Manoach, D. S. (2007). Where left becomes right: a magnetoencephalographic study of sensorimotor transformation for antisaccades. *Neuroimage*, 36(4):1313–1323.

Moore, T. and Armstrong, K. M. (2003). Selective gating of visual signals by microstimulation of frontal cortex. *Nature*, 421(6921):370–373.

Moore, T. and Fallah, M. (2001). Control of eye movements and spatial attention. *Proc. Natl. Acad. Sci. U.S.A.*, 98(3):1273–1276.

Moster, M. L. and Goldberg, G. (1990). Topography of scalp potentials preceding self-initiated saccades. *Neurology*, 40(4):644–648.

Moster, M. L., Roemer, R. A., Shagass, C., Polansky, M., and Shan, Y. (1997). Presaccadic spike potential in normal subjects. *Neuro-Ophthalmology*, 18(4):185–190.

Mowrer, O. H., Ruch, T. C., and Miller, N. E. (1935). The corneo-retinal potential difference as the basis of the galvanometric method of recording eye movements. *Am J Physiol*, 114(2):423–428.

Müller, K.-R., Tangermann, M., Dornhege, G., Krauledat, M., Curio, G., and Blankertz, B. (2008). Machine learning for real-time single-trial EEG-analysis: from brain-computer interfacing to mental state monitoring. *J Neurosci Methods*, 167(1):82–90.

Munoz, D. P. and Everling, S. (2004). Look away: the anti-saccade task and the voluntary control of eye movement. *Nat Rev Neurosci*, 5(3):218–228.

Mysore, S. P. and Knudsen, E. I. (2011). The role of a midbrain network in competitive stimulus selection. *Curr Opin Neurobiol*, 21(4):653–660.

Najemnik, J. and Geisler, W. S. (2005). Optimal eye movement strategies in visual search. *Nature*, 434(7031):387–391.

Najemnik, J. and Geisler, W. S. (2008). Eye movement statistics in humans are consistent with an optimal search strategy. *J Vis*, 8(3):4.1–14.

Nakamura, K. and Colby, C. L. (2002). Updating of the visual representation in monkey striate and extrastriate cortex during saccades. *Proc. Natl. Acad. Sci. U.S.A.*, 99(6):4026–4031.

Nakano, T. and Kitazawa, S. (2010). Eyeblink entrainment at breakpoints of speech. *Exp Brain Res*, 205(4):577–581.

Nazir, T. A. and O'Regan, J. K. (1990). Some results on translation invariance in the human visual system. *Spatial Vision*, 5(2):81–100.

Newell, A. and Simon, A. H. (1963). GPS, a program that simulates human thought. In Feigenbaum, E. A. and Feldman, J., editors, *Computers and Thought*, pages 279–293. McGraw-Hill, New York, reprint, 1961 original edition.

Newell, A. and Simon, H. A. (1972). *Human Problem Solving*. Prentice-Hall, Englewood Cliffs, NJ.

Nichols, T. E. and Holmes, A. P. (2002). Nonparametric permutation tests for functional neuroimaging: a primer with examples. *Hum Brain Mapp*, 15(1):1–25.

Noë, A. (2005). *Action in perception*. Representation and Mind. MIT Press, Cambridge, MA.

Nolan, H., Whelan, R., and Reilly, R. B. (2010). FASTER: Fully automated statistical thresholding for EEG artifact rejection. *J Neurosci Methods*, 192(1):152–162.

Nolte, G. (2003). The magnetic lead field theorem in the quasi-static approximation and its use for magnetoencephalography forward calculation in realistic volume conductors. *Phys Med Biol*, 48(22):3637–3652.

Nottage, J. F. (2010). Uncovering gamma in visual tasks. *Brain Topogr*, 23(1):58–71.

Nunez, P. l. and Srinivasan, P. L. N. R. (2006). *Electric fields of the brain: the neurophysics of EEG*. Oxford University Press, New York, 2nd edition.

Oh, J., Han, M., Peterson, B. S., and Jeong, J. (2012). Spontaneous eyeblinks are correlated with responses during the Stroop task. *PLoS ONE*, 7(4):e34871.1–11.

Oliveira, F. T. P., Diedrichsen, J., Verstynen, T., Duque, J., and Ivry, R. B. (2010). Transcranial magnetic stimulation of posterior parietal cortex affects decisions of hand choice. *Proc Natl Acad Sci USA*, 107(41):17751–17756.

Oostenveld, R., Fries, P., Maris, E., and Schoffelen, J.-M. (2011). FieldTrip: Open source software for advanced analysis of MEG, EEG, and invasive electrophysiological data. *Comput Intell Neurosci*, 2011:156869.1–9.

O'Regan, J. K. and Noë, A. (2001). A sensorimotor account of vision and visual consciousness. *Behav Brain Sci*, 24(5):939–73– discussion 973–1031.

Ossandón, J. P., Helo, A. V., Montefusco-Siegmund, R., and Maldonado, P. E. (2010). Superposition model predicts EEG occipital activity during free viewing of natural scenes. *J Neurosci*, 30(13):4787–4795.

Otero-Millan, J., Macknik, S. L., Langston, R. E., and Martinez-Conde, S. (2013). An oculomotor continuum from exploration to fixation. *Proc Natl Acad Sci USA*, 110(15):6175–6180.

Parks, N. A. and Corballis, P. M. (2008). Electrophysiological correlates of presaccadic remapping in humans. *Psychophysiology*, 45(5):776–783.

Parks, N. A. and Corballis, P. M. (2010). Human transsaccadic visual processing: presaccadic remapping and postsaccadic updating. *Neuropsychologia*, 48(12):3451–3458.

Pasik, P., Pasik, T., and Bender, M. B. (1965). Recovery of the electro-oculogram after total ablation of the retina in monkeys. *Electroencephalogr Clin Neurophysiol*, 19(3):291–297.

Pastor-Bernier, A. and Cisek, P. (2011). Neural correlates of biased competition in premotor cortex. *J Neurosci*, 31(19):7083–7088.

Pastor-Bernier, A., Tremblay, E., and Cisek, P. (2012). Dorsal premotor cortex is involved in switching motor plans. *Front Neuroeng*, 5:5.1–15.

Pelz, J. B. and Canosa, R. (2001). Oculomotor behavior and perceptual strategies in complex tasks. *Vision Res*, 41(25-26):3587–3596.

Pertzov, Y., Avidan, G., and Zohary, E. (2011). Multiple reference frames for saccadic planning in the human parietal cortex. *J Neurosci*, 31(3):1059–1068.

Pesaran, B., Nelson, M. J., and Andersen, R. A. (2008). Free choice activates a decision circuit between frontal and parietal cortex. *Nature*, 453(7193):406–409.

Pesaran, B., Pezaris, J. S., Sahani, M., Mitra, P. P., and Andersen, R. A. (2002). Temporal structure in neuronal activity during working memory in macaque parietal cortex. *Nat Neurosci*, 5(8):805–811.

Peterburs, J., Gajda, K., Hoffmann, K.-P., Daum, I., and Bellebaum, C. (2011). Electrophysiological correlates of inter- and intrahemispheric saccade-related updating of visual space. *Behav Brain Res*, 216(2):496–504.

Pham, T. T. H., Croft, R. J., Cadusch, P. J., and Barry, R. J. (2011). A test of four EOG correction methods using an improved validation technique. *Int J Psychophysiol*, 79(2):203–210.

Picton, T. W., van Roon, P., Armilio, M. L., Berg, P., Ille, N., and Scherg, M. (2000a). Blinks, Saccades, Extraocular Muscles and Visual Evoked Potentials (Reply to Verleger). *Journal of Psychophysiology*, 14(4):210–217.

Picton, T. W., van Roon, P., Armilio, M. L., Berg, P., Ille, N., and Scherg, M. (2000b). The correction of ocular artifacts: a topographic perspective. *Neurophysiol Clin*, 111(1):53–65.

Pieszek, M., Widmann, A., Gruber, T., and Schröger, E. (2013). The human brain maintains contradictory and redundant auditory sensory predictions. *PLoS ONE*, 8(1):e53634.1–13.

Platt, M. L. and Glimcher, P. W. (1999). Neural correlates of decision variables in parietal cortex. *Nature*, 400(6741):233–238.

Plöchl, M., Ossandón, J. P., and König, P. (2012). Combining EEG and eye tracking: identification, characterization, and correction of eye movement artifacts in electroencephalographic data. *Front Hum Neurosci*, 6:278.1–23.

Powell, K. D. and Goldberg, M. E. (2000). Response of neurons in the lateral intraparietal area to a distractor flashed during the delay period of a memory-guided saccade. *J Neurophysiol*, 84(1):301–310.

Premereur, E., Vanduffel, W., Roelfsema, P. R., and Janssen, P. (2012). Frontal eye field microstimulation induces task-dependent gamma oscillations in the lateral intraparietal area. *J Neurophysiol*, 108(5):1392–1402.

Prime, S. L., Vesia, M., and Crawford, J. D. (2010). TMS over human frontal eye fields disrupts trans-saccadic memory of multiple objects. *Cereb Cortex*, 20(4):759–772.

Pulvermüller, F. and Fadiga, L. (2010). Active perception: sensorimotor circuits as a cortical basis for language. *Nat Rev Neurosci*, 11(5):351–360.

Quilter, P. M., McGillivray, B. B., and Wadbrook, D. G. (1977). The removal of eye movement artefact from EEG signals using correlation techniques. In *Random Signal Analysis IEEE Conference Publication*, volume 159, pages 93–100.

Raabe, M., Fischer, V., Bernhardt, D., and Greenlee, M. W. (2013). Neural correlates of spatial working memory load in a delayed match-to-sample saccade task. *Neuroimage*, 71:84–91.

Rajkai, C., Lakatos, P., Chen, C.-M., Pincze, Z., Karmos, G., and Schroeder, C. E. (2008). Transient cortical excitation at the onset of visual fixation. *Cereb Cortex*, 18(1):200–209.

Reingold, E. M. and Stampe, D. M. (2002). Saccadic inhibition in voluntary and reflexive saccades. *J Cogn Neurosci*, 14(3):371–388.

Reva, N. V. and Aftanas, L. I. (2004). The coincidence between late non-phase-locked gamma synchronization response and saccadic eye movements. *Int J Psychophysiol*, 51(3):215–222.

Riemslag, F. C., Van der Heijde, G. L., Van Dongen, M. M., and Ottenhoff, F. (1988). On the origin of the presaccadic spike potential. *Electroencephalogr Clin Neurophysiol*, 70(4):281–287.

Rizzolatti, G., Riggio, L., Dascola, I., and Umiltá, C. (1987). Reorienting attention across the horizontal and vertical meridians: evidence in favor of a premotor theory of attention. *Neuropsychologia*, 25(1A):31–40.

Rohde, M. (2010). *Enaction, Embodiment, Evolutionary Robotics Simulation Models for a Post-Cognitivist Science of Mind*, volume 1 of *Atlantis thinking machines*. Atlantis Press, Paris.

Rolfs, M. (2009). Microsaccades: small steps on a long way. *Vision Res*, 49(20):2415–2441.

Rolfs, M., Engbert, R., and Kliegl, R. (2004). Microsaccade orientation supports attentional enhancement opposite a peripheral cue: commentary on Tse, Sheinberg, and Logothetis (2003). *Psychol Sci*, 15(10):705–707.

Rolfs, M., Kliegl, R., and Engbert, R. (2008). Toward a model of microsaccade generation: the case of microsaccadic inhibition. *J Vis*, 8(11):5.1–23.

Rowe, J. B., Hughes, L., and Nimmo-Smith, I. (2010). Action selection: a race model for selected and non-selected actions distinguishes the contribution of premotor and prefrontal areas. *Neuroimage*, 51(2):888–896.

Rubehn, B., Bosman, C., Oostenveld, R., Fries, P., and Stieglitz, T. (2009). A MEMS-based flexible multichannel ECoG-electrode array. *J. Neural Eng.*, 6(3):036003.1–10.

Sajda, P., Philiastides, M. G., and Parra, L. C. (2009). Single-trial analysis of neuroimaging data: inferring neural networks underlying perceptual decision-making in the human brain. *IEEE Rev Biomed Eng*, 2:97–109.

Salinas, E. and Sejnowski, T. J. (2001). Correlated neuronal activity and the flow of neural information. *Nat Rev Neurosci*, 2(8):539–550.

Salvucci, D. D. and Goldberg, J. H. (2000). Identifying fixations and saccades in eye-tracking protocols. In *ETRA '00*, pages 71–78. ACM Press, New York.

Savitzky, A. and Golay, M. (1964). Smoothing and differentiation of data by simplified least squares procedures. *Analytical chemistry*, 36(8):1627–1639.

Saxberg, B. V. (1987a). Projected free fall trajectories. I. Theory and simulation. *Biol Cybern*, 56(2-3):159–175.

Saxberg, B. V. (1987b). Projected free fall trajectories. II. Human experiments. *Biol Cybern*, 56(2-3):177–184.

Schafer, R. J. and Moore, T. (2007). Attention governs action in the primate frontal eye field. *Neuron*, 56(3):541–551.

Schall, J. D. and Hanes, D. P. (1998). Neural mechanisms of selection and control of visually guided eye movements. *Neural Netw*, 11(7-8):1241–1251.

Schall, J. D., Stuphorn, V., and Brown, J. W. (2002). Monitoring and control of action by the frontal lobes. *Neuron*, 36(2):309–322.

Scherberger, H. and Andersen, R. A. (2007). Target selection signals for arm reaching in the posterior parietal cortex. *J Neurosci*, 27(8):2001–2012.

Schlögl, A., Keinrath, C., Zimmermann, D., Scherer, R., Leeb, R., and Pfurtscheller, G. (2007). A fully automated correction method of EOG artifacts in EEG recordings. *Neurophysiol Clin*, 118(1):98–104.

Schroeder, C. E., Wilson, D. A., Radman, T., Scharfman, H., and Lakatos, P. (2010). Dynamics of active sensing and perceptual selection. *Curr Opin Neurobiol*, 20(2):172–176.

Schumann, F., Einhäuser-Treyer, W., Vockeroth, J., Bartl, K., Schneider, E., and König, P. (2008). Salient features in gaze-aligned recordings of human visual input during free exploration of natural environments. *J Vis*, 8(14):12.1–17.

Schütz, A. C., Braun, D. I., and Gegenfurtner, K. R. (2011). Eye movements and perception: a selective review. *J Vis*, 11(5):9.1–30.

Schwartzman, D. J. and Kranczioch, C. (2011). In the blink of an eye: the contribution of microsaccadic activity to the induced γ band response. *Int J Psychophysiol*, 79(1):73–82.

Searle, J. R. (1980). Minds, brains, and programs. *Behav Brain Sci*, 3(3):417–424.

Shackman, A. J., McMenamin, B. W., Maxwell, J. S., Greischar, L. L., and Davidson, R. J. (2010). Identifying robust and sensitive frequency bands for interrogating neural oscillations. *Neuroimage*, 51(4):1319–1333.

Shadlen, M. N., Kiani, R., Hanks, T. D., and Churchland, A. K. (2008). Neurobiology of decision making: An intentional framework. In Engel, C. and Singer, W., editors, *Better than conscious? Decision making, the human mind, and implications for institutions*, pages 71–101. MIT Press, Cambridge, MA.

Shadlen, M. N. and Newsome, W. T. (2001). Neural basis of a perceptual decision in the parietal cortex (area LIP) of the rhesus monkey. *J Neurophysiol*, 86(4):1916–1936.

Shaffer, D. M. and McBeath, M. K. (2005). Naive beliefs in baseball: Systematic distortion in perceived time of apex for fly balls. *Journal of Experimental Psychology: Learning, Memory, and Cognition*, 31(6):1492–1501.

Shapiro, L. (2011). *Embodied Cognition*. Routledge, London.

Siegel, M., Donner, T. H., and Engel, A. K. (2012). Spectral fingerprints of large-scale neuronal interactions. *Nat Rev Neurosci*, 3(2):121–134.

Siegel, M., Donner, T. H., Oostenveld, R., Fries, P., and Engel, A. K. (2008). Neuronal synchronization along the dorsal visual pathway reflects the focus of spatial attention. *Neuron*, 60(4):709–719.

Siegel, M., Engel, A. K., and Donner, T. H. (2011). Cortical network dynamics of perceptual decision-making in the human brain. *Front Hum Neurosci*, 5:21.1–12.

Siegle, G. J., Ichikawa, N., and Steinhauer, S. (2008). Blink before and after you think: blinks occur prior to and following cognitive load indexed by pupillary responses. *Psychophysiology*, 45(5):679–687.

Silver, M. A. and Kastner, S. (2009). Topographic maps in human frontal and parietal cortex. *Trends Cogn Sci*, 13(11):488–495.

Silvis, J. D. and Van der Stigchel, S. (2013). How memory mechanisms are a key component in the guidance of our eye movements: Evidence from the global effect. *Psychonomic Bulletin & Review*, Advance online publication, doi:10.3758/s13423-013-0498-9.

Skrandies, W. and Laschke, K. (1997). Topography of visually evoked brain activity during eye movements: lambda waves, saccadic suppression, and discrimination performance. *Int J Psychophysiol*, 27(1):15–27.

Smilek, D., Carriere, J. S. A., and Cheyne, J. A. (2010). Out of mind, out of sight: eye blinking as indicator and embodiment of mind wandering. *Psychol Sci*, 21(6):786–789.

Sommer, M. A. and Wurtz, R. H. (2008). Brain circuits for the internal monitoring of movements. *Annu Rev Neurosci*, 31:317–338.

Soon, C. S., Brass, M., Heinze, H.-J., and Haynes, J.-D. (2008). Unconscious determinants of free decisions in the human brain. *Nat Neurosci*, 11(5):543–545.

Sparks, D. L. (2002). The brainstem control of saccadic eye movements. *Nat Rev Neurosci*, 3(12):952–964.

Spüler, M., Rosenstiel, W., and Bogdan, M. (2012). Online adaptation of a c-VEP Brain-computer Interface(BCI) based on error-related potentials and unsupervised learning. *PLoS ONE*, 7(12):e51077.1–11.

Sugrue, L. P., Corrado, G. S., and Newsome, W. T. (2004). Matching behavior and the representation of value in the parietal cortex. *Science*, 304(5678):1782–1787.

Sugrue, L. P., Corrado, G. S., and Newsome, W. T. (2005). Choosing the greater of two goods: neural currencies for valuation and decision making. *Nat Rev Neurosci*, 6(5):363–375.

Sweeney, J. A., Luna, B., Keedy, S. K., McDowell, J. E., and Clementz, B. A. (2007). fMRI studies of eye movement control: investigating the interaction of cognitive and sensorimotor brain systems. *Neuroimage*, 36 Suppl 2:T54–60.

Sylvester, R., Haynes, J.-D., and Rees, G. (2005). Saccades differentially modulate human LGN and V1 responses in the presence and absence of visual stimulation. *Curr Biol*, 15(1):37–41.

Tallon-Baudry, C., Bertrand, O., Delpuech, C., and Pernier, J. (1996). Stimulus specificity of phase-locked and non-phase-locked 40 Hz visual responses in human. *J Neurosci*, 16(13):4240–4249.

Talsma, D. and Woldorff, G. M. (2005). Methods for the estimation and removal of artifacts and overlap in ERP data. In Handy, T. C., editor, *Brain signal analysis: Advances in neuroelectric and neuromagnetic methods*, pages 115–148. MIT Press, Cambridge , MA.

Tatler, B. W., Hayhoe, M. M., Land, M. F., and Ballard, D. H. (2011). Eye guidance in natural vision: reinterpreting salience. *J Vis*, 11(5):5.1–23.

Thelen, E., Schöner, G., Scheier, C., and Smith, L. B. (2001). The dynamics of embodiment: a field theory of infant perseverative reaching. *Behav Brain Sci*, 24(1):1–34– discussion 34–86.

Thickbroom, G. W., Knezevic, W., Carroll, W. M., and Mastaglia, F. L. (1991). Saccade onset and offset lambda waves: relation to pattern movement visually evoked potentials. *Brain Res*, 551(1-2):150–156.

Thickbroom, G. W. and Mastaglia, F. L. (1985). Presaccadic 'spike' potential: investigation of topography and source. *Brain Res*, 339(2):271–280.

Thickbroom, G. W. and Mastaglia, F. L. (1986). Presaccadic spike potential. Relation to eye movement direction. *Electroencephalogr Clin Neurophysiol*, 64(3):211–214.

Thickbroom, G. W. and Mastaglia, F. L. (1987). Presaccadic spike potential: a computer model based upon motor unit recruitment patterns in the extraocular muscles. *Brain Res*, 422(2):377–380.

Thomson, D. J. (1982). Spectrum estimation and harmonic analysis. *Proc. IEEE*, 70(9):1055–1096.

Thut, G., Nietzel, A., Brandt, S. A., and Pascual-Leone, A. (2006). Alpha-band electroencephalographic activity over occipital cortex indexes visuospatial attention bias and predicts visual target detection. *J Neurosci*, 26(37):9494–9502.

Trommershäuser, J., Glimcher, P. W., and Gegenfurtner, K. R. (2009). Visual processing, learning and feedback in the primate eye movement system. *Trends Neurosci*, 32(11):583–590.

Troncoso, X. G., Macknik, S. L., Otero-Millan, J., and Martinez-Conde, S. (2008). Microsaccades drive illusory motion in the Enigma illusion. *Proc Natl Acad Sci USA*, 105(41):16033–16038.

Trujillo, L. T., Peterson, M. A., Kaszniak, A. W., and Allen, J. J. B. (2005). EEG phase synchrony differences across visual perception conditions may depend on recording and analysis methods. *Neurophysiol Clin*, 116(1):172–189.

Turatto, M., Valsecchi, M., Tamè, L., and Betta, E. (2007). Microsaccades distinguish between global and local visual processing. *Neuroreport*, 18(10):1015–1018.

Valsecchi, M., Betta, E., and Turatto, M. (2007). Visual oddballs induce prolonged microsaccadic inhibition. *Exp Brain Res*, 177(2):196–208.

Valsecchi, M., Dimigen, O., Kliegl, R., Sommer, W., and Turatto, M. (2009). Microsaccadic inhibition and P300 enhancement in a visual oddball task. *Psychophysiology*, 46(3):635–644.

Valsecchi, M. and Turatto, M. (2008). Microsaccadic responses in a bimodal oddball task. *Psychol Res*, 73(1):23–33.

van Dam, L. C. J. and van Ee, R. (2006). Retinal image shifts, but not eye movements per se, cause alternations in awareness during binocular rivalry. *J Vis*, 6(11):1172–1179.

Van Der Werf, J., Buchholz, V. N., Jensen, O., and Medendorp, W. P. (2009). Neuronal synchronization in human parietal cortex during saccade planning. *Behav Brain Res*, 205(2):329–335.

Van Der Werf, J., Buchholz, V. N., Jensen, O., and Medendorp, W. P. (2013). Reorganization of oscillatory activity in human parietal cortex during spatial updating. *Cereb Cortex*, 23(3):508–519.

Van Der Werf, J., Jensen, O., Fries, P., and Medendorp, W. P. (2008). Gamma-band activity in human posterior parietal cortex encodes the motor goal during delayed prosaccades and antisaccades. *J Neurosci*, 28(34):8397–8405.

Van Der Werf, J., Jensen, O., Fries, P., and Medendorp, W. P. (2010). Neuronal synchronization in human posterior parietal cortex during reach planning. *J Neurosci*, 30(4):1402–1412.

van Gompel, R. P. G., Fischer, M. H., Murray, W. S., and Hill, R. L. (2007). Eye-movement research: An overview of current and past developments. In van Gompel, R. P. G., Fischer, M. H., Murray, W. S., and Hill, R. L., editors, *Eye movements: A window on mind and brain*, pages 1–28. Elsevier, Amsterdam.

Van Pelt, S., Toni, I., Diedrichsen, J., and Medendorp, W. P. (2010). Repetition suppression dissociates spatial frames of reference in human saccade generation. *J Neurophysiol*, 104(3):1239–1248.

Van Veen, B. D., Van Drongelen, W., Yuchtman, M., and Suzuki, A. (1997). Localization of brain electrical activity via linearly constrained minimum variance spatial filtering. *IEEE Trans Biomed Eng*, 44(9):867–880.

Varela, F., Thompson, E., and Rosch, E. (1993). *The embodied mind: Cognitive science and human experience*. MIT Press, Cambridge, MA, 1st paperback edition.

Verleger, R., Gasser, T., and Möcks, J. (1982). Correction of EOG artifacts in event-related potentials of the EEG: aspects of reliability and validity. *Psychophysiology*, 19(4):472–480.

Vigario, R., Jousmäki, V., Haemaelaeninen, M., Haft, R., and Oja, E. (1998). Independent component analysis for identification of artifacts in magnetoencephalographic recordings. In *Advances in Neural Information Processing Systems 10, [NIPS Conference, Denver, CO, 1997]*, pages 229–235.

Vigario, R. and Oja, E. (2008). BSS and ICA in neuroinformatics: from current practices to open challenges. *IEEE Rev Biomed Eng*, 1:50–61.

Vigario, R., Sarela, J., Jousmiki, V., Hämäläinen, M., and Oja, E. (2000). Independent component approach to the analysis of EEG and MEG recordings. *IEEE Trans Biomed Eng*, 47(5):589–593.

von Helmholtz, H. (1867). *Handbuch der physiologischen Optik [Guide of physiological optics]*. Voss, Leipzig.

Wallstrom, G. L., Kass, R. E., Miller, A., Cohn, J. F., and Fox, N. A. (2004). Automatic correction of ocular artifacts in the EEG: a comparison of regression-based and component-based methods. *Int J Psychophysiol*, 53(2):105–119.

Watson, T. L. and Krekelberg, B. (2009). The relationship between saccadic suppression and perceptual stability. *Curr Biol*, 19(12):1040–1043.

Wauschkuhn, B., Verleger, R., Wascher, E., Klostermann, W., Burk, M., Heide, W., and Kömpf, D. (1998). Lateralized human cortical activity for shifting visuospatial attention and initiating saccades. *J Neurophysiol*, 80(6):2900–2910.

Whitton, J. L., Lue, F., and Moldofsky, H. (1978). A spectral method for removing eye movement artifacts from the EEG. *Electroencephalogr Clin Neurophysiol*, 44(6):735–741.

Wilson, A. D. and Golonka, S. (2013). Embodied Cognition is Not What you Think it is. *Front Psychol*, 4:58.1–13.

Wilson, M. (2002). Six views of embodied cognition. *Psychonomic Bulletin & Review*, 9(4):625–636.

Womelsdorf, T., Schoffelen, J.-M., Oostenveld, R., Singer, W., Desimone, R., Engel, A. K., and Fries, P. (2007). Modulation of Neuronal Interactions Through Neuronal Synchronization. *Science*, 316(5831):1609–1612.

Wurtz, R. H. (2008). Neuronal mechanisms of visual stability. *Vision Res*, 48(20):2070–2089.

Wyart, V., de Gardelle, V., Scholl, J., and Summerfield, C. (2012). Rhythmic fluctuations in evidence accumulation during decision making in the human brain. *Neuron*, 76(4):847–858.

Wyart, V. and Tallon-Baudry, C. (2008). Neural dissociation between visual awareness and spatial attention. *J Neurosci*, 28(10):2667–2679.

Yang, T. and Shadlen, M. N. (2007). Probabilistic reasoning by neurons. *Nature*, 447(7148):1075–1080.

Yarbus, A. L. (1957). The perception of an image fixed with respect to the retina. *Biophysics*, 2:683–690.

Yarbus, A. L. (1967). *Eye movements and vision*. (Haigh, B., translator) Plenum Press, New York, 1965 original edition.

Yuval-Greenberg, S., Tomer, O., Keren, A. S., Nelken, I., and Deouell, L. Y. (2008). Transient induced gamma-band response in EEG as a manifestation of miniature saccades. *Neuron*, 58(3):429–441.

Yuval-Greenberg, S. S. and Deouell, L. Y. L. (2011). Scalp-recorded induced γ-band responses to auditory stimulation and its correlations with saccadic muscle-activity. *Brain Topogr*, 24(1):30–39.

Zhang, J., Hughes, L. E., and Rowe, J. B. (2012). Selection and inhibition mechanisms for human voluntary action decisions. *Neuroimage*, 63(1):392–402.

Zhang, M. and Barash, S. (2000). Neuronal switching of sensorimotor transformations for antisaccades. *Nature*, 408(6815):971–975.

Zhang, M. and Barash, S. (2004). Persistent LIP activity in memory antisaccades: working memory for a sensorimotor transformation. *J Neurophysiol*, 91(3):1424–1441.

List of Publications and Conference Abstracts

The projects presented in this thesis have been published in the following journals and conferences:

Carl C, Açık A, König P, Engel AK, Hipp JF (2011). The saccadic spike artifact in MEG. Neuroimage, 59(2):1657–67. (Study 2)

Carl C, Hipp JF, König P, Engel AK (submitted). Spectral signatures of action selection. J Neurosci. (Study 3)

Carl C, Açık A, König P, Engel AK, Hipp JRF (2011). The saccadic spike potential in magnetoencephalography. Front Hum Neurosci. (142). (Study 2)

Carl C, König P, Engel AK, Hipp JF (2010). Eye movement artifacts during active human vision in MEG. International Summer School on multimodal approaches in Neuroscience. International Research School on Neuroscience of Communication Max Planck Institute for Human Cognitive and Brain Science, Leipzig. (Study 1,2)

Carl C, Hipp JF, König P, Engel AK (2009). Neural synchronization during saccade planning and execution in the human brain [Abstract]. Society for Neuroscience Abstracts, Chicago. (Study 3)

Declaration

I hereby confirm that I contributed significantly to all materials used in this thesis, and that I wrote this thesis independently and made no use of resources other than those indicated. This thesis has not been used, either in the same or different form, to fulfill any other examination requirements. This thesis was neither published in Germany nor abroad, except for the parts indicated above. Copyright of text and figures has been or will be transferred to the respective publishers.

Date, Location Signature